QUANTUM MONTE CARLO STUDY OF THE MULTI-ORBITAL ANDERSON MODEL INCLUDING THE SU(2) INVARIANT HUND'S COUPLING

A Thesis Submitted to
the Graduate School of Engineering and Sciences of
İzmir Institute of Technology
in Partial Fulfillment of the Requirements for the Degree of

MASTER OF SCIENCE

in Physics

by
Gökhan Öztarhan

June 2018
İZMİR

We approve the thesis of **Gökhan Öztarhan**

Examining Committee Members:

Prof. Dr. Nejat BULUT
Department of Physics, İzmir Institute of Technology

Assoc. Prof. Dr. A. Devrim GÜÇLÜ
Department of Physics, İzmir Institute of Technology

Prof. Dr. Hamza POLAT
Department of Physics, Dokuz Eylül University

26 June 2018

Prof. Dr. Nejat BULUT
Supervisor, Department of Physics
İzmir Institute of Technology

Prof. Dr. R. Tuğrul SENGER
Head of the Department of
Physics

Prof. Dr. Aysun SOFUOĞLU
Dean of the Graduate School of
Engineering and Sciences

ACKNOWLEDGMENTS

I would like to thank my supervisor Prof. Dr. Nejat Bulut for his academic guidance and encouragement throughout my graduate study.

I am thankful to the committee members of my thesis Assoc. Prof. Dr. A. Devrim Güçlü and Prof. Dr. Hamza Polat for their participations and proofreading.

I also would like to thank my group mates Selma Mayda Bacaksız and Zafer Kandemir.

I would like to express my gratitude to Gün Deniz Akkoç, who is one of my best friends, for his patience, valuable discussions and support along the way to complete my studies.

I am also grateful to my friends Caner Mengü, Çağatay Odabaşı, Batuhan Kalkan and Elif Ünsal for their friendship and entertaining moments.

I am also thankful to my family for their endless support.

ABSTRACT

QUANTUM MONTE CARLO STUDY OF THE MULTI-ORBITAL ANDERSON MODEL INCLUDING THE SU(2) INVARIANT HUND'S COUPLING

In this study, an SU(2) invariant multi-orbital Anderson impurity model is discussed to obtain the electronic properties of metalloproteins. Metalloproteins are organic molecules containing transition metal atoms. They have important roles in the chemical reactions taking place in organisms. The electronic properties of metalloproteins can be modeled by an effective Anderson impurity model. The effective Anderson impurity model can be studied with the quantum Monte Carlo algorithm developed by Hirsch and Fye (1986). In the quantum Monte Carlo simulations of the Anderson impurity model so far, only the longitudinal component of the Hund's coupling term which arises from the Coulomb interactions between the 3d orbitals is taken into account. Spin-flip and pair-hopping terms (the transverse terms of the Hund's coupling) are not considered. They are required to make the Hamiltonian SU(2) invariant, which is related to the spin rotations, so that the Hamiltonian is more realistic. The treatment of the transverse Hund's coupling with the Hirsch-Fye algorithm has been difficult because of the problems encountered in the Trotter decomposition. Instead, a series expansion method was developed by Sakai et al. (2006). Here, we combine the Hirsch-Fye quantum Monte Carlo algorithm with the series expansion method to study the SU(2) invariant multi-orbital Anderson impurity model. Therefore, we present results from quantum Monte Carlo simulations with the new algorithm.

ÖZET

SU(2)-DEĞİŞMEZ HUND ETKİLEŞİMİ İÇEREN ÇOK-ORBİTALLİ ANDERSON MODELİNİN KUANTUM MONTE CARLO ÇALIŞMASI

Bu çalışmada metaloproteinlerin elektronik özelliklerini elde etmek için bir SU (2)-değişmez çok-orbitalli Anderson safsızlık modeli tartışılmaktadır. Metaloproteinler geçiş atomu içeren organik moleküllerdir. Mikroorganizmalarda gerçekleşen kimyasal reaksiyonlarda önemli rollere sahiptirler. Metaloproteinlerin elektronik özellikleri bir etkin Anderson safsızlık modeliyle modellenebilmektedir. Etkin Anderson safsızlık modeli Hirsch and Fye (1986) tarafından geliştirilen kuantum Monte Carlo algoritması ile çalışılabilmek- tedir. Şimdiye kadar olan Anderson safsızlık modelinin kuantum Monte Carlo simülasyonlarında 3d orbitalleri arasındaki Coulumb etkileşimlerinden kaynaklanan, Hund etkileşiminin sadece enine bileşeni hesaba katılmıştır. Spin-çevirme ve çift-atlama (Hund etkileşiminin boyuna bileşenleri) terimleri hesaba katılmamıştır. Bu terimler Hamiltoniyeni spin rotasyonlarıyla alakalı olan SU(2)-değişmez yapmak için gereklidir, böylece Hamiltoniyen daha gerçekçi olacaktır. Boyuna Hund etkileşiminin Hirsch-Fye algoritmasıyla işleyişi Trotter ayrışmasında karşılaşılan problemler yüzünden zordur. Bunun yerine, bir seri açılımı metodu Sakai et al. (2006) tarafından geliştirilmiştir. Burada, SU(2)-değişmez çok-orbitalli Anderson safsızlık modelini çalışmak için Hirsch-Fye kuantum Monte Carlo algoritması ile seri açılımı metodunu birleştiriyoruz. Sonuç olarak, yeni algoritma ile kuantum Monte Carlo simülasyon sonuçlarını sunuyoruz.

TABLE OF CONTENTS

LIST OF FIGURES

Figure **Page**

temperature $T = 300$ K. In these calculations $H_U \neq 0$ and $H_{U'-J} \neq 0$. $U = 4$ eV, $U = 2.2$ eV and $U' - J = 1.3$ eV. In QMC simulations $\Delta\tau = 0.13063$ and $L = 296$. The chemical potential is constant as $\mu = 7$ eV. 1000 warm up and 1000 measurement sweeps were taken at 32 processors for each point on the graph in QMC simulations. Red empty dots for calculations with the QMC simulations, black filled dots for the exact diagonalization results. (a) Total occupation number of the 3d orbitals $\langle n_{3d} \rangle$ versus chemical potential μ. (b) Square of the total magnetic moment at the 3d orbitals $\langle (M_{3d})^2 \rangle$ versus chemical potential μ. (c) Expectation value of H_J versus chemical potential μ. 78

LIST OF TABLES

LIST OF ABBREVIATIONS

DMS . . . . . Dilute Magnetic Semiconductors
QMC . . . . . Quantum Monte Carlo
HF+SE QMC . . . . . Hirsch-Fye + Series Expansion Quantum Monte Carlo

CHAPTER 1

INTRODUCTION

Obtaining solutions to the strongly correlated electron systems consisting of transition metal atoms has always been a challenge in physics. There are several Hamiltonians constructed to approach this problems such as Hubbard (Hubbard (1963)) and Anderson Hamiltonians (Anderson (1961)). These Hamiltonians can be used to model the materials of which the electronic and magnetic properties are determined or affected by the d orbitals of the transition metals they contain. The high-dimensionality of these complex systems makes it difficult to obtain analytical solutions, consequently the numerical methods have been developed to solve them. The advances in the computer technologies allow us to have realistic numerical calculations. One of the most popular methods is quantum Monte Carlo simulations.

The Anderson impurity model has been introduced in order to study the properties of a localized magnetic impurity in a metallic host (Anderson (1961)), after that it was extended to the semiconductor hosts (Haldane and Anderson (1976)). The single-orbital Anderson impurity model in second-quantized form is

$$H = \sum_{m,\sigma}(\varepsilon_m - \mu)n_{m\sigma} + \sum_{\sigma}(\varepsilon_\nu - \mu)n_{\nu\sigma} + \sum_{m,\sigma} V_{m\nu}\left(c^\dagger_{m\sigma}d_{\nu\sigma} + h.c.\right) + Un_{\nu\uparrow}n_{\nu\downarrow} \quad (1.1)$$

where $c^\dagger_{m\sigma}(c_{m\sigma})$ and $d^\dagger_{\nu\sigma}(d_{\nu\sigma})$ are creation(annihilation) operators for the host state m and the localized state at ν, σ spin. ε_m and ε_ν are the energies of the host and impurity states. $V_{m\nu}$ is the hybridization matrix elements between host and impurity orbitals. μ is the chemical potential, $n_{\nu\sigma}$ is the occupation number of the impurity orbital, $n_{m\sigma}$ is the occupation at the host orbitals. U is the Coulomb repulsion between the d electron at the impurity site. The single-orbital Hamiltonian can be easily generalized to multi-orbital systems. Many physical phenomena can be analyzed, such as presence of the localized states or effects of them in semiconductors and metals, even with this simple model.

The first studies on the magnetic properties of transition metal impurities in semiconductor hosts within the Anderson impurity model (Haldane and Anderson (1976)) shows the existence of the localized energy levels which lies in the semiconductor gap triggered by the occupations of the d-orbitals of those transition metals, changing the

magnetic properties of the materials. The same principles have been observed in the dilute magnetic semiconductors (DMS) (Ohno et al. (1992, 1996)) such as (Ga,Mn)As. They are semiconductors which exhibit magnetic properties, and they contain transition metal atoms substituted into non-magnetic host atoms. An impurity bound state has been found in the semiconductor gap of (Ga,Mn)As (Jungwirth et al. (2007)). The theoretical studies within the Anderson impurity model show that this impurity bound states determines the electronic and magnetic properties of (Ga,Mn)As (Tomoda et al. (2009)). On the other hand, the comparisons between the DMS materials and the metalloproteins show that the same mechanism exists for the metalloproteins and metalloenzymes which have been studied within the framework of multi-orbital Anderson impurity model (Kandemir et al. (2016); Mayda et al. (2017)).

Metalloproteins are basically proteins which contain transition metal atoms. They have several functions within the organisms from oxygen-carrying to catalyzing the vital reactions in cells. The preceding studies for metalloproteins examined within the Anderson model have given very promising results (Kandemir et al. (2016); Mayda et al. (2017)). Although the impurity bound states have been found for metalloproteins, the models did not consist of SU(2) invariant terms. Thus, there has not been any studies for these materials within a SU(2) invariant Anderson Hamiltonian.

SU(2) invariant Anderson Hamiltonian consists of spin-flip and pair-hopping terms (the transverse components of the Hund's coupling) along with the inter- and intra-orbital Coulomb repulsion and the z-component (longitudinal) of the Hund's coupling. Addition of spin-flip and the pair-hopping terms makes the Hamiltonian invariant under SU(2) transformations which are basically rotations in the spin degrees of freedom. The studies within the multi-orbital Hubbard model for t_{2g} orbitals of Sr_2RuO_4 show that the preservation of the rotational symmetries and Hund's exchange coupling are important not only for ferromagnetism in materials containing transition metal atoms, but also for superconductivity and metal-insulator transitions (Sakai et al. (2006)). If the symmetry is broken, transverse spin fluctuations are ignored. This means that if the transverse components of the Hund's coupling term (spin-flip and pair hopping terms) is not taken into account, the longitudinal component of the Hund's coupling makes systems to exhibit a tendency to ferromagnetic behavior. Thus, it can lead to wrong or overestimated results in the details of the magnetic and electronic properties calculated. The transverse terms can suppress the behavior of the longitudinal component.

In this manner, we propose that studies with an SU(2) invariant multi-orbital Anderson Hamiltonian give more detailed and accurate results for metalloproteins. In this

study, 3d orbitals of the transition metal atom in the molecules are taken as impurity orbitals and remaining orbitals of the molecules are the host orbitals for Anderson model. The Anderson model parameters, which are the energy eigenvalues of the single-particle part and the hybridization matrix elements of the Hamiltonian, are obtained from the density functional theory calculations as explained in Kandemir et al. (2016). SU(2) invariant Anderson Hamiltonian is constructed with these values to be solved. We focus on hemoglobin molecule which consist of 4 heme group, each of them includes an iron atom in the center. However, we examine a part of one heme group. The electronic and magnetic properties of human hemoglobin, HbA, is calculated. Two molecules are chosen: $C_{32}H_{30}FeN_{10}O_2$ which is called deoxyheme, $C_{32}H_{30}FeN_{10}O_4$ called oxyheme in this study. These molecules are important since hemoglobin molecule exhibits a transition from high-spin state to low-spin state upon binding of oxygen molecules to the Fe atoms (Pauling and Coryell (1936)). 3d orbitals of Fe atom acts as the transition metal impurities in the semiconductor hosts, thus making these molecules perfect candidates to model them with Anderson impurity model.

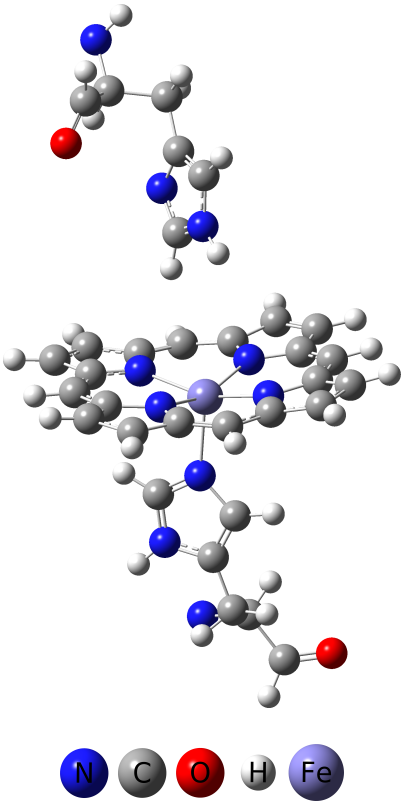

Figure 1.1. Molecular structure of $C_{32}H_{30}FeN_{10}O_2$

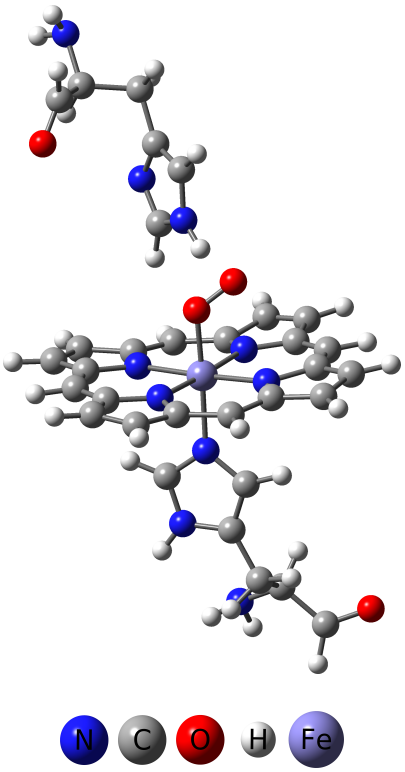

Figure 1.2. Molecular structure of $C_{32}H_{30}FeN_{10}O_4$

In order to solve our model, we implement a quantum Monte Carlo method developed for the multi-orbital Hubbard model to simulate the t_{2g} orbitals of Sr_2RuO_4 by Sakai et al. (2006). In this QMC method, there is a combined approach of series expansion to the partition function and Trotter decomposition. The reason of a combined method is the difficulty in the decoupling of the spin-flip and the pair-hopping terms. The renowned auxiliary-field QMC algorithm developed by Hirsch and Fye (1986) uses Trotter decomposition to discretize the imaginary-time interval, β, of the Boltzmann operator in the partition function, then the Hubbard-Stratonovich transformation (Hirsch (1983)) to decompose the interaction terms in order to get quadratic terms with respect to the electron creation and annihilation operators. The density-density type interactions in the intra- and inter-orbital Coulomb interactions along with the z-component of the Hund's coupling can be decoupled easily with Hubbard-Stratonovich transformation. However, the spin-flip and pair-hopping terms consist of off-diagonal terms with respect to the electron creation and annihilation operators, thus another transformation is required for these terms. This transformation exactly map the quartic terms in the spin-flip and pair-hopping terms to their quadratic ones (Rombouts et al. (1998)). In order to use this transforma-

tion, we need to expand the partition function in series and use a discretized version of the continuous-time QMC algorithm developed by Rombouts et al. (1999) to combine it with Hirsch-Fye QMC algorithm. We named this new algorithm as Hirsch-Fye + Series Expansion QMC (HF+SE QMC) introduced by Sakai et al. (2006).

There were several attempts to decouple the Hund's coupling term and to solve it within the framework of the dynamical mean field theory or QMC (Held and Vollhardt (1998); Motome and Imada (1997); Han (2004); Sakai et al. (2004)). These transformations have serious problems: sign problem, neglecting the equality of spins or the orbitals, orbital rotational symmetries, or works for some special cases. However, HF+SE QMC algoritm uses an exact discrete transformation to the Hund's coupling term. Therefore, this algorithm is an numerically exact solver to the problem after the results are extrapolated due to the errors caused by the time discretization and the series expansion.

CHAPTER 2

MULTI-ORBITAL ANDERSON IMPURITY MODEL

In this study, we will use multi-orbital Anderson Hamiltonian to model the transition metal impurities in organic molecules such as hemoglobin molecule. The construction of the model starts with the second-quantized Hamiltonian which includes kinetic energy of the electrons, ionic potential on them and the electron-electron interaction.

$$h_1(\mathbf{r}) = -\frac{\hbar^2}{2m}\nabla^2 + V_{ion}(\mathbf{r}) \tag{2.1}$$

$$h_2(\mathbf{r}, \mathbf{r}') = V_{ee}(\mathbf{r} - \mathbf{r}') \tag{2.2}$$

The second-quantized Hamiltonian is

$$\begin{aligned} H = &\sum_{\sigma} \int d\mathbf{r} \Psi_{\sigma}^{\dagger}(\mathbf{r}) \left[-\frac{\hbar^2}{2m}\nabla^2 + V_{ion}(\mathbf{r}) \right] \Psi_{\sigma}(\mathbf{r}) \\ &+ \frac{1}{2} \sum_{\sigma,\sigma'} \iint d\mathbf{r} d\mathbf{r}' \Psi_{\sigma}^{\dagger}(\mathbf{r}) \Psi_{\sigma'}^{\dagger}(\mathbf{r}') V_{ee}(\mathbf{r} - \mathbf{r}') \Psi_{\sigma'}(\mathbf{r}') \Psi_{\sigma}(\mathbf{r}) \end{aligned} \tag{2.3}$$

We can expand the field operators, $\Psi_{\sigma}(\mathbf{r})$, in terms of the Wannier orbitals for the host and the impurity orbitals as

$$\Psi_{\sigma}(\mathbf{r}) = \sum_{i} \varphi_i(\mathbf{r}) c_{i,\sigma} \tag{2.4}$$

where $c_{m,\sigma}$ is the annihilation operator for the host states and $d_{\nu,\sigma}$ is for the impurity states. In summation over i, the impurity orbitals are denoted as ν and host orbitals are m. After using 2.4, there are several terms as integrals in equation 2.3. We can define them separately to construct the model. The kinetic energies of the host and impurity orbitals

are

$$\varepsilon_m - \mu = \int d\mathbf{r}\varphi_m^*(\mathbf{r}) \left[-\frac{\hbar^2}{2m}\nabla^2 + V_{ion}(\mathbf{r}) \right] \varphi_m(\mathbf{r}) \tag{2.5}$$

$$\varepsilon_\nu - \mu = \int d\mathbf{r}\varphi_\nu^*(\mathbf{r}) \left[-\frac{\hbar^2}{2m}\nabla^2 + V_{ion}(\mathbf{r}) \right] \varphi_\nu(\mathbf{r}) \tag{2.6}$$

The hybridization terms between the host and the impurity orbitals, which indicates the hopping of electrons from host to impurity or impurity to host, are

$$V_{m\nu} = \int d\mathbf{r}\varphi_m^*(\mathbf{r}) \left[-\frac{\hbar^2}{2m}\nabla^2 + V_{ion}(\mathbf{r}) \right] \varphi_\nu(\mathbf{r}) \tag{2.7}$$

$$V_{\nu m} = \int d\mathbf{r}\varphi_\nu^*(\mathbf{r}) \left[-\frac{\hbar^2}{2m}\nabla^2 + V_{ion}(\mathbf{r}) \right] \varphi_m(\mathbf{r}) \tag{2.8}$$

The electron-electron interaction is defined on the impurity orbitals in this model. These integrals are defined in the following.

$$U = \iint d\mathbf{r}d\mathbf{r}'|\varphi_\nu^\dagger(\mathbf{r})|^2 V_{ee}(\mathbf{r}-\mathbf{r}')|\varphi_\nu(\mathbf{r}')|^2 \tag{2.9}$$

$$U' = \iint d\mathbf{r}d\mathbf{r}'|\varphi_\nu^\dagger(\mathbf{r})|^2 V_{ee}(\mathbf{r}-\mathbf{r}')|\varphi_{\nu'}(\mathbf{r}')|^2 \tag{2.10}$$

$$J = \iint d\mathbf{r}d\mathbf{r}'\varphi_\nu^\dagger(\mathbf{r})\varphi_{\nu'}^\dagger(\mathbf{r}')V_{ee}(\mathbf{r}-\mathbf{r}')\varphi_\nu(\mathbf{r}')\varphi_{\nu'}(\mathbf{r}) \tag{2.11}$$

$$J' = \iint d\mathbf{r}d\mathbf{r}'\varphi_\nu^\dagger(\mathbf{r})\varphi_\nu^\dagger(\mathbf{r}')V_{ee}(\mathbf{r}-\mathbf{r}')\varphi_{\nu'}(\mathbf{r}')\varphi_{\nu'}(\mathbf{r}) \tag{2.12}$$

The integrals other than U, U', J and J' are expected to be smaller than these integrals or to be zero. The real space rotations interchange the d orbitals to each other, in order to ensure this equality the integrals the results of the integrals U, U', J and J' should be related to each other by

$$U = U' + 2J \tag{2.13}$$

With this condition the Hamiltonian is rotationally invariant in real space, as well. If we take the Wannier orbitals real for impurity orbitals, then it holds $J' = J$. After these definition, we construct the multi-orbital Anderson Model with inter-orbital and intra-

orbital interaction including spin-flip and pair-hopping terms which is defined as

$$
\begin{aligned}
H = & \sum_{m,\sigma}(\varepsilon_m - \mu)c^{\dagger}_{m\sigma}c_{m\sigma} + \sum_{\nu,\sigma}(\varepsilon_\nu - \mu)d^{\dagger}_{\nu\sigma}d_{\nu\sigma} + \sum_{m,\nu,\sigma} V_{m\nu}\left(c^{\dagger}_{m\sigma}d_{\nu\sigma} + h.c.\right) \\
& + \sum_{\nu} U n_{\nu\uparrow}n_{\nu\downarrow} + \sum_{\nu>\nu',\sigma}\left[U' n_{\nu\sigma}n_{\nu',-\sigma} + (U'-J)\, n_{\nu\sigma}n_{\nu'\sigma}\right] \\
& + \sum_{\nu>\nu'} J(d^{\dagger}_{\nu\uparrow}d^{\dagger}_{\nu'\downarrow}d_{\nu\downarrow}d_{\nu'\uparrow} + d^{\dagger}_{\nu\uparrow}d^{\dagger}_{\nu\downarrow}d_{\nu'\downarrow}d_{\nu'\uparrow} + h.c.)
\end{aligned}
\tag{2.14}
$$

where $c^{\dagger}_{m\sigma}(c_{m\sigma})$ and $d^{\dagger}_{\nu\sigma}(d_{\nu\sigma})$ are creation(annihilation) operators for the host state m and the localized state at ν'th d orbital, σ spin. ε_m and ε_ν are the energies of the host and d states. $V_{m\nu}$ is the hybridization matrix elements between host and impurity orbitals. μ is the chemical potential and $n_{\nu\sigma}$ is the occupation number of the ν'th d orbital. U is the Coulomb repulsion between the d electron at the same impurity state, U' and $U'-J$ is the Coulomb interaction between the d electrons at the different impurity state with opposite spins and parallel spins. J is the Hund's coupling between the different orbital pairs. $U'-J$ term includes the z-component of the Hund's coupling. And the remaining part with J term is the x and y component of the Hund's coupling, which are the spin-flip and the pair-hopping terms.

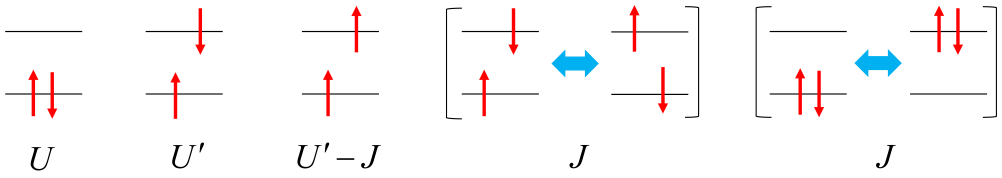

Figure 2.1. Visualization of $U, U', U'-J$ and J terms.

We can seperate the Hamiltonian into 3 parts for further calculations.

$$
\begin{aligned}
H_0 &= \sum_{m,\sigma}(\varepsilon_m - \mu)c^{\dagger}_{m\sigma}c_{m\sigma} + \sum_{\nu,\sigma}(\varepsilon_\nu - \mu)d^{\dagger}_{\nu\sigma}d_{\nu\sigma} + \sum_{m,\nu,\sigma} V_{m\nu}\left(c^{\dagger}_{m\sigma}d_{\nu\sigma} + h.c.\right) \\
H_U &= \sum_{\nu} U n_{\nu\uparrow}n_{\nu\downarrow} + \sum_{\nu>\nu',\sigma}\left[U' n_{\nu\sigma}n_{\nu',-\sigma} + (U'-J)\, n_{\nu\sigma}n_{\nu'\sigma}\right] \\
H_J &= \sum_{\nu>\nu'} J(d^{\dagger}_{\nu\uparrow}d^{\dagger}_{\nu'\downarrow}d_{\nu\downarrow}d_{\nu'\uparrow} + d^{\dagger}_{\nu\uparrow}d^{\dagger}_{\nu\downarrow}d_{\nu'\downarrow}d_{\nu'\uparrow} + h.c.)
\end{aligned}
\tag{2.15}
$$

2.1. The Effect of the SU(2) Invariant Hamiltonian in the Atomic Limit

The preservation of the orbital and spin rotational symmetries affect many of the aspects for our calculations. Although it exhibits a little difference in the total occupations of the orbitals, an apparent distinction in the total magnetization is seen from the calculations. In order to show that we have done simple calculations with hemoglobin molecule. After the parameters of the Anderson model are calculated from the DFT results (as in Kandemir et al. (2016)), the hybridization matrix elements are set to zero. In this way, the connection between the host and the impurity orbitals is lost, and the Hamiltonian consisting of only five 3d orbitals can be diagonalized.The energy eigenvalues of the 3d orbitals can be seen from the table 2.1. The comparisons (Figures: 2.2 and 2.4) show that the total magnetization varies with respect to the absence of spin-flip and pair-hopping terms.

Table 2.1. Energy eigenvalues of the 3d orbitals of the heme molecules in eV.

ε_ν	xy	xz	yz	$3z^2-r^2$	x^2-y^2
deoxyheme	-3.5048	-3.4912	-3.0422	-3.3714	-3.4368
oxyheme	-4.5551	-4.1687	-4.2150	-4.0599	-4.3048

For deoxy molecule in figure 2.2b we observed that the calculations with H_J exhibit lower magnetization values than the calculations without H_J at chemical potential values $\mu \approx -1.5$ eV and $\mu \approx 12.5$ eV. The effect of H_J is seen when the molecule starts to have higher magnetic moment values, and just before losing its magnetic moment. After these values of μ, there are sudden jumps in the magnetic moment values, $\langle n_{3d} \rangle$. Thus, H_J is more effective before these transitions. However, the total electron occupations of the 3d orbitals are $\langle n_{3d} \rangle \approx 2$ and $\langle n_{3d} \rangle \approx 8$ at $\mu \approx -1.5$ eV and $\mu \approx 12.5$ eV, and there are no apparent differences in the total electron numbers.

The expection value of H_J is nonzero just for these chemical potential two intervals from figure 2.3a. $\langle H_J \rangle \approx -0.3$ at chemical potentials $\mu \approx -1.5$ eV and $\mu \approx 12.5$ eV. When we compare $\langle H_J \rangle$ with the other parts of the Hamiltonian, the values $\langle H_U \rangle \approx 1.6$ and $\langle H_0 + H_U \rangle \approx -2.2$ at $\mu \approx -1.5$. The effect of H_J is comparable with the other parts of the Hamiltonian. For chemical potential $\mu \approx 12.5$ eV, however, the values $\langle H_U \rangle \approx 55.6$ and $\langle H_0 + H_U \rangle \approx -72.5$ seem much higher than $\langle H_J \rangle$ at that chemical potential. In fact,

the chemical potential and the Coulomb interaction terms add up for 5 orbitals, thus the values seem higher, but H_J is still effective as seen from total magnetic moment 2.2b.

For oxy molecule in figure 2.4 we observed the same behavior with the deoxy molecule, but at lower chemical potential values, $\mu \approx -2.5$ eV and $\mu \approx 11.5$ eV. The reason is that the calculations were carried out in the atomic limit. There is no hybridization between the host and the impurity orbitals. The presence of the oxygen molecule lowers the eigenenergies of the Fe(3d) orbitals by approximately 1 eV as in table 2.1, but its effect on the hosts cannot be seen because of the absence of hybridization. Therefore, in the atomic limit the same behavior is seen but at lower chemical potential values. H_J is effective just before the first dramatic increment in the total magnetic moments.

The expection value of H_J of oxyheme also exhibits the same behavior with the oxyheme in the atomic limit as seen from figure 2.4a. The expection values of H_U and $H_0 + H_U$ are the same but shifted with respect to chemical potential approximately 1 eV. The reason for the same behavior is not only eigenenergy differences of Fe(3d) orbitals approximately 1 eV between the two molecules, but also the similiarities in the closeness of the eigenenergies of each Fe(3d) orbital within each molecule.

Therefore, even in the atomic limit we saw that the effect of spin-flip and pair-hopping terms is not negligible, it can be effective where a transition occurs. It can contribute to the antiferromagnetic correlations since it lowers the magnetization on certain points in two of the molecules.

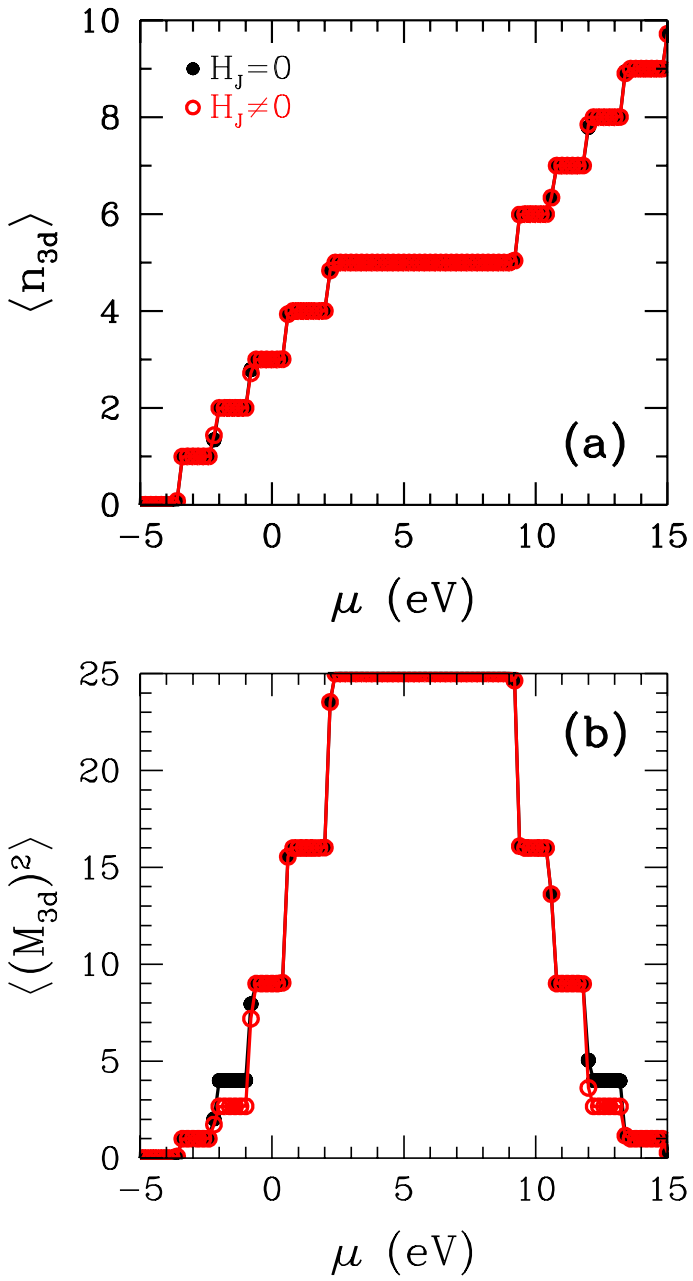

Figure 2.2. Exact diagonalization results for Fe(3d) orbitals in deoxyheme molecule in the atomic limit. Coulomb interaction between the 3d orbitals $U = 4$ eV and Hund's coupling $J = 0.9$ eV at temperature $T = 300$ K. Red empty dots indicates the calculations with H_J, black filled dots indicates the calculations without H_J. (a) Total occupation number of the Fe(3d) orbitals $\langle n_{3d} \rangle$ versus chemical potential μ. (b) Square of the total magnetic moment at the Fe(3d) orbitals $\langle (M_{3d})^2 \rangle$ versus chemical potential μ.

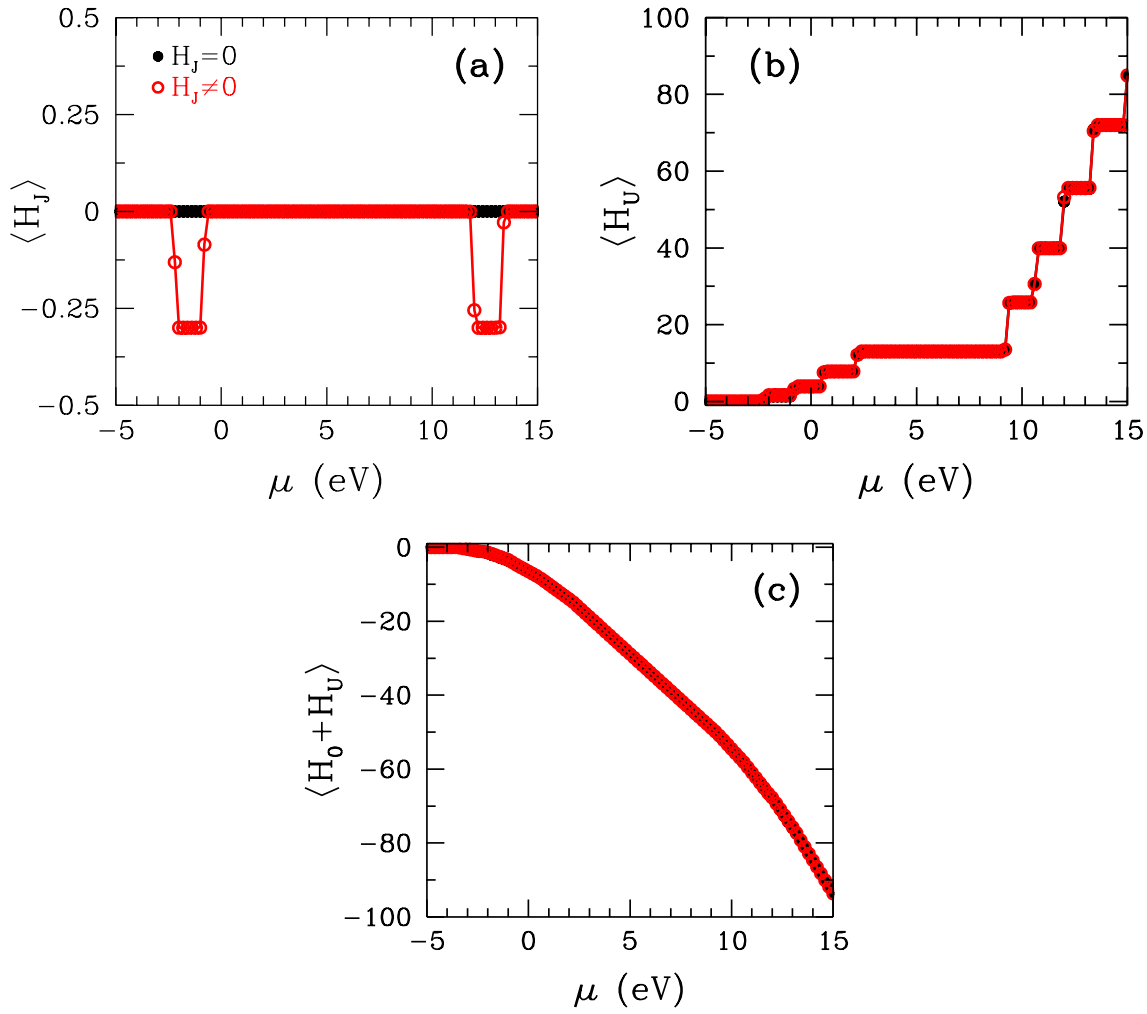

Figure 2.3. Exact diagonalization results for Fe(3d) orbitals in deoxyheme molecule in the atomic limit. Coulomb interaction between the 3d orbitals $U = 4$ eV and Hund's coupling $J = 0.9$ eV at temperature $T = 300$ K. Red empty dots indicates the calculations with H_J, black filled dots indicates the calculations without H_J. (a) Expectation value of H_J versus chemical potential μ. (b) Expectation value of H_U versus chemical potential μ. (c) Expectation value of $H_0 + H_U$ versus chemical potential μ.

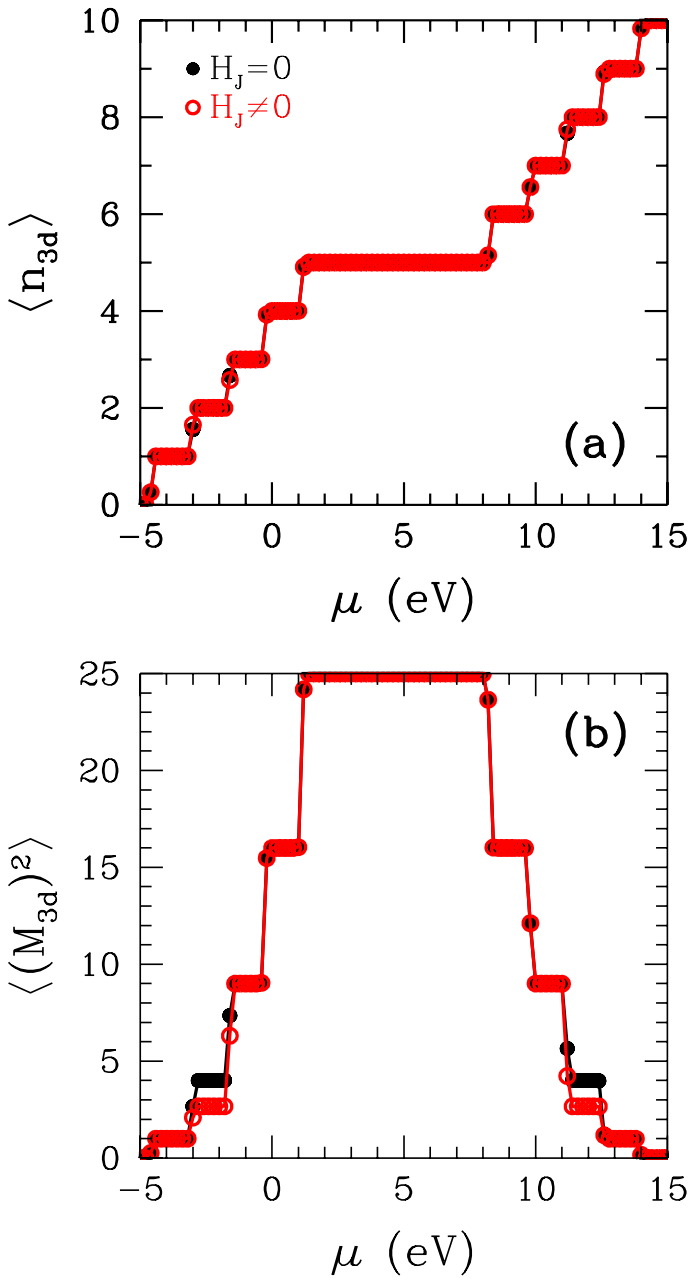

Figure 2.4. Exact diagonalization results for Fe(3d) orbitals in oxyheme molecule in the atomic limit. Coulomb interaction between the 3d orbitals $U = 4$ eV and Hund's coupling $J = 0.9$ eV at temperature $T = 300$ K. Red empty dots indicates the calculations with H_J, black filled dots indicates the calculations without H_J. (a) Total occupation number of the Fe(3d) orbitals $\langle n_{3d} \rangle$ versus chemical potential μ. (b) Square of the total magnetic moment at the Fe(3d) orbitals $\langle (M_{3d})^2 \rangle$ versus chemical potential μ.

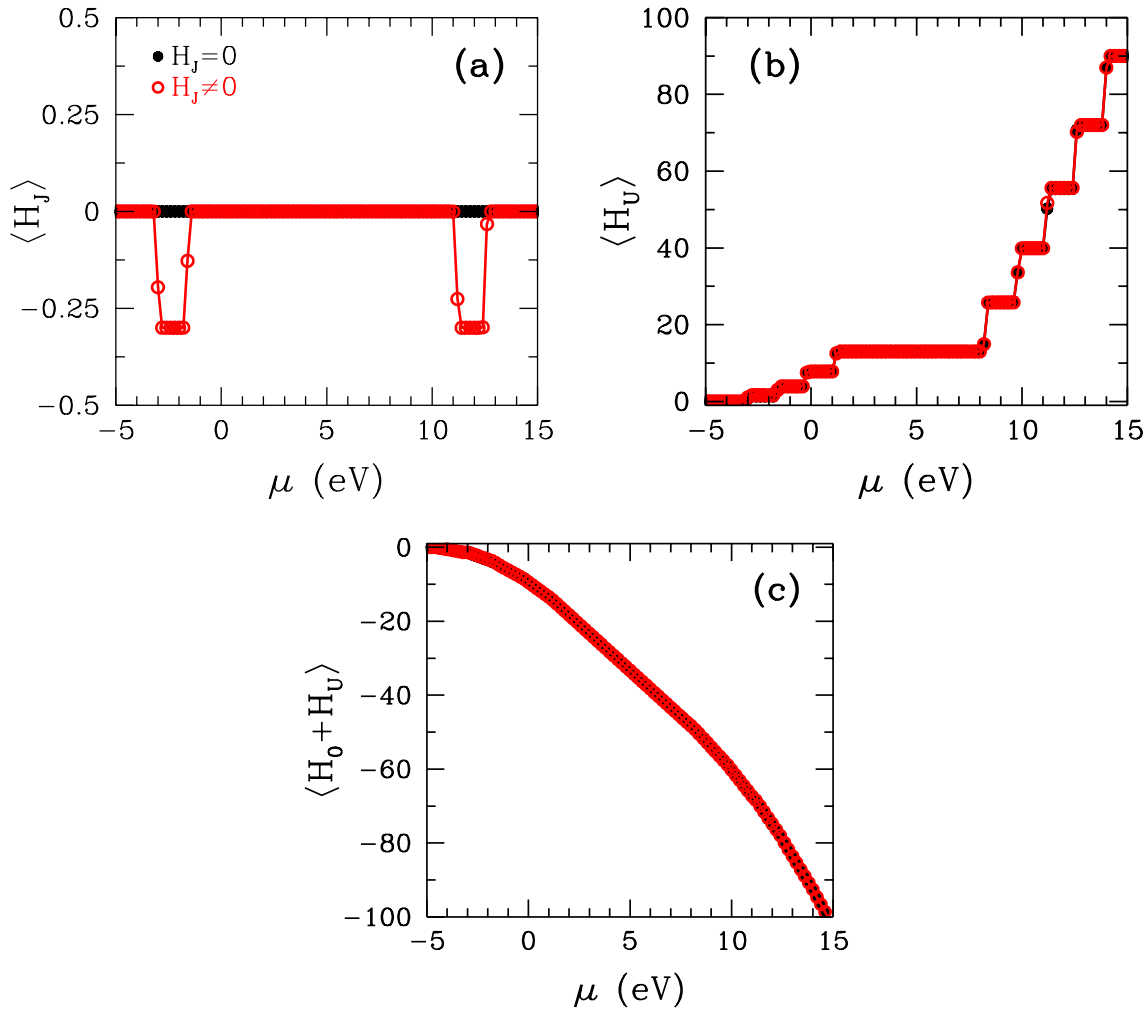

Figure 2.5. Exact diagonalization results for Fe(3d) orbitals in oxyheme molecule in the atomic limit. Coulomb interaction between the 3d orbitals $U = 4$ eV and Hund's coupling $J = 0.9$ eV at temperature $T = 300$ K. Red empty dots indicates the calculations with H_J, black filled dots indicates the calculations without H_J. (a) Expectation value of H_J versus chemical potential μ. (b) Expectation value of H_U versus chemical potential μ. (c) Expectation value of $H_0 + H_U$ versus chemical potential μ.

CHAPTER 3

MONTE CARLO METHOD

Monte Carlo method is a random sampling technique in order to estimate a probability distribution functions, or to obtain results for numerical integration problems. There are several methods, leading to the term "quantum Monte Carlo (QMC)", to sample the terms of partition in quantum mechanics in order to evaluate the expectation values of the observables (Gull et al. (2011)). Some methods involve sampling of the wavefunctions of the many-body systems (McMillan (1965); Ceperley et al. (1977); Foulkes et al. (2001)), while the others stochastically sample the action of the many-body system or the path integrals (Ceperley (1995); Sandvik and Kurkijärvi (1991)). On the other hand, auxiliary-field algorithms (Hirsch and Fye (1986)) discretize the Boltzmann operator or the action so that the partition function integral can be reformulated as a discrete sum over a high-dimensional configuration space, and these algorithms sample the terms of the discretized sum of the partition function instead of dealing with the whole configuration space.

This chapter covers the basic principles of the Monte Carlo integration and sampling from the configuration spaces.

3.1. Monte Carlo Integration

There are high-dimensional integrals and sums over high-dimensional configuration spaces to be solved in order to evaluate the properties of the thermodynamical systems. The basic numerical integration techniques, i.e. Simpson's Rule, are not sufficient when the dimensions of the integrals increase due to the fact that in these methods the error scales with the number of the integration points or the dimensionality of the integrals. For high-dimensional integrals, they are not efficient.

Monte Carlo integration, however, is not dependent on the dimensionality of the integrals. The elements of the integration domain are randomly sampled in Monte Carlo integration. For uniformly selected elements x_i of the configuration space C, any integral can be approximated as

$$\frac{1}{\Omega}\int_C f(x)dx = \lim_{N\to\infty}\frac{1}{N}\sum_{i=1}^{N} f(x_i) \tag{3.1}$$

where Ω is the volume of configuration space C. The statistical error, Δ, can be estimated as

$$\Delta = \sqrt{\frac{\mathrm{var} f}{N}} = \sqrt{\frac{\overline{f^2} - \overline{f}^2}{N-1}} \tag{3.2}$$

Therefore, the error of this method decreases with the number of samples, and it is independent of dimensionality of the integrals.

3.2. Importance Sampling

Calculation of the integrals with uniformly chosen random elements is not efficient for high-dimensional integrals. Instead, the elements which has more impact on the integral can be chosen with importance sampling and decrease the variance more quickly. The configurations can be generated with a general probability distribution $p(x)$ on configuration space C, where

$$\int_C p(x)dx = 1 \tag{3.3}$$

then equation 3.1 becomes

$$\langle f \rangle = \frac{1}{\Omega}\int_C \frac{f(x)}{p(x)}p(x)dx = \lim_{N\to\infty}\frac{1}{N}\sum_{i=1}^{N}\frac{f(x_i)}{p(x_i)} \tag{3.4}$$

and the integration error is

$$\Delta = \sqrt{\frac{\text{var}(f/p)}{N}} \tag{3.5}$$

The expectation value of an observable in a system in equilibrium can be calculated using the partition in statistical mechanics. The configurations can be generated according to their contribution to the partition function. The expectation value of an observable, A, is

$$\langle A \rangle = \frac{1}{Z} \int_C A(x)\rho(x)dx \tag{3.6}$$

where

$$Z = \int_C \rho(x)dx \tag{3.7}$$

In order to use importance sampling, equation 3.6 becomes

$$\langle A \rangle = \frac{1}{Z} \int_C A(x)\frac{\rho(x)}{p(x)}p(x)dx = \lim_{N\to\infty} \frac{\sum_{i=1}^{N} A(x_i)\frac{\rho(x_i)}{p(x_i)}}{\sum_{i=1}^{N} \frac{\rho(x_i)}{p(x_i)}} \tag{3.8}$$

3.3. Markov Process, Metropolis and Heat-bath Algorithms

There is a method called Markov process to generate the configurations according to their contribution to partition function or some probability distribution. In the Markov chain the configurations are generated randomly but their values are dependent on their previous values. The chain starts from a random elements $x_0 \in C$, and can be visualized as

$$x_0 \to x_1 \to x_2 \to \cdots \to x_k \to \ldots$$

These configurations are generated via the transition probabilities between the states x_k and x_{k+1}. To ensure that the probability distribution of the generated configurations asymptotically approaches the right probability distribution, the transition probabilities should satisfy detailed balance and ergodicity conditions. Ergodicity means that reaching any x from any configuration y should be possible in a finite number of steps in the Markov chain. To fulfill the detailed balance condition, the equation between the probability distribution $p(x)$ and transition matrix W_{xy} should be

$$\frac{W_{xy}}{W_{yx}} = \frac{p_y}{p_x} \tag{3.9}$$

Metropolis and heat-bath algorithms satisfies detailed balance condition. The transition matrix elements are splitted into two parts as proposal and acceptance parts (Gull et al. (2011)).

$$W_{xy} = W_{prop}(x \to y) W_{acc}(x \to y) \tag{3.10}$$

Using equation 3.9 detailed balance condition becomes

$$\frac{W_{acc}(x \to y)}{W_{acc}(y \to x)} = \frac{p_y}{p_x} \frac{W_{prop}(y \to x)}{W_{prop}(x \to y)} \tag{3.11}$$

To satisfy that the Metropolis algorithm then reads

$$W_{acc}^{metropolis}(x \to y) = \min\left\{1, \frac{p_y}{p_x} \frac{W_{prop}(y \to x)}{W_{prop}(x \to y)}\right\} \tag{3.12}$$

while the heat-bath algorithm is

$$W_{acc}^{heat-bath}(x \to y) = \frac{P}{1+P} \tag{3.13}$$

where

$$P = \frac{p_y}{p_x} \frac{W_{prop}(y \to x)}{W_{prop}(x \to y)} \tag{3.14}$$

CHAPTER 4

HIRSCH-FYE + SERIES EXPANSION ALGORITHM

In this chapter, we present detailed derivations of the steps of the HF+SE QMC algorithm. We start with the partition function for the measurements in the finite temperature. After the series expansion of the Boltzmann factor, the transformation formulas are applied to the two-body interaction terms. These decoupling formulas map the quantum mechanical problem to its exactly classical one, an extra dimension to the problem in return. Thus, we can classically sample the terms of the partition function with Monte Carlo methods. To perform the physical measurements, we use a Green's function method. In order to use it in the algorithm, for decoupling and calculating the Green's functions, we need to make one more modification to the 3 parts of the Hamiltonian. Thus, H_0, H_U and H_J becomes

$$H_0 = \sum_{m,\sigma}(\varepsilon_m - \mu)c^\dagger_{m\sigma}c_{m\sigma} + \sum_{\nu,\sigma}(\varepsilon_\nu - \mu)d^\dagger_{\nu\sigma}d_{\nu\sigma} + \sum_{m,\nu,\sigma} V_{m\nu}\left(c^\dagger_{m\sigma}d_{\nu\sigma} + h.c.\right) + \frac{U}{2}\sum_{\nu,\sigma} n_{\nu\sigma} + \sum_{\nu>\nu',\sigma}\left[\frac{U'}{2}(n_{\nu\sigma} + n_{\nu',-\sigma}) + \frac{(U'-J)}{2}(n_{\nu\sigma} + n_{\nu'\sigma})\right] \tag{4.1}$$

$$H_U = \sum_{\nu}\left[Un_{\nu\uparrow}n_{\nu\downarrow} - \frac{U}{2}(n_{\nu\uparrow} + n_{\nu\downarrow})\right] + \sum_{\nu>\nu',\sigma}\left[U'n_{\nu\sigma}n_{\nu',-\sigma} - \frac{U'}{2}(n_{\nu\sigma} + n_{\nu',-\sigma})\right] + \sum_{\nu>\nu',\sigma}\left[(U'-J)n_{\nu\sigma}n_{\nu'\sigma} - \frac{(U'-J)}{2}(n_{\nu\sigma} + n_{\nu'\sigma})\right] \tag{4.2}$$

$$H_J = \sum_{\nu>\nu'} J(d^\dagger_{\nu\uparrow}d^\dagger_{\nu'\downarrow}d_{\nu\downarrow}d_{\nu'\uparrow} + d^\dagger_{\nu\uparrow}d^\dagger_{\nu\downarrow}d_{\nu'\downarrow}d_{\nu'\uparrow} + h.c.) \tag{4.3}$$

The partition function is

$$\begin{aligned} Z &= \mathrm{Tr} e^{-\beta \hat{H}} \\ &= \mathrm{Tr} e^{-\beta(H_0+H_U+H_J)} \end{aligned} \tag{4.4}$$

We add and subtract a constant, γ, to the Hamiltonian in order to make a discrete decomposition to H_J. We split the Hamiltonian into two parts as H_1 and H_2 where

$$H_1 = H_0 + H_U + \frac{\gamma}{\beta} \tag{4.5}$$

$$H_2 = H_J - \frac{\gamma}{\beta} \tag{4.6}$$

The partition function becomes

$$\begin{aligned} Z &= \mathrm{Tr} e^{-\beta(H_1+H_2)} \\ &= e^{-\gamma} \mathrm{Tr} e^{-\beta(H_0+H_U)+(\gamma-\beta H_J)} \end{aligned} \tag{4.7}$$

In the following sections, we drop the constant term, $e^{-\gamma}$, in the partition function since it is just a constant and does not change the physics.

4.1. Series Expansion of the Boltzmann Factor

We expand the Boltzmann operator, $e^{-\beta \hat{H}}$ with respect to $\gamma - \beta H_J$.

$$\begin{aligned} e^{-\beta(H_0+H_U)+(\gamma-\beta H_J)} &= e^{-\beta(H_0+H_U)} \\ &+ \sum_{k=1}^{\infty} \int_0^1 d\tau_k \cdots \int_0^{\tau_2} d\tau_1 \\ &\times \prod_{i=1}^{k} \left[e^{-\tau_i \beta(H_0+H_U)} (\gamma - \beta H_J) e^{\tau_i \beta(H_0+H_U)} \right] e^{-\beta(H_0+H_U)} \end{aligned} \tag{4.8}$$

Derivation of this expansion is given in Appendix A. After discretization of the integrals for numerical calculations, the equation becomes

$$\begin{aligned} e^{-\beta H} &= e^{-\beta(H_0+H_U)} \\ &+ \sum_{k=1}^{\infty} L^{-k} \sum_{j_k=1}^{L} \cdots \sum_{j_1=1}^{j_2} \prod_{i=1}^{k} \left[e^{-j_i \Delta\tau (H_0+H_U)} (\gamma - \beta H_J) e^{j_i \Delta\tau (H_0+H_U)} \right] \\ &\times e^{-\beta(H_0+H_U)} + O(\Delta\tau) \end{aligned} \tag{4.9}$$

where

$$\Delta\tau = \beta \Big/ L. \tag{4.10}$$

The summations in equation 4.9 are cut at L. This expression is valid only for the condition $\langle k \rangle \ll L$. To reduce the computation time and the number of configurations, the terms having consecutive $\gamma - \beta H_J$ in the same imaginary-time interval is changed into approximate terms. We use the notation

$$\chi \equiv \gamma - \beta H_J \tag{4.11}$$

After these changes equation 4.9 becomes

$$e^{-\beta H} = \sum_{r_1, r_2, \cdots, r_L = 0,1} F(k; r_1, r_2, \cdots, r_L) \prod_{\ell=1}^{L} \left[e^{-\Delta\tau (H_0+H_U)} \chi_{r_\ell} \right] + O(\Delta\tau) \tag{4.12}$$

where

$$k = \sum_{\ell=1}^{L} r_\ell \quad \text{and} \quad \chi_0 = 1. \tag{4.13}$$

F is a positive weight factor. Detailed derivation of F terms is given in Appendix B.

We use Trotter approximation to decompose H_U and to separate it from H_0.

$$e^{-\Delta\tau(H_0+H_U)} \cong e^{-\Delta\tau H_0} e^{-\Delta\tau H_U} + O(\Delta\tau^2) \tag{4.14}$$

Now, we can use discrete Hubbard-Stratonovich transformation to decompose $e^{-\Delta\tau H_U}$. The Hubbard-Stratonovich transformation is following.

$$e^{-\Delta\tau V\left[n_\nu n_{\nu'} - \frac{1}{2}(n_\nu + n_{\nu'})\right]} = \frac{1}{2} \sum_{S_V=\pm 1} e^{\lambda_V S_V (n_\nu - n_{\nu'})} \quad for \quad V \geq 0 \tag{4.15}$$

where

$$\cosh(\lambda_V) = e^{\frac{1}{2}\Delta\tau V} \tag{4.16}$$

Thus, the decomposition of $e^{-\Delta\tau H_U}$ can be done with Hubbard-Stratonovich transformation.

$$\begin{aligned} e^{-\Delta\tau H_U} = \exp\Bigg\{ -\Delta\tau \Bigg[& \sum_\nu \left(U n_{\nu\uparrow} n_{\nu\downarrow} - \frac{U}{2}(n_{\nu\sigma} + n_{\nu'\sigma}) \right) \\ & + \sum_{\nu>\nu',\sigma} \left(U' n_{\nu\sigma} n_{\nu',-\sigma} - \frac{U'}{2}(n_{\nu\sigma} + n_{\nu',-\sigma}) \right) \\ & + \sum_{\nu>\nu',\sigma} \left((U'-J) n_{\nu\sigma} n_{\nu'\sigma} - \frac{(U'-J)}{2}(n_{\nu\sigma} + n_{\nu'\sigma}) \right) \Bigg] \Bigg\} \end{aligned} \tag{4.17}$$

After the discrete Hubbard-Stratonovich transformation, equation 4.17 becomes as in

Hirsch and Fye (1986)

$$e^{-\Delta\tau H_U(\ell)} = \frac{1}{2^{(2N_d-1)N_d}} \sum_{\{S^U_{\nu,\ell}=\pm1\}} \sum_{\{S^{U'}_{\nu\nu',\ell}=\pm1\}} \sum_{\{S^{U'-J}_{\nu\nu',\ell,\sigma}=\pm1\}} \exp\left\{ \sum_{\nu=1}^{N_d} \sum_{\sigma} \sigma\lambda_1 S^U_{\nu,\ell} n_{\nu\sigma} + \sum_{\nu=1}^{N_d} \sum_{\substack{\nu'=1 \\ \nu'\neq\nu}}^{N_d} \lambda_2 S^{U'}_{\nu\nu',\ell}(n_{\nu\uparrow} + n_{\nu\downarrow}) + \sum_{\nu=1}^{N_d} \sum_{\substack{\nu'=1 \\ \nu'\neq\nu}}^{N_d} \sum_{\sigma} \lambda_3 S^{U'-J}_{\nu\nu',\ell,\sigma}(n_{\nu\sigma} - n_{\nu'\sigma}) \right\} \tag{4.18}$$

where

$$\cosh(\lambda_1) = e^{\frac{1}{2}\Delta\tau U} \tag{4.19}$$

$$\cosh(\lambda_2) = e^{\frac{1}{2}\Delta\tau U'} \tag{4.20}$$

$$\cosh(\lambda_3) = e^{\frac{1}{2}\Delta\tau (U'-J)} \tag{4.21}$$

and N_d is the number of the d orbitals. There are $(2N_d - 1)N_d$ density-density type interactions which are transformed, leaving $1/2$ for each after the transformation. We can write equation 4.18 in terms of $W_{\nu\sigma}(\ell)$'s

$$e^{-\Delta\tau H_U(\ell)} = \frac{1}{2^{(2N_d-1)N_d}} \sum_{\{S^U_{\nu,\ell}=\pm1\}} \sum_{\{S^{U'}_{\nu\nu',\ell}=\pm1\}} \sum_{\{S^{U'-J}_{\nu\nu',\ell,\sigma}=\pm1\}} \exp\left\{ \sum_{\nu,\sigma} W_{\nu\sigma}(\ell) n_{\nu\sigma} \right\} \tag{4.22}$$

where

$$W_{\nu\sigma}(\ell) = W^U_{\nu\sigma}(\ell) + W^{U'}_{\nu\sigma}(\ell) + W^{U'-J}_{\nu\sigma}(\ell) \tag{4.23}$$

$$W^U_{\nu\sigma}(\ell) = \sigma\lambda_1 S^U_{\nu,\ell} \tag{4.24}$$

$$W^{U'}_{\nu\uparrow} = \lambda_2 \sum_{\substack{\nu'=1 \\ \nu'\neq\nu}}^{N_d} S^{U'}_{\nu\nu',\ell}$$
$$W^{U'}_{\nu\downarrow} = -\lambda_2 \sum_{\substack{\nu'=1 \\ \nu'\neq\nu}}^{N_d} S^{U'}_{\nu'\nu,\ell} \tag{4.25}$$

$$W^{U'-J}_{\nu\sigma} = \lambda_3 \sum_{\nu'=1}^{\nu-1} S^{U'-J}_{\nu\nu',\ell,\sigma} - \lambda_3 \sum_{\nu'=\nu+1}^{N_d} S^{U'-J}_{\nu'\nu,\ell,\sigma} \tag{4.26}$$

Here we can make one more simplification to ease the notation for configurations $\{S^{U}_{\nu,\ell}, S^{U'}_{\nu\nu',\ell}, S^{U'-J}_{\nu\nu',\ell,\sigma}\}$ which is

$$\{\widetilde{S}_\ell\} \equiv \{S^{U}_{\nu,\ell}, S^{U'}_{\nu\nu',\ell}, S^{U'-J}_{\nu\nu',\ell,\sigma}\} \tag{4.27}$$

Using equation 4.22, equation 4.12 becomes

$$e^{-\beta H} = \frac{1}{2^{(2N_d-1)N_dL}} \sum_{\{r_\ell=0,1\}} \sum_{\{\widetilde{S}_\ell=\pm 1\}} F(k; r_1, r_2, \cdots, r_L)$$
$$\times \prod_{\ell=1}^{L} \left[e^{-\Delta\tau H_0} e^{\sum_{\nu,\sigma} W_{\nu\sigma}(\ell) n_{\nu\sigma}} \chi_{r_\ell} \right] + O(\Delta\tau) \tag{4.28}$$

Since H_0, H_U and H_J are separated out, we can decompose $\chi(= \gamma - \beta H_J)$ now. Firstly, we need to decompose χ_{r_ℓ} into all distinct two-orbital pairs as in Sakai et al. (2006).

$$\gamma - \beta H_J(\ell) = \sum_{\nu>\nu'} \left[\gamma^{\nu\nu'} - \beta H_J^{\nu\nu'}(\ell) \right] \tag{4.29}$$

where

$$\gamma = \sum_{\nu>\nu'} \gamma^{\nu\nu'} \tag{4.30}$$

Decomposition of H_J is following as in Appendix C;

$$\gamma^{\nu\nu'} - \beta H_J^{\nu\nu'}(\ell) = \frac{\gamma^{\nu\nu'} - \beta J}{8} \sum_{\{q_\ell^{\nu\nu'}, t_{\uparrow\ell}^{\nu\nu'}, t_{\downarrow\ell}^{\nu\nu'} = \pm 1\}} \times \prod_\sigma \exp\left\{\lambda_4 \left[\sigma q_\ell^{\nu\nu'} f_\sigma^{\nu\nu'} + t_{\sigma\ell}^{\nu\nu'}(n_{\nu\sigma} + n_{\nu'\sigma} - 1)\right]\right\} \tag{4.31}$$

where

$$H_J^{\nu\nu'} = J f_\uparrow^{\nu\nu'} f_\downarrow^{\nu\nu'} \tag{4.32}$$

$$f_\sigma^{\nu\nu'} = d_{\nu\sigma}^\dagger d_{\nu'\sigma} + d_{\nu'\sigma}^\dagger d_{\nu\sigma} \tag{4.33}$$

$$\lambda_4 = \frac{1}{2} \ln \frac{1+\kappa}{1-\kappa} \tag{4.34}$$

$$\kappa = \sqrt{\frac{\beta J}{\gamma^{\nu\nu'}}} < 1 \tag{4.35}$$

Using equation 4.29 and 4.31 together, we obtain the decomposition for χ_{r_ℓ} and it is

$$\gamma - \beta H_J(\ell) = \sum_{\nu > \nu'} \sum_{\{q_\ell^{\nu\nu'}, t_{\uparrow\ell}^{\nu\nu'}, t_{\downarrow\ell}^{\nu\nu'}\} = \pm 1} Q_{r_\ell}^{\nu\nu'} \tag{4.36}$$

where

$$Q_{r_\ell}^{\nu\nu'} = \frac{\gamma^{\nu\nu'} - \beta J}{8} \prod_\sigma e^{\lambda_4 \left[\sigma q_\ell^{\nu\nu'} f_\sigma^{\nu\nu'} + t_{\sigma\ell}^{\nu\nu'}(n_{\nu\sigma} + n_{\nu'\sigma} - 1)\right]} \tag{4.37}$$

Using what we find after the decomposition of χ_{r_ℓ}, the final form of the Boltzmann operator is

$$e^{-\beta H} = \frac{1}{2^{(2N_d - 1)N_d L}} \sum_{\{r_\ell = 0, 1\}} \sum_{\{\widetilde{S}_\ell = \pm 1\}} \sum_{\substack{\eta > \eta', \\ \{q_\ell^{\eta\eta'}, t_{\uparrow\ell}^{\eta\eta'}, t_{\downarrow\ell}^{\eta\eta'} = \pm 1\}}} F(k; r_1, r_2, \cdots, r_L) \times \prod_{\ell=1}^{L} \left[e^{-\Delta\tau H_0} e^{\sum_{\nu,\sigma} W_{\nu\sigma}(\ell) n_{\nu\sigma}} Q_{r_\ell}^{\eta\eta'}\right] + O(\Delta\tau) \tag{4.38}$$

where

$$Q_{r_\ell}^{\eta\eta'} = \begin{cases} 1 & \text{if} \quad r_\ell = 0 \\ \frac{\gamma^{\eta\eta'} - \beta J}{8} \prod_\sigma e^{\lambda_4 \left[\sigma q_\ell^{\eta\eta'} f_\sigma^{\eta\eta'} + t_{\sigma\ell}^{\eta\eta'} (n_{\eta\sigma} + n_{\eta'\sigma} - 1)\right]} & \text{if} \quad r_\ell = 1 \end{cases} \tag{4.39}$$

and

$$k = \sum_{\ell=1}^{L} r_\ell \tag{4.40}$$

In equation 4.38 we changed the notation for $Q_{r_\ell}^{\nu\nu'}$ term (ν, ν' to η, η') and we used the fact that expanding the ℓ multiplication with "$\eta > \eta'$" summation being inside of it gives different pairs of orbitals multiplied in different terms of the summation. We expanded the ℓ multiplication and then took the "$\eta > \eta'$" summation out of the ℓ multiplication. This means that in different imaginary-time slices there can be different pairs of orbitals active in $Q_{r_\ell}^{\eta\eta'}$ term.

4.2. Partition Function

Before calculating the partition function, we make other simplifications to ease the notations. We change $\eta\eta'$ pair notations and configurations obtained from 4.31, $\{q_\ell^{\eta\eta'}, t_{\uparrow\ell}^{\eta\eta'}, t_{\downarrow\ell}^{\eta\eta'}\}$. According to this change

$$\alpha \equiv \eta\eta' \tag{4.41}$$

$$\sum_\alpha \equiv \sum_{\eta > \eta'} \tag{4.42}$$

$$\{q_\ell^\alpha, t_{\uparrow\ell}^\alpha, t_{\downarrow\ell}^\alpha\} \equiv \{q_\ell^{\eta\eta'}, t_{\uparrow\ell}^{\eta\eta'}, t_{\downarrow\ell}^{\eta\eta'}\} \tag{4.43}$$

$$\{P_\ell^\alpha\} \equiv \{q_\ell^\alpha, t_{\uparrow\ell}^\alpha, t_{\downarrow\ell}^\alpha\} \tag{4.44}$$

α stands for the orbitals pairs on which H_J is acting and $\{P_\ell^\alpha\}$ is for the configurations $\{q_\ell^{\eta\eta'}, t_{\uparrow\ell}^{\eta\eta'}, t_{\downarrow\ell}^{\eta\eta'}\}$. Thus, the partition function is

$$\begin{aligned} Z &= \mathrm{Tr} e^{-\beta H} \\ &= \frac{1}{2^{(2N_d-1)N_d L}} \sum_{\{r_\ell=0,1\}} \sum_{\{\widetilde{S}_\ell=\pm 1\}} \sum_{\alpha} \sum_{\{P_\ell^\alpha \pm 1\}} F(k; r_1, r_2, \cdots, r_L) \\ &\times \mathrm{Tr} \prod_{\ell=1}^{L} \left[e^{-\Delta\tau H_0} e^{\sum_{\nu,\sigma} W_{\nu\sigma}(\ell) n_{\nu\sigma}} Q_{r_\ell}^\alpha \right] + O(\Delta\tau) \end{aligned} \tag{4.45}$$

We can drop another constant term, $1/2^{(2N_d-1)N_d L}$, from the partition function. Let us focus on the trace over fermion degrees of freedom.

$$\mathrm{Tr} \prod_{\ell=1}^{L} \left[e^{-\Delta\tau H_0} e^{\sum_{\nu,\sigma} W_{\nu\sigma}(\ell) n_{\nu\sigma}} Q_{r_\ell}^\alpha \right] \tag{4.46}$$

This trace has three parts to evaluate. First part is coming from H_0, second part is coming from H_U and the third part is coming from $\gamma - \beta H_J$. First part is represented as

$$e^{-\Delta\tau H_0} \tag{4.47}$$

The second part is

$$e^{\sum_{\nu,\sigma} W_{\nu\sigma}(\ell) n_{\nu\sigma}} = e^{\sum_{\nu,\sigma} d_{\nu\sigma}^\dagger W_{\nu\sigma}(\ell) d_{\nu\sigma}} \tag{4.48}$$

And the third part is

$$\begin{aligned} Q_{r_\ell}^\alpha &= \frac{\gamma^\alpha - \beta J}{8} \prod_\sigma e^{\lambda_4 \left[\sigma q_\ell^\alpha f_\sigma^\alpha + t_{\sigma\ell}^\alpha (n_{\eta\sigma} + n_{\eta'\sigma} - 1) \right]} \\ &= \frac{\gamma^\alpha - \beta J}{8} \prod_\sigma e^{-\lambda_4 t_{\sigma\ell}^\alpha} e^{\left[d_{\eta\sigma}^\dagger \left(\lambda_4 \sigma q_\ell^\alpha \right) d_{\eta'\sigma} + d_{\eta'\sigma}^\dagger \left(\lambda_4 \sigma q_\ell^\alpha \right) d_{\eta\sigma} + d_{\eta\sigma}^\dagger \left(\lambda_4 t_{\sigma\ell}^\alpha \right) d_{\eta\sigma} + d_{\eta'\sigma}^\dagger \left(\lambda_4 t_{\sigma\ell}^\alpha \right) d_{\eta'\sigma} \right]} \end{aligned} \tag{4.49}$$

In equation 4.49, $\frac{\gamma^{\alpha}-\beta J}{8}e^{-\lambda_4(t_{\uparrow\ell}+t_{\downarrow\ell})}$ is just a constant with respect to the trace over fermion degrees of freedom. Therefore, we can take this terms out of the trace. Let us define the $N_d \times N_d$ matrices

$$[W_\sigma(\ell)]_{\nu_1,\nu_2} = W_{\nu_1\sigma}(\ell)\delta_{\nu_2,\nu_1} \tag{4.50}$$

$$[T^{\alpha}_{\sigma}(\ell)]_{\nu_1,\nu_2} = \lambda_4\sigma q^{\alpha}_{\ell}\left(\delta_{\nu_1,\eta}\delta_{\nu_2,\eta'} + \delta_{\nu_1,\eta'}\delta_{\nu_2,\eta}\right) + \lambda_4 t^{\alpha}_{\sigma\ell}\left(\delta_{\nu_1,\eta}\delta_{\nu_2,\eta} + \delta_{\nu_1,\eta'}\delta_{\nu_2,\eta'}\right) \tag{4.51}$$

The dimension of these matrices is $N_d \times N_d$ since the interaction part of the Hamiltonian includes only N_d impurity orbitals. Using these matrices we can easily take the trace over fermion degrees of freedom. The trace becomes

$$\begin{aligned}\mathrm{Tr}\prod_{\sigma}\prod_{\ell=1}^{L}\left[e^{-\Delta\tau H_0}e^{\sum_{\nu,\nu'} d^{\dagger}_{\nu\sigma}[W_\sigma(\ell)]_{\nu,\nu'}d_{\nu'\sigma}}e^{\sum_{\nu,\nu'} d^{\dagger}_{\nu\sigma}[T^{\alpha}_{\sigma}(\ell)]_{\nu,\nu'}d_{\nu'\sigma}}\right] = \\ \prod_{\sigma}\det\left[I + B^{\sigma}_{L}B^{\sigma}_{L-1}\cdots B^{\sigma}_{1}\right]\end{aligned} \tag{4.52}$$

where

$$B^{\sigma}_{\ell} = \begin{cases} e^{-\Delta\tau K}e^{W_\sigma(\ell)}e^{T^{\alpha}_{\sigma}(\ell)} & \text{for} \quad r_\ell = 1 \\ e^{-\Delta\tau K}e^{W_\sigma(\ell)} & \text{for} \quad r_\ell = 0 \end{cases} \tag{4.53}$$

where K is the kinetic part of the Hamiltonian. Calculation of the trace can be found in Appendix D. Let us define the product of the matrices $e^{W_\sigma(\ell)}$ and $e^{T^{\alpha}_{\sigma}(\ell)}$ by $\Lambda_\sigma(\ell)$.

$$\Lambda_\sigma(\ell) = e^{W_\sigma(\ell)}e^{T^{\alpha}_{\sigma}(\ell)} \tag{4.54}$$

By using these results, the partition function becomes

$$Z = \sum_{\{r_\ell=0,1\}}\sum_{\{\widetilde{S}_\ell=\pm1\}}\sum_{\alpha}\sum_{\{P^{\alpha}_{\ell}\pm1\}}\widetilde{F}(\{r_\ell\})\prod_{\sigma}\det\left[I + B^{\sigma}_{L}B^{\sigma}_{L-1}\cdots B^{\sigma}_{1}\right] \tag{4.55}$$

where

$$B_\ell^\sigma = e^{-\Delta\tau K}\Lambda_\sigma(\ell) \tag{4.56}$$

$$\Lambda_\sigma(\ell) = \begin{cases} e^{W_\sigma(\ell)}e^{T_\sigma^\alpha(\ell)} & \text{for} \quad r_\ell = 1 \\ e^{W_\sigma(\ell)} & \text{for} \quad r_\ell = 0 \end{cases} \tag{4.57}$$

$$\widetilde{F}(\{r_\ell\}) = F(k; r_1, \cdots, r_L)\left(\frac{\widetilde{\gamma} - \beta J}{8}\right)^k \exp\left\{-\lambda_4 \sum_{\ell=1}^{L}\left(t_{\uparrow\ell} + t_{\downarrow\ell}\right)\delta_{r_\ell,1}\right\} \tag{4.58}$$

$$k = \sum_{\ell=1}^{L} r_\ell \tag{4.59}$$

$$\{P_\ell^\alpha\} \equiv \{q_\ell^\alpha, t_{\uparrow\ell}^\alpha, t_{\downarrow\ell}^\alpha\} \tag{4.60}$$

$$\{\widetilde{S}_\ell\} \equiv \{S_{\nu,\ell}^U, S_{\nu\nu',\ell}^{U'}, S_{\nu\nu',\ell,\sigma}^{U'-J}\} \tag{4.61}$$

and α were indicated as the orbital pairs $\eta\eta'$ on which the H_J is acting. Recall that the α summation has the condition $\eta > \eta'$. In equation 4.58, we took the weights of the orbital pairs coming from $\gamma - \beta H_J$ term equal. Thus, we set γ^α as constant, $\widetilde{\gamma}$.

$$\gamma = \sum_\alpha \widetilde{\gamma} \tag{4.62}$$

Furthermore, determinants of the products of B_ℓ^σ being $N_d \times N_d$ matrices can be repre-

sented as the determinants of $N_d \cdot L \times N_d \cdot L$ matrices,

$$\prod_{\sigma} \det \left[I + B_L^{\sigma} B_{L-1}^{\sigma} \cdots B_1^{\sigma} \right] = \det M_{\uparrow} M_{\downarrow} \tag{4.63}$$

where

$$M_{\sigma} = \begin{bmatrix} I & 0 & \cdots & & & B_L^{\sigma} \\ -B_1^{\sigma} & I & 0 & & & 0 \\ 0 & -B_2^{\sigma} & I & & & \vdots \\ \vdots & \vdots & \vdots & \ddots & & \vdots \\ & & & & I & 0 \\ 0 & 0 & \cdots & 0 & -B_{L-1}^{\sigma} & I \end{bmatrix}_{N_d \cdot L \times N_d \cdot L} \tag{4.64}$$

and

$$G^{\sigma} = [M_{\sigma}]^{-1} \tag{4.65}$$

Relation between the single particle Green's functions and M_σ matrices is in Appendix D.

4.3. $\Lambda_\sigma(\ell)$ Matrices

Let us look at the form of $\Lambda_\sigma(\ell)$ matrices.

$$\Lambda_{\sigma}(\ell) = e^{W_{\sigma}(\ell)} e^{T_{\sigma}^{\alpha}(\ell)} \tag{4.66}$$

$$e^{W_\sigma(\ell)} = \begin{bmatrix} e^{W_{1,\sigma}(\ell)} & & & & 0 \\ & e^{W_{2,\sigma}(\ell)} & & & \\ & & \ddots & & \\ & & & e^{W_{N_d-1,\sigma}(\ell)} & \\ 0 & & & & e^{W_{N_d,\sigma}(\ell)} \end{bmatrix}_{N_d \times N_d} \tag{4.67}$$

We keep in mind that $\Lambda_\sigma(\ell) = e^{W_\sigma(\ell)}$ if $r_\ell = 0$. However, $T^\alpha_\sigma(\ell)$ has only four non-zero elements.

$$T^\alpha_\sigma(\ell) = \begin{bmatrix} 0 & & & & & & 0 \\ & \ddots & \overset{\boldsymbol{\eta',\eta'}}{\downarrow} & & \overset{\boldsymbol{\eta',\eta}}{\downarrow} & & \\ & & \lambda_4 t^\alpha_{\sigma\ell} & \cdots & \lambda_4 \sigma q^\alpha_\ell & & \\ & & \vdots & & \vdots & & \\ & & \lambda_4 \sigma q^\alpha_\ell & \cdots & \lambda_4 t^\alpha_{\sigma\ell} & & \\ & & \underset{\boldsymbol{\eta,\eta'}}{\uparrow} & & \underset{\boldsymbol{\eta,\eta}}{\uparrow} & \ddots & \\ 0 & & & & & & 0 \end{bmatrix}_{N_d \times N_d} \tag{4.68}$$

Exponential of this matrix is quite simple.

$$e^{T^\alpha_\sigma(\ell)} = \begin{bmatrix} 1 & & & & & & 0 \\ & \ddots & \overset{\boldsymbol{\eta',\eta'}}{\downarrow} & & \overset{\boldsymbol{\eta',\eta}}{\downarrow} & & \\ & & e^{\lambda_4 t^\alpha_{\sigma\ell}} \cosh(\lambda_4 \sigma q^\alpha_\ell) & \cdots & e^{\lambda_4 t^\alpha_{\sigma\ell}} \sinh(\lambda_4 \sigma q^\alpha_\ell) & & \\ & & & 1 & & & \\ & & e^{\lambda_4 t^\alpha_{\sigma\ell}} \sinh(\lambda_4 \sigma q^\alpha_\ell) & \cdots & e^{\lambda_4 t^\alpha_{\sigma\ell}} \cosh(\lambda_4 \sigma q^\alpha_\ell) & & \\ & & \underset{\boldsymbol{\eta,\eta'}}{\uparrow} & & \underset{\boldsymbol{\eta,\eta}}{\uparrow} & \ddots & \\ 0 & & & & & & 1 \end{bmatrix}_{N_d \times N_d} \tag{4.69}$$

Now, we can form $\Lambda_\sigma(\ell)$ matrix which is the product of $e^{W_\sigma(\ell)}$ and $e^{T^\alpha_\sigma(\ell)}$ matrices. From equation 4.66;

$$\Lambda_\sigma(\ell) = \begin{bmatrix} \ddots & & & 0 \\ & e^{\lambda_4 t^\alpha_{\sigma\ell}} \cosh(\lambda_4 \sigma q^\alpha_\ell) e^{W_{\eta',\sigma}(\ell)} & e^{\lambda_4 t^\alpha_{\sigma\ell}} \sinh(\lambda_4 \sigma q^\alpha_\ell) e^{W_{\eta',\sigma}(\ell)} & \\ & & \ddots & \\ & e^{\lambda_4 t^\alpha_{\sigma\ell}} \sinh(\lambda_4 \sigma q^\alpha_\ell) e^{W_{\eta,\sigma}(\ell)} & e^{\lambda_4 t^\alpha_{\sigma\ell}} \cosh(\lambda_4 \sigma q^\alpha_\ell) e^{W_{\eta,\sigma}(\ell)} & \\ 0 & & & \ddots \end{bmatrix} \tag{4.70}$$

In matrix $\Lambda_\sigma(\ell)$, all elements are zero except the diagonal, $[\Lambda_\sigma(\ell)]_{\eta,\eta'}$ and $[\Lambda_\sigma(\ell)]_{\eta',\eta}$ elements. And the inverse of this matrix is

$$[\Lambda_\sigma(\ell)]^{-1} = \begin{bmatrix} \ddots & & & 0 \\ & e^{-\lambda_4 t^\alpha_{\sigma\ell}} \cosh(\lambda_4 \sigma q^\alpha_\ell) e^{-W_{\eta',\sigma}(\ell)} & -e^{-\lambda_4 t^\alpha_{\sigma\ell}} \sinh(\lambda_4 \sigma q^\alpha_\ell) e^{-W_{\eta,\sigma}(\ell)} & \\ & & \ddots & \\ & -e^{-\lambda_4 t^\alpha_{\sigma\ell}} \sinh(\lambda_4 \sigma q^\alpha_\ell) e^{-W_{\eta',\sigma}(\ell)} & e^{-\lambda_4 t^\alpha_{\sigma\ell}} \cosh(\lambda_4 \sigma q^\alpha_\ell) e^{-W_{\eta,\sigma}(\ell)} & \\ 0 & & & \ddots \end{bmatrix} \tag{4.71}$$

Always keep in mind that $\eta > \eta'$ and the dimensions of the $\Lambda_\sigma(\ell)$ matrices are $N_d \times N_d$.

4.4. Expansion Parameter γ

The expansion parameter γ not only affects the strength of the auxiliary spins introduced in the decomposition of $\gamma - \beta H_J$ term as in equation 4.31, but also affects the expansion order. It is related to the expectation value of H_J since we expand the partition function as powers of it. However, the expectation values of any observable should not be depended on γ since it is the free parameter of the expansion.

In this chapter, we have split the Hamiltonian in two parts as H_1 and H_2.

$$H_1 = H_0 + H_U + \frac{\gamma}{\beta} \tag{4.72}$$

$$H_2 = H_J - \frac{\gamma}{\beta} \tag{4.73}$$

Let us rewrite the expansion formula in equation 4.8 by using H_1 and H_2.

$$\begin{aligned} Z &= e^{-\beta(H_1+H_2)} \\ &= \sum_{k=0}^{\infty} \int_0^1 d\tau_k \cdots \int_0^{\tau_2} d\tau_1 \prod_{i=1}^{k} \left[-\beta H_2(\tau_i\beta)\right] e^{-\beta H_1} \end{aligned} \tag{4.74}$$

where

$$H_2(\tau_i\beta) = e^{-\tau_i\beta H_1} H_2 e^{\tau_i\beta H_1} \tag{4.75}$$

We need to change the upper limits of the integrals to 1. In order to do that, the equation should be multiplied by $1/k!$ to cancel out the overcounted terms.

$$Z = \sum_{k=0}^{\infty} \frac{1}{k!} \int_0^1 d\tau_k \cdots \int_0^1 d\tau_1 \prod_{i=1}^{k} \left[-\beta H_2(\tau_i\beta)\right] e^{-\beta H_1} \tag{4.76}$$

Let us calculate the expectation value of $-H_2$ using 4.76.

$$\begin{aligned}\langle -H_2\rangle &= \frac{1}{\beta}\int_0^\beta d\tau \langle -H_2(\tau)\rangle \\ &= \frac{1}{\beta}\int_0^1 d\tau \langle -\beta H_2(\tau\beta)\rangle \\ &= \frac{1}{\beta}\frac{1}{Z}\sum_{k=0}^{\infty}\frac{1}{k!}\int_0^1 d\tau\int_0^1 d\tau_k\cdots\int_0^1 d\tau_1 \\ &\times(-\beta H_2(\tau\beta))(-\beta H_2(\tau_1\beta))\ldots(-\beta H_2(\tau_k\beta))e^{-\beta H_1}\end{aligned} \tag{4.77}$$

If the equation is multiplied and divided by $k+1$ and the summation over k is shifted to $k+1$, it is simply the expectation value of the expansion order k.

$$\begin{aligned}\langle -H_2\rangle &= \frac{1}{\beta}\frac{1}{Z}\sum_{k=0}^{\infty}\frac{k+1}{(k+1)!}\int_0^1 d\tau\int_0^1 d\tau_k\cdots\int_0^1 d\tau_1 \\ &\times(-\beta H_2(\tau\beta))(-\beta H_2(\tau_1\beta))\ldots(-\beta H_2(\tau_k\beta))e^{-\beta H_1} \\ &= \frac{1}{\beta}\frac{1}{Z}\sum_{k=0}^{\infty}\frac{k}{k!}\int_0^1 d\tau_k\cdots\int_0^1 d\tau_1(-\beta H_2(\tau_1\beta))\ldots(-\beta H_2(\tau_k\beta))e^{-\beta H_1}\end{aligned} \tag{4.78}$$

Now, let us go back to our notation, make the integrals time-ordered and arrange the limits of the integrals to their old values.

$$\begin{aligned}\langle -H_2\rangle &= \frac{1}{\beta}\frac{1}{Z}\sum_{k=0}^{\infty}k\int_0^1 d\tau_k\cdots\int_0^{\tau_2} d\tau_1\prod_{i=1}^{k}\left[-\beta H_2(\tau_i\beta)\right]e^{-\beta H_1} \\ &= \frac{1}{\beta}\langle k\rangle\end{aligned} \tag{4.79}$$

If we look at $\langle -H_2\rangle$ from the other way, the equation is

$$\langle -H_2\rangle = \frac{\gamma}{\beta} - \langle H_J\rangle \tag{4.80}$$

Using equations 4.79 and 4.80, the relation between the expansion parameter, γ, and $\langle H_J\rangle$

becomes

$$\langle k \rangle = \gamma - \beta \langle H_J \rangle \tag{4.81}$$

CHAPTER 5

CALCULATIONS OF THE GREEN'S FUNCTIONS

In this chapter, we focus on the calculations of the Green's functions, updates of them in the Monte Carlo steps and the physical measurements.

5.1. New Green's Function $(G^\sigma)'$ From Old Green's Function G^σ

Here, we will give a derivation of the new Green's function $(G^\sigma)'$ with a new spin configuration when we know the old one with old spin configuration. Since Λ_σ is not diagonal, we cannot use Hirsh-Fye algorithm directly. We have to find out the form of the equations. We omit the spin indices, η and α indices for simplicity. Λ' represents the new spin configuration and Λ represents the old spin configuration. Let us define the matrices G^{-1} and Λ.

$$G^{-1} = \begin{bmatrix} I & 0 & \cdots & & & B_L \\ -B_1 & I & 0 & & & 0 \\ 0 & -B_2 & I & & & \vdots \\ \vdots & \vdots & \vdots & \ddots & & \vdots \\ & & & & I & 0 \\ 0 & 0 & \cdots & 0 & -B_{L-1} & I \end{bmatrix}_{N_d \cdot L \times N_d \cdot L} \tag{5.1}$$

$$(\Lambda)^{-1} = \begin{bmatrix} [\Lambda(1)]^{-1}_{N_d \times N_d} & & & 0 \\ & [\Lambda(2)]^{-1}_{N_d \times N_d} & & \\ & & \ddots & \\ 0 & & & [\Lambda(L)]^{-1}_{N_d \times N_d} \end{bmatrix}_{N_d \cdot L \times N_d \cdot L} \tag{5.2}$$

Here Λ is a $N_d \cdot L \times N_d \cdot L$ matrix, and there are $N_d \times N_d$ matrices in the diagonal elements which are denoted as $\Lambda(\ell)$. $\Lambda(\ell)$ can be written as

$$[\Lambda(\ell)]_{i,j} = [\Lambda]_{i\ell,j\ell} \tag{5.3}$$

And the multiplication of these matrices

$$G^{-1}\left(\Lambda\right)^{-1} = \begin{bmatrix} [\Lambda(1)]^{-1} & 0 & \cdots & & & e^{-\Delta\tau K} \\ -e^{-\Delta\tau K} & [\Lambda(2)]^{-1} & 0 & & & 0 \\ 0 & -e^{-\Delta\tau K} & [\Lambda(3)]^{-1} & & & \vdots \\ \vdots & & & \ddots & & \\ & & & & [\Lambda(L-1)]^{-1} & 0 \\ 0 & 0 & \cdots & 0 & -e^{-\Delta\tau K} & [\Lambda(L)]^{-1} \end{bmatrix} \tag{5.4}$$

Because $B_\ell = e^{-\Delta\tau K}\Lambda(\ell)$.

Let us define $\widetilde{G}$ which is

$$\widetilde{G} = \Lambda G \tag{5.5}$$

$$(\widetilde{G})^{-1} = G^{-1}\left(\Lambda\right)^{-1} \tag{5.6}$$

With these definitions we clearly see that we can get $\widetilde{G}'$ from $\widetilde{G}$.

$$\implies \quad (\widetilde{G}')^{-1} = \widetilde{G}^{-1} - \Lambda^{-1} + (\Lambda')^{-1} \tag{5.7}$$

$$(\widetilde{G}')^{-1} - \widetilde{G}^{-1} = (\Lambda')^{-1} - \Lambda^{-1} \tag{5.8}$$

Multiplying both sides $\widetilde{G}$ from the left and $\widetilde{G}'$ from the right, we get

$$\widetilde{G} - \widetilde{G}' = \widetilde{G}\left[(\Lambda')^{-1} - \Lambda^{-1}\right]\widetilde{G}' \tag{5.9}$$

$$\widetilde{G}' = \widetilde{G} - \widetilde{G}\left[(\Lambda')^{-1} - \Lambda^{-1}\right]\widetilde{G}' \tag{5.10}$$

Using equation 5.5, the expression becomes

$$\Lambda' G' = \Lambda G - \Lambda G\left[(\Lambda')^{-1} - \Lambda^{-1}\right]\Lambda' G' \tag{5.11}$$

$$(\Lambda)^{-1}\Lambda' G' = G + G\left(\Lambda^{-1}\Lambda' - I\right)G' \tag{5.12}$$

Add G' to both sides;

$$G' = G + (G - I)\left(\Lambda^{-1}\Lambda' - I\right)G' \tag{5.13}$$

Therefore, we find the relation between the old Green's function and the new Green's function which is

$$\boxed{G' = \left\{I - (G - I)\left(\Lambda^{-1}\Lambda' - I\right)\right\}^{-1} G} \tag{5.14}$$

5.2. Initial Calculation of Green's Function G^σ from G^0 and Λ_σ

In Hirsh-Fye quantum Monte Carlo method they used a relation to find G from G' which is represented as

$$G' = G + (G - I)(e^{V'-V} - I)G' \tag{5.15}$$

They used this relation to find G^σ from G^0 which can be found analytically, as well. However, the Hamiltonian that they used includes only the intra-orbital Coulomb interaction. The Hamiltonian that we use includes inter-orbital Coulomb interaction, pair-hopping and

spin-flip terms along with the intra-orbital Coulomb interaction. Therefore, we cannot use this relation. In section 5.1 we have found that the relation between the old and the new Green's function is

$$G' = \left\{ I - (G - I) \left(\Lambda^{-1} \Lambda' - I \right) \right\}^{-1} G \tag{5.16}$$

In order to find the relation for the initial calculation of Green's function we need to modify some variables in a way that;

$$\begin{aligned} G' &\longrightarrow G^{\sigma} \\ G &\longrightarrow G^{0} \\ \Lambda^{-1}\Lambda' &\longrightarrow \Lambda_{\sigma} \end{aligned} \tag{5.17}$$

The equation for the initial calculation of Green's function G^{σ} from G^{0} is

$$\boxed{G^{\sigma} = \left\{ I - (G^{0} - I) \left(\Lambda_{\sigma} - I \right) \right\}^{-1} G^{0}} \tag{5.18}$$

where G^{0} is the Green's function for the case in which the auxiliary fields, $\{\widetilde{S}_{\ell}\}$ and $\{P_{\ell}^{\alpha}\}$, are set to zero, and we can calculate it analytically. Since the Green's function was defined with plus sign in Hirsh-Fye paper, we defined it the same way. Green's function is represented as

$$G^{\sigma}_{\nu\nu'}(\ell, \ell') = + \left\langle T d_{\nu\sigma}(\ell) d^{\dagger}_{\nu'\sigma}(\ell') \right\rangle \tag{5.19}$$

in our algorithm. Here G^{0} is calculated from the H_{0} part of the Hamiltonian which is

$$\begin{aligned} H_{0} = &\sum_{m,\sigma} (\varepsilon_{m} - \mu) c^{\dagger}_{m\sigma} c_{m\sigma} + \sum_{\nu,\sigma} (\varepsilon_{\nu} - \mu) d^{\dagger}_{\nu\sigma} d_{\nu\sigma} + \sum_{m,\nu,\sigma} V_{m\nu} \left(c^{\dagger}_{m\sigma} d_{\nu\sigma} + h.c. \right) \\ &+ \frac{U}{2} \sum_{\nu,\sigma} n_{\nu\sigma} + \sum_{\nu > \nu',\sigma} \left[\frac{U'}{2} (n_{\nu\sigma} + n_{\nu',-\sigma}) + \frac{(U' - J)}{2} (n_{\nu\sigma} + n_{\nu'\sigma}) \right] \end{aligned} \tag{5.20}$$

G^0 is calculated from the Dyson's equation which is

$$G^0_{\nu\nu'}(i\omega_n) = G^{00}_{\nu\nu'}(i\omega_n) + \sum_{\nu'',\nu'''} G^{00}_{\nu\nu''}(i\omega_n) \sum_{m,m'} V_{\nu'' m} G^{00}_{mm'}(i\omega_n) V_{m'\nu'''} G^{00}_{\nu'''\nu'}(i\omega_n) \tag{5.21}$$

where $G^{00}_{\nu\nu'}(i\omega_n)$ and $G^{00}_{mm'}(i\omega_n)$ are impurity and host Green's functions when the hybridization terms, $V_{m\nu}$, are zero. $G^{00}_{\nu\nu'}(i\omega_n)$ and $G^{00}_{mm'}(i\omega_n)$ are calculated from the Hamiltonian H_{00}.

$$H_{00} = \sum_{m,\sigma} (\varepsilon_m - \mu) c^\dagger_{m\sigma} c_{m\sigma} + \sum_{\nu,\sigma} (\varepsilon_\nu - \mu) d^\dagger_{\nu\sigma} d_{\nu\sigma} + \sum_{\nu,\sigma} Y n_{\nu\sigma} \tag{5.22}$$

where

$$\sum_{\nu,\sigma} Y n_{\nu\sigma} = \frac{U}{2} \sum_{\nu,\sigma} n_{\nu\sigma} + \sum_{\nu>\nu',\sigma} \left[\frac{U'}{2} (n_{\nu\sigma} + n_{\nu',-\sigma}) + \frac{(U'-J)}{2} (n_{\nu\sigma} + n_{\nu'\sigma}) \right] \tag{5.23}$$

and if sums over ν, ν' and σ are taken

$$Y = (N_d - 1) \left(\frac{U}{2} + \frac{U'}{2} + \frac{U' - J}{2} \right) \tag{5.24}$$

for $N_d > 1$. N_d is the number of d orbitals. The Green's functions, $G^{00}_{\nu\nu'}(i\omega_n)$ and $G^{00}_{mm'}(i\omega_n)$, for zero hybridization are

$$G^{00}_{\nu\nu'}(i\omega_n) = \frac{\delta_{\nu\nu'}}{i\omega_n - (\varepsilon_\nu - \mu + Y)} \tag{5.25}$$

$$G^{00}_{mm'}(i\omega_n) = \frac{\delta_{mm'}}{i\omega_n - (\varepsilon_m - \mu)} \tag{5.26}$$

Notice that $G^0_{\nu\nu'}(i\omega_n)$ is calculated in Matsubara frequency, $i\omega_n$. After the calculation, it should be transformed to Matsubara time, $\tau = it$.

5.3. Ratio of the Determinants

In this section we will calculate the ratio of the determinants which are used for updating the Green's functions and weight comparison while progressing in the Markov chain.

$$\widetilde{G}' = \widetilde{G} - \widetilde{G}\left[(\Lambda')^{-1} - \Lambda^{-1}\right]\widetilde{G}' \tag{5.27}$$

where we omitted the spin and η indices and $\widetilde{G} = \Lambda G$. Multiplying with $(\widetilde{G}')^{-1}$ on the right

$$I = \widetilde{G}(\widetilde{G}')^{-1} - \widetilde{G}\left[(\Lambda')^{-1} - \Lambda^{-1}\right] \tag{5.28}$$

$$\widetilde{G}(\widetilde{G}')^{-1} = I + \widetilde{G}\left[(\Lambda')^{-1} - \Lambda^{-1}\right] \tag{5.29}$$

Recall that $G = M^{-1}$ from equation 4.65.

$$\widetilde{G} = \Lambda G \tag{5.30}$$

$$= \Lambda M^{-1} \tag{5.31}$$

Using that equation 5.29 becomes

$$\left(\Lambda M^{-1}\right)\left[\Lambda'(M')^{-1}\right]^{-1} = I + \Lambda G\left[(\Lambda')^{-1} - \Lambda^{-1}\right] \tag{5.32}$$

Multiplying Λ^{-1} on the left, Λ' on the right

$$M^{-1}M' = \Lambda^{-1}\Lambda' + G\left(I - \Lambda^{-1}\Lambda'\right) \tag{5.33}$$

$$= \Lambda^{-1}\Lambda' + (G - I)\left(I - \Lambda^{-1}\Lambda'\right) + \left(I - \Lambda^{-1}\Lambda'\right) \tag{5.34}$$

$$\Rightarrow \quad M^{-1}M' = I + (I - G)\left(\Lambda^{-1}\Lambda' - I\right) \tag{5.35}$$

After taking the determinant of the both sides, expression becomes

$$\frac{\det M'}{\det M} = \det\left[I + (I - G)\left(\Lambda^{-1}\Lambda' - I\right)\right] \tag{5.36}$$

Therefore, the ratio of the determinants of the new and the old spin configuration without omitting the indices is

$$\boxed{R_\sigma = \frac{\det M'_\sigma}{\det M_\sigma} = \det A_\sigma} \tag{5.37}$$

where

$$\boxed{A_\sigma = I + (I - G^\sigma)\left(\Lambda_\sigma^{-1}\Lambda'_\sigma - I\right)} \tag{5.38}$$

5.4. Calculation of Updated Green's Functions

In this section we will derive the expressions for the updated Green's functions. First, look at the equations for the relation between the old and the new Green's function;

$$(G^\sigma)' = G^\sigma + (G^\sigma - I)\left(\Lambda_\sigma^{-1}\Lambda'_\sigma - I\right)(G^\sigma)' \tag{5.39}$$

and

$$(G^{\sigma})' = \left\{ I - (G^{\sigma} - I) \left(\Lambda_{\sigma}^{-1} \Lambda_{\sigma}' - I \right) \right\}^{-1} G^{\sigma} \tag{5.40}$$

solving them together gives the expression for the update algorithm that we used in the program which is represented as

$$\boxed{(G^{\sigma})' = G^{\sigma} + (G^{\sigma} - I) \left(\Lambda_{\sigma}^{-1} \Lambda_{\sigma}' - I \right) A_{\sigma}^{-1} G^{\sigma}} \tag{5.41}$$

where

$$\boxed{A_{\sigma} = I + (I - G^{\sigma}) \left(\Lambda_{\sigma}^{-1} \Lambda_{\sigma}' - I \right)} \tag{5.42}$$

The matrix A_{σ} is used in fast update scheme to make a more efficient and fast algorithm. The derivations of the equations required for fast update scheme is given in Appendix E.

There are two types of updates in this algorithm: single spin flip and expansion order updates. Expansion order updates increase or decrease the expansion order by one at a random imaginary-time slice for one Monte Carlo move by introducing or removing 3 spin for H_J term. Single spin flip updates changes the values of the spins while the expansion order is constant. While making these changes, we need to consider the detailed balance of the Monte Carlo steps. The η and α indices is dropped for simplicity.

5.5. Monte Carlo Transition Probabilities for Single Spin-flips

The acceptance probabilities for a single spin-flip are calculated using heat-bath algorithm using equation 3.13;

$$W_{acc}(s \to s') = \frac{P}{1 + P} \tag{5.43}$$

where

$$P = \frac{p_{s'}}{p_s} \frac{W_{prop}(s' \to s)}{W_{prop}(s \to s')} \tag{5.44}$$

Here the term $p_{s'}/p_s$ is simply the ratio of the determinants multiplied by the ratio of the weight terms for expansion orders.

$$\frac{p_{s'}}{p_s} = \frac{\widetilde{F}'}{\widetilde{F}} R_\uparrow R_\downarrow \tag{5.45}$$

where the ratio of the determinants, R_σ, is calculated in section 5.3 which is

$$R_\sigma = \frac{\det M'_\sigma}{\det M_\sigma} = \det A_\sigma \tag{5.46}$$

where

$$A_\sigma = I + (I - G^\sigma)\left(\Lambda_\sigma^{-1}\Lambda'_\sigma - I\right) \tag{5.47}$$

We should consider $\widetilde{F}(k; r_1, r_2, \cdots, r_L)$ as weights of the configurations along with the determinants of the fermion matrices.

$$\widetilde{F}(k; r_1, r_2, \cdots, r_L) = F(k; r_1, r_2, \cdots, r_L) \left(\frac{\widetilde{\gamma} - \beta J}{8}\right)^k \exp\left\{-\lambda_4 \sum_{\ell=1}^{L} (t_{\uparrow\ell} + t_{\downarrow\ell})\, \delta_{r_\ell,1}\right\} \tag{5.48}$$

Therefore, the equation 5.44 becomes

$$P = \frac{\widetilde{F}'}{\widetilde{F}} R_\uparrow R_\downarrow \frac{W_{prop}(s' \to s)}{W_{prop}(s \to s')} \tag{5.49}$$

In this study the proposal probabilities are different only when there is an order change. We will show that the calculation of the acceptance probabilities for each spin-

flip.

5.5.1. Single Spin-flip for "r_ℓ"

Spin-flip for r_ℓ occurs in two ways. First one is turning on the effect of H_J for imaginary-time slice ℓ, and the second one is turning it off for imaginary-time slice ℓ.

5.5.1.1. Turning on the effect of H_J

Let us look at the turning on case which is following;

$$r_\ell = 0 \quad \longrightarrow \quad r'_\ell = 1$$

This move turns on three auxiliary field variables at time slice ℓ, and impurity sites η, η'. These variables are q_ℓ, $t_{\uparrow\ell}$ and $t_{\downarrow\ell}$.

$$\begin{aligned} q_\ell = 0 \quad &\longrightarrow \quad q'_\ell = \pm 1 \\ t_{\uparrow\ell} = 0 \quad &\longrightarrow \quad t'_{\uparrow\ell} = \pm 1 \\ t_{\downarrow\ell} = 0 \quad &\longrightarrow \quad t'_{\downarrow\ell} = \pm 1 \end{aligned}$$

Let us calculate the ratio of the weight variables $\widetilde{F}$. If we turn on the effects of H_J for imaginary-time slice ℓ, it is turned on for $k+1$ imaginary-time slices.

$$\begin{aligned} \frac{\widetilde{F}'}{\widetilde{F}} &= \frac{\widetilde{F}(k+1; r_1, r_2, \cdots, r'_\ell = 1, \cdots, r_L)}{\widetilde{F}(k; r_1, r_2, \cdots, r_\ell = 0, \cdots, r_L)} \\ &= \frac{F(k+1; r_1, r_2, \cdots, r'_\ell = 1, \cdots, r_L)}{F(k; r_1, r_2, \cdots, r_\ell = 0, \cdots, r_L)} \frac{\left(\frac{\widetilde{\gamma}-\beta J}{8}\right)^{k+1}}{\left(\frac{\widetilde{\gamma}-\beta J}{8}\right)^{k}} e^{-\lambda_4\left(t_{\uparrow\ell}+t_{\downarrow\ell}\right)} \end{aligned} \tag{5.50}$$

The ratio of the weight variables becomes

$$\frac{\widetilde{F}'}{\widetilde{F}} = \frac{F(k+1; r_1, r_2, \cdots, r'_\ell = 1, \cdots, r_L)}{F(k; r_1, r_2, \cdots, r_\ell = 0, \cdots, r_L)} \left(\frac{\widetilde{\gamma} - \beta J}{8}\right) e^{-\lambda_4 (t_{\uparrow\ell} + t_{\downarrow\ell})} \tag{5.51}$$

We should consider the ratio of the proposal probabilities, as well. For order change updates, the steps in the Markov chain are not symmetrical. Increasing order by one adds 3 auxiliary field variables at the same time. Thus, there are 8 configurations from which we can choose. The proposal probability from r_ℓ to r'_ℓ is

$$W_{prop}(r_\ell \to r'_\ell) = \frac{1}{8} \tag{5.52}$$

and the proposal probabilities for reverse move is chosen from one possible configuration, it is

$$W_{prop}(r'_\ell \to r_\ell) = 1 \tag{5.53}$$

Using 5.49 the probability of the change "$r_\ell = 0 \longrightarrow r'_\ell = 1$" is

$$P = \frac{\widetilde{F}'}{\widetilde{F}} R_\uparrow R_\downarrow \frac{1}{1/8} \tag{5.54}$$

Therefore, the acceptance probability of the change "$r_\ell = 0 \longrightarrow r'_\ell = 1$" is

$$\boxed{W_{acc}(r_\ell \to r'_\ell) = \frac{P}{1+P}} \tag{5.55}$$

where

$$\boxed{P = 8 \times \frac{\widetilde{F}'}{\widetilde{F}} R_\uparrow R_\downarrow} \tag{5.56}$$

and

$$\boxed{\frac{\widetilde{F}'}{\widetilde{F}} = \frac{F(k+1; r_1, r_2, \cdots, r'_\ell = 1, \cdots, r_L)}{F(k; r_1, r_2, \cdots, r_\ell = 0, \cdots, r_L)} \left(\frac{\widetilde{\gamma} - \beta J}{8}\right) e^{-\lambda_4 \left(t_{\uparrow\ell} + t_{\downarrow\ell}\right)}} \tag{5.57}$$

5.5.1.2. Turning off the effect of H_J

Let us look at the turning on case which is following;

$$r_\ell = 1 \quad \longrightarrow \quad r'_\ell = 0$$

This move turns off three auxiliary field variables at time slice ℓ, and impurity sites η, η'. These variables are q_ℓ, $t_{\uparrow\ell}$ and $t_{\downarrow\ell}$.

$$\begin{aligned} q_\ell = \pm 1 \quad &\longrightarrow \quad q'_\ell = 0 \\ t_{\uparrow\ell} = \pm 1 \quad &\longrightarrow \quad t'_{\uparrow\ell} = 0 \\ t_{\downarrow\ell} = \pm 1 \quad &\longrightarrow \quad t'_{\downarrow\ell} = 0 \end{aligned}$$

Let us calculate the ratio of the weight variables $\widetilde{F}$. If we turn of the effects of H_J for imaginary-time slice ℓ, it is turned on for $k-1$ imaginary-time slices.

$$\begin{aligned} \frac{\widetilde{F}'}{\widetilde{F}} &= \frac{\widetilde{F}(k-1; r_1, r_2, \cdots, r'_\ell = 0, \cdots, r_L)}{\widetilde{F}(k; r_1, r_2, \cdots, r_\ell = 1, \cdots, r_L)} \\ &= \frac{F(k-1; r_1, r_2, \cdots, r'_\ell = 0, \cdots, r_L)}{F(k; r_1, r_2, \cdots, r_\ell = 1, \cdots, r_L)} \frac{\left(\frac{\widetilde{\gamma} - \beta J}{8}\right)^{k-1}}{\left(\frac{\widetilde{\gamma} - \beta J}{8}\right)^{k}} e^{+\lambda_4 \left(t_{\uparrow\ell} + t_{\downarrow\ell}\right)} \end{aligned} \tag{5.58}$$

The ratio of the weight variables becomes

$$\frac{\widetilde{F}'}{\widetilde{F}} = \frac{F(k-1; r_1, r_2, \cdots, r'_\ell = 0, \cdots, r_L)}{F(k; r_1, r_2, \cdots, r_\ell = 1, \cdots, r_L)} \left(\frac{\widetilde{\gamma} - \beta J}{8}\right)^{-1} e^{+\lambda_4 \left(t_{\uparrow\ell} + t_{\downarrow\ell}\right)} \tag{5.59}$$

We should consider the ratio of the proposal probabilities, as well. Decreasing order by one removes 3 auxiliary field variables at the same time. There is only one configuration for removing case. The proposal probability from r_ℓ to r'_ℓ is

$$W_{prop}(r_\ell \to r'_\ell) = 1 \tag{5.60}$$

and the proposal probabilities for reverse move is chosen from 8 possible configurations, it is

$$W_{prop}(r'_\ell \to r_\ell) = \frac{1}{8} \tag{5.61}$$

Using 5.49 the probability of the change "$r_\ell = 1 \longrightarrow r'_\ell = 0$" is

$$P = \frac{\widetilde{F}'}{\widetilde{F}} R_\uparrow R_\downarrow \frac{1/8}{1} \tag{5.62}$$

Therefore, the acceptance probability of the change "$r_\ell = 1 \longrightarrow r'_\ell = 0$" is

$$\boxed{W_{acc}(r_\ell \to r'_\ell) = \frac{P}{1+P}} \tag{5.63}$$

where

$$\boxed{P = \frac{1}{8} \times \frac{\widetilde{F}'}{\widetilde{F}} R_\uparrow R_\downarrow} \tag{5.64}$$

and

$$\boxed{\frac{\widetilde{F}'}{\widetilde{F}} = \frac{F(k-1; r_1, r_2, \cdots, r'_\ell = 0, \cdots, r_L)}{F(k; r_1, r_2, \cdots, r_\ell = 1, \cdots, r_L)} \left(\frac{\widetilde{\gamma} - \beta J}{8}\right)^{-1} e^{+\lambda_4 (t_{\uparrow\ell} + t_{\downarrow\ell})}} \tag{5.65}$$

5.5.2. Single Spin-flip for "q_ℓ"

The spin-flip for q_ℓ occurs in the following way.

$$q_\ell \quad \longrightarrow \quad q'_\ell = -q_\ell$$

Let us calculate the ratio of the weight variables $\widetilde{F}$. There is nothing related to q_ℓ in $\widetilde{F}$. Therefore, $\widetilde{F}' = \widetilde{F}$ The ratio of the weight variables becomes

$$\frac{\widetilde{F}'}{\widetilde{F}} = 1 \tag{5.66}$$

The proposal probabilities for this change is the same since there is no order change. Using 5.49 the acceptance probability of the change "$q_\ell \longrightarrow q'_\ell = -q_\ell$" is

$$\boxed{W_{acc}(q_\ell \to q'_\ell) = \frac{P}{1+P}} \tag{5.67}$$

where

$$\boxed{P = R_\uparrow R_\downarrow} \tag{5.68}$$

5.5.3. Single Spin-flip for "$t_{\sigma\ell}$"

The spin-flip for $t_{\sigma\ell}$ occurs in the following way.

$$t_{\sigma\ell} \quad \longrightarrow \quad t'_{\sigma\ell} = -t_{\sigma\ell}$$

Let us calculate the ratio of the weight variables $\widetilde{F}$.

$$\begin{aligned}\frac{\widetilde{F}'}{\widetilde{F}} &= \frac{\widetilde{F}(k;r_1,r_2,\cdots,r_L)}{\widetilde{F}(k;r_1,r_2,\cdots,r_L)} \\ &= \frac{F(k;r_1,r_2,\cdots,r_L)}{F(k;r_1,r_2,\cdots,r_L)} \frac{\left(\frac{\widetilde{\gamma}-\beta J}{8}\right)^k}{\left(\frac{\widetilde{\gamma}-\beta J}{8}\right)^k} e^{+2\lambda_4 t_{\sigma\ell}}\end{aligned} \tag{5.69}$$

The ratio of the weight variables becomes

$$\frac{\widetilde{F}'}{\widetilde{F}} = e^{+2\lambda_4 t_{\sigma\ell}} \tag{5.70}$$

The proposal probabilities for this change is the same since there is no order change. Using 5.49 the acceptance probability of the change "$t_{\sigma\ell} \longrightarrow t'_{\sigma\ell} = -t_{\sigma\ell}$" is

$$\boxed{W_{acc}(t_{\sigma\ell} \to t'_{\sigma\ell}) = \frac{P}{1+P}} \tag{5.71}$$

where

$$\boxed{P = \frac{\widetilde{F}'}{\widetilde{F}} R_\uparrow R_\downarrow} \tag{5.72}$$

5.5.4. Single Spin-flip for "$S^{U}_{\nu\ell}$", "$S^{U'}_{\nu\nu',\ell}$" and "$S^{U'-J}_{\nu\nu',\ell,\sigma}$"

Spin-flips of these variables are explained in sections E.7, E.8 and E.9. From the results it is seen that these changes do not include any variables changing in the $\widetilde{F}$ weights. Therefore, the ratio of the weights is

$$\frac{\widetilde{F}'}{\widetilde{F}} = 1 \tag{5.73}$$

for these spin-flips. The proposal probabilities for this change is the same since there is no order change. The probability of acceptance of these spin changes is

$$\boxed{W_{acc}(s_\ell \to s'_\ell) = \frac{P}{1+P}} \tag{5.74}$$

where

$$\boxed{P = R_\uparrow R_\downarrow} \tag{5.75}$$

where the matrices $A_\uparrow$ and $\det A_\downarrow$ is calculated in sections E.7, E.8 and E.9.

5.6. Quantum Monte Carlo Measurements

We use Green's function method in order to calculate the physical measurements. The key point is that the Green's functions are sampled from the configurations $\left\{\{r_\ell\}, \{\widetilde{S}_\ell\}, \{\alpha\}, \{P_\ell^\alpha\}\right\}$. Thus, after the Green's functions are calculated, we need to average them over the QMC samples.

The single particle Green's functions in Matsubara time are

$$G^\uparrow_{\nu\nu'}(\tau) = -\left\langle T_\tau d_{\nu\uparrow}(\tau'+\tau) d^\dagger_{\nu'\uparrow}(\tau')\right\rangle \tag{5.76}$$

$$G^\downarrow_{\nu\nu'}(\tau) = -\left\langle T_\tau d_{\nu\downarrow}(\tau'+\tau) d^\dagger_{\nu'\downarrow}(\tau')\right\rangle \tag{5.77}$$

The physical quantities that we measure can be represented as the single particle Green's functions using the commutation relation between the electron creation/annihilation operators.

$$\left\{d_{\nu\sigma}, d^\dagger_{\nu'\sigma'}\right\} = \delta_{\nu\nu'}\delta_{\sigma\sigma'} \tag{5.78}$$

The electron number operator and magnetization operators are

$$n_\nu = d^\dagger_{\nu\uparrow} d_{\nu\uparrow} + d^\dagger_{\nu\downarrow} d_{\nu\downarrow} \tag{5.79}$$

$$M^Z_\nu = d^\dagger_{\nu\uparrow} d_{\nu\uparrow} - d^\dagger_{\nu\downarrow} d_{\nu\downarrow} \tag{5.80}$$

These are static measurements, using commutation relations representations of them with the Green's functions are

$$\begin{aligned} \langle n_\nu \rangle &= \langle n_\nu \rangle_{mc} \\ &= \frac{1}{L} \sum_{i=1}^{L} \left\langle (1 - G^\uparrow_{\nu\nu}(\tau_i, \tau_i)) + (1 - G^\downarrow_{\nu\nu}(\tau_i, \tau_i)) \right\rangle_{mc} \end{aligned} \tag{5.81}$$

$$\begin{aligned} \left\langle \left(M^Z_\nu M^Z_{\nu'} \right) \right\rangle &= \left\langle (d^\dagger_{\nu\uparrow} d_{\nu\uparrow} - d^\dagger_{\nu\downarrow} d_{\nu\downarrow})(d^\dagger_{\nu'\uparrow} d_{\nu'\uparrow} - d^\dagger_{\nu'\downarrow} d_{\nu'\downarrow}) \right\rangle_{mc} \\ &= \frac{1}{L} \sum_{i=1}^{L} \Big\langle (G^\uparrow_{\nu\nu}(\tau_i, \tau_i) - G^\downarrow_{\nu\nu}(\tau_i, \tau_i)) \\ &\qquad \times (G^\uparrow_{\nu'\nu'}(\tau_i, \tau_i) - G^\downarrow_{\nu'\nu'}(\tau_i, \tau_i)) \\ &\qquad + G^\uparrow_{\nu\nu'}(\tau_i, \tau_i)(\delta_{\nu\nu'} - G^\uparrow_{\nu'\nu}(\tau_i, \tau_i)) \\ &\qquad + G^\uparrow_{\nu'\nu}(\tau_i, \tau_i)(\delta_{\nu\nu'} - G^\uparrow_{\nu\nu'}(\tau_i, \tau_i)) \Big\rangle_{mc} \end{aligned} \tag{5.82}$$

where n_ν is the occupation of the impurity orbital ν, $\left(M^Z_\nu M^Z_{\nu'} \right)$ is the magnetic correlation between the impurit orbitals ν and ν'. Since HF+SE QMC algorithm uses time discretization, measurements need to be averaged over L time slices. $\langle \cdots \rangle_{mc}$ indicates the average over the configurations sampled during the Monte Carlo simulations.

The other physical quantities such as total occupation, square of the total magnetic moment and dynamical quantities can be calculated in the same way.

CHAPTER 6

QUANTUM MONTE CARLO RESULTS

In this chapter, we will show the results of our calculations. We have implemented two kinds of algorithms to test here:

• First, HF+SE algorithm was tested which we developed it for Anderson impurity model. It includes spin-flip and pair-hopping terms along with the U, U' and $U'-J$ terms. Rombouts' transformation is applied to spin-flip and pair-hopping terms. Spin-flip and pair-hopping terms have off-diagonal terms in the occupation number basis.

• Second, in order to check the reliability of a combined method with Hubbard-Stratonovich transformation and Rombouts' transformation together, we have applied Rombouts' transformation on $U'-J$ term to expand it with series expansion since $U'-J$ only includes diagonal terms in the occupation number basis. It is easier to combine them when all terms have diagonal elements. Thus, we have done tests with this algorithm including Hubbard-Stronovich transformation on U, U' and Rombouts' transformation on $U'-J$ terms.

6.1. Tests of the HF+SE QMC Algorithm for Spin-flip and Pair-hopping Terms

These first tests have been carried out for the algorithm that we developed for SU(2) invariant Anderson impurity model.

In order to test our algorithm, we compared the results of the program with the inputs of an exactly solvable model. The results from the runs for average expansion order, $\langle k\rangle$, and the value of $\gamma-\beta\langle H_J\rangle$ were compared which is a self-check mechanism since they should be equal. Additionally, the results should not be changed with respect to the free parameter γ in the expansion.

The first tests of the algorithm is on a 2 orbital Anderson model with no hybridization between the host and the impurity orbitals. In this theoretical situation, the Hamiltonian can be diagonalized for 2 orbitals. The tests were carried out at temperatures $T=3020$ K, $T=700$ K, $T=300$ K. However, the correlation times are less in high temperatures. Thus, we get the results quickly in high temperatures.

Firstly, we set H_U term to zero. The Hamiltonian becomes

$$H = H_0 + H_J \tag{6.1}$$

Figure 6.1 shows the effect of the H_J term from the exact diagonalization results for Hamiltonian. Spin-flip and pair-hopping terms affect the results considerably when H_U is absent. From the expectation value of H_J it is clearly seen that the total energy of the system is decreased which is expected since H_J contains off-diagonal terms with respect to the electron creation/annihilation operators. For this case H_J changes both total magnetic moment and total occupation numbers. It lowers the magnetic moment as expected.

For testing our algorithm, we compared the results with these exact calculations of $\langle n_{3d} \rangle$, $\langle (M_{3d})^2 \rangle$ and $\langle H_J \rangle$. Then we will show that the results do not change with respect to the free parameter γ.

In figure 6.2, 2000 warm up and 5000 measurement sweeps were taken from the QMC simulations for each point. Our QMC calculations exactly match to the exact diagonalization results for $H = H_0 + H_J$ as seen from figure 6.2 plotted as a function of chemical potential μ. Here, the number of imaginary-time slices $L = 64$ and the time discretization parameter $\Delta\tau = 0.06$. $J = 0.9$ but $H_U = 0$. Free expansion parameter $\gamma - \beta J = 0.3$. The energy values of the impurity orbitals are $\varepsilon_1 = 0$ eV and $\varepsilon_2 = 0$ eV. All points are within the error bars. Here, the only error is the statistical error caused by the Monte Carlo samples. In 6.2b, the error on the total magnetic moment at chemical potential $\mu = -0.2$ can be fixed with more Monte Carlo samples.

For the calculations in figure 6.3, 5000 warm up and 10000 measurement sweeps were taken from the QMC simulations for each point. Here, the results are plotted as a function of the free expansion parameter γ. It is clearly seen that the results does not change as a function of γ and exactly on the line of the exact diagonalization result. The number of imaginary-time slices $L = 64$ and the time discretization parameter $\Delta\tau = 0.06$. $J = 0.9$ but $H_U = 0$. This time the chemical potential is constant as $\mu = -0.2$. The energy values of the impurity orbitals are $\varepsilon_1 = 0$ eV and $\varepsilon_2 = 0$ eV. The value of the total magnetic moment is fluctuating about the exact value, because of the degeneracy in the energy eigenvalues. It can be a smooth function of γ, if there are more Monte Carlo samples. If we look at our bare data, the expectation value of the expansion order $\langle k \rangle$ and $\gamma - \beta \langle H_J \rangle$ are equal for all data points.

We have carried out tests for only H_J term at $T = 300$ K to check the algorithm

in more realistic temperatures. Figure 6.4 shows the exact diagonalization calculations to observe the effect of H_J term at 300 K and non-degenerate impurity energy eigenvalues. The energy values of the impurity orbitals are $\varepsilon_1 = 0$ eV and $\varepsilon_2 = 2$ eV. It is seen that the magnetization values are lowered more than the previous case. At lower temperatures, the strength of the spin-flip and pair-hopping interactions are higher. They nearly suppresses ferromagnetic behavior of the system for this case.

The comparison between the QMC results and the exact diagonalization calculations in 300 K and non-degenerate energy case shows that they also match for these parameters. Figure 6.5 shows the comparison between QMC results and the exact diagonalization calculations. 5000 warm up and 5000 measurement sweeps and 32 CPU per points are used in the QMC simulations for each point. Here, the number of imaginary-time slices $L = 296$ and the time discretization parameter $\Delta\tau = 0.13063$. $J = 0.9$ but $H_U = 0$. Free expansion parameter $\gamma - \beta J = 0.3$. The energy values of the impurity orbitals are $\varepsilon_1 = 0$ eV and $\varepsilon_2 = 2$ eV. All points match the exact calculations except for two points. More Monte Carlo samples can lower the error bars of these points and they can converge the exact results. In figure 6.6, the QMC results are plotted as a function of the free parameter γ, with the parameters used in the figure 6.5 but at constant chemical potential $\mu = 1$ eV. The results are independent of the free parameter as expected.

We continue our tests by extend this calculations to 3 orbital and 5 orbital systems with a degenerate energy levels. The Hamiltonian is again

$$H = H_0 + H_J \tag{6.2}$$

In the calculations of figure 6.7, 3 orbital system is tested. The comparison between the QMC results and the exact diagonalization calculations shows that the QMC results have little errors. For these calculations The free parameter is taken as $\gamma - \beta J = 0.3$. The number of imaginary-time slices $L = 64$ and the time discretization parameter $\Delta\tau = 0.06$. $J = 0.9$ but $H_U = 0$. The energy eigenvalues are all zero, $\varepsilon_\nu = 0$. 5000 warm up and 10000 measurement sweeps were taken for each point. The temperature is $T = 3020$ K. The expectation value of H_J is overestimated a little bit in these calculations. Thus, there are unmatched points in the magnetization and the occupation values.

For those calculations in figure 6.8 we compare the results of the QMC simulations with the exact diagonalization results for 5 orbitals, plotted as a function of μ. The free parameter is taken as $\gamma - \beta J = 0.3$. The number of imaginary-time slices $L = 64$ and the

time discretization parameter $\Delta\tau = 0.06$. $J = 0.9$ but $H_U = 0$. The energy eigenvalues are all zero, $\varepsilon_\nu = 0$. 100 warm up and 100 measurement sweeps were taken from 10 cores for each point. Sweeps are lower than the two orbital case, because matrix sizes bigger and the number of processes are much more to calculate the observables. However, the results do not match to the exact diagonalization results. It may be caused by a bug in the source code of the program or the treatment of free expansion parameter γ implemented mistakenly. As seen from figure 6.8, the expectation value of H_J is underestimated.

Although the results do not match to the exact ones, if we plot them as a function of free parameter γ, they are constant as in 2 orbital case. In figure 6.8, results do not change as a function of γ. Here, the number of imaginary-time slices $L = 32$ and the time discretization parameter $\Delta\tau = 0.12$. $J = 0.9$ but $H_U = 0$. The energy eigenvalues are all zero, $\varepsilon_\nu = 0$. 100 warm up and 100 measurement sweeps were taken from 10 cores for each point. A lower number of imaginary-time slices are chosen, because of the bigger matrix sizes.

The last tests of the program involve H_U and H_J together for 2 orbital case. The Hamiltonian becomes

$$H = H_0 + H_U + H_J \tag{6.3}$$

For this Hamiltonian we compared the exact diagonalization results to see the effect of H_J when H_U is present. Figure 6.10 shows the exact diagonalization comparison when $H_U \neq 0$ for $H_J = 0$ and $H_J \neq 0$. The energy eigenvalues are $\varepsilon_1 = 0$ eV and $\varepsilon_2 = 0$ eV. Coulomb interaction between the 3d orbitals $U = 4$ eV and Hund's coupling $J = 0.9$ eV at temperature $T = 3020$ K for this calculation. For chemical potential values between $\mu = 0.5$ and $\mu = 6.5$, H_J is effective and its value is approximately $\langle H_J \rangle = -0.3$. At these chemical potential values, spin-flip and pair-hopping terms suppress the ferromagnetic tendency of the z-component of the Hund's coupling, as seen in figure 6.10b. However, no apparent change in the total occupation.

In figure 6.11, the comparison between the QMC results and the exact diagonalization results are for $U = 4$ eV and $J = 0.9$ eV at temperature $T = 3020$ K. In QMC simulations $\Delta\tau = 0.12$ and $L = 32$, the free parameter $\gamma - \beta J = 0.3$, 10000 warm up and 50000 measurement sweeps were taken at 30 processors for each point on the graph in QMC simulations, and the energy eigenvalues are $\varepsilon_1 = 0$ eV and $\varepsilon_2 = 0$ eV. The QMC measurements do not match to exact diagonalization results for these calculations. However, the behavior is similar to the exact results. The expectation value of H_J

is overestimated here. Thus, it lowers the value of the total magnetic moment more than expected.

For 2 orbital case, we have tested our algorithm at $T = 700$ K, as well. In figure 6.12, QMC results and exact diagonalization calculations are compared for for $U = 4$ eV and $J = 0.9$ eV at $T = 700$ K, $\Delta\tau = 0.13810$ and $L = 120$, the free parameter $\gamma - \beta J = 0.3$, and 1000 warm up and 4000 measurement sweeps were taken at 32 processors for each point on the graph. The energy eigenvalues are $\varepsilon_1 = 0$ eV and $\varepsilon_2 = 0$ eV. Here, the behavior is similar with 6.11. For total occupation numbers, the jumps are located at different chemical potential values compared to exact diagonalization calculations since the expectation value of H_J is overestimated in QMC results. This causes the magnetization values to be lowered more than expected.

In 6.13, we have compared QMC results and the exact diagonalization results for non-degenerate impurity energies for $U = 4$ eV and $J = 0.9$ eV at $T = 700$ K, $\Delta\tau = 0.13810$ and $L = 120$, the free parameter $\gamma - \beta J = 0.3$. The energy eigenvalues are $\varepsilon_1 = 0$ eV and $\varepsilon_2 = 2$ eV. 1000 warm up and 4000 measurement sweeps were taken at 32 processors for each point on the graph. The jumps are located at different chemical potential values similar to the previous cases 6.11 and 6.12. The expectation value of H_J is overestimated again. Resulting a dramatic decrement in the magnetization values.

In figure 6.14, we present the distributions of the expansion orders sampled in the QMC simulations. These results are for theoretical 2-orbital case. $H_U = 0$ and $H_J \neq 0$. The energy eigenvalues are $\varepsilon_1 = 0$ eV and $\varepsilon_2 = 0$ eV. Hund's coupling $J = 0.9$ eV at temperature $T = 3020$ K for this calculations. As the free parameter $\gamma - \beta J$ increases, the distribution shifts to the right so that the contribution from the higher orders can be sampled. The expansion orders are sampled from a normally distributed space as seen in the figures. However, for the figures 6.15, the expansion orders for Monte Carlo samples are not normally distributed. For the calculation in figure 6.15, the only difference is $H_U \neq 0$ and Coulomb interaction is $U = 4$ eV. This may be related to the overestimated expectation values of H_J terms and transition probabilities that we choose. The distributions have skewness and for high values of measurement sweeps, they converge to a certain skewness value.

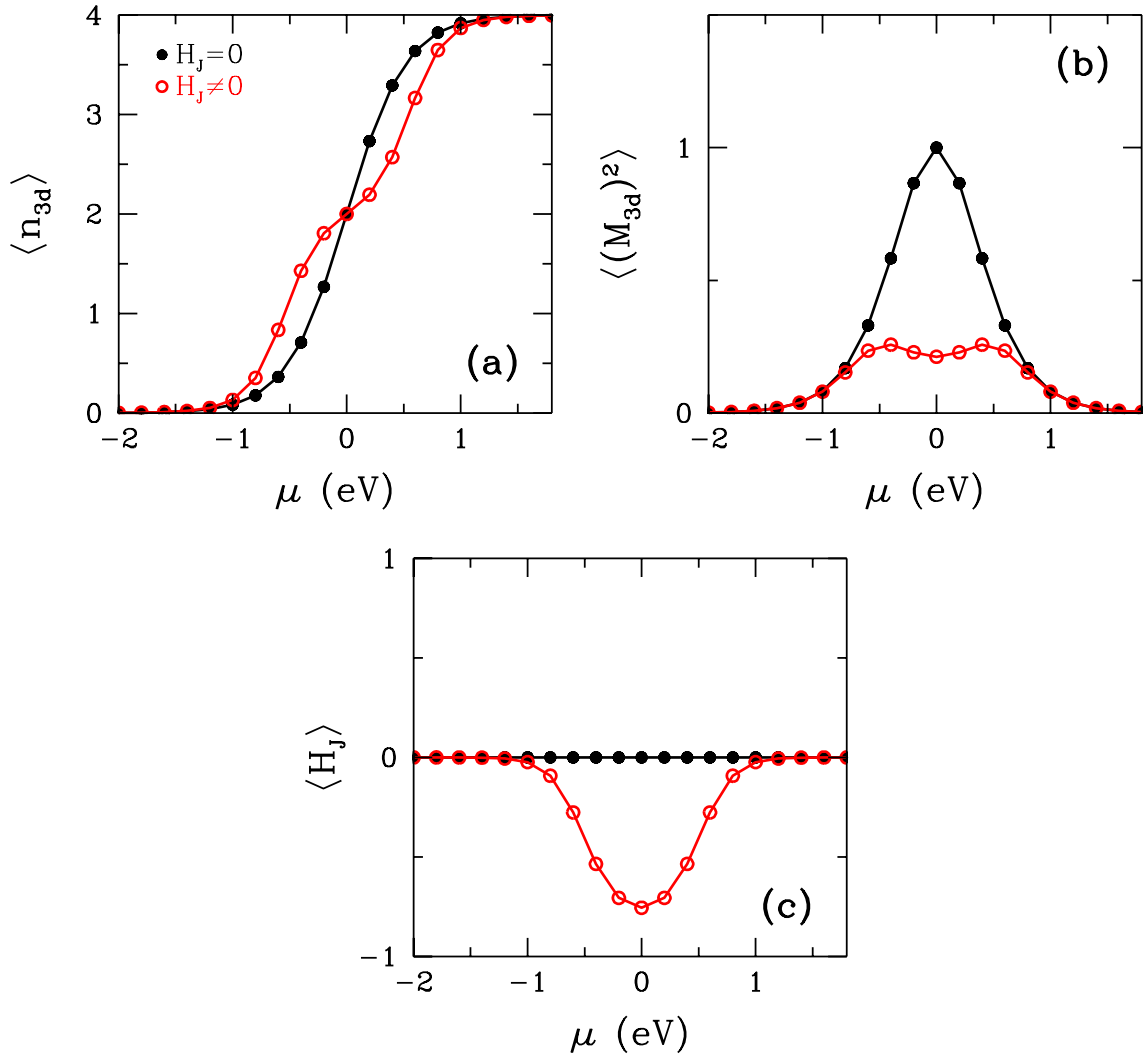

Figure 6.1. Exact diagonalization results plotted as a function of chemical potential μ, for theoretical 2-impurity orbitals of degenerate energy levels, and no hybridization between the host and the impurity. $\varepsilon_1 = 0$ eV and $\varepsilon_2 = 0$ eV. Coulomb interaction between the 3d orbitals $U = 0$ eV and Hund's coupling $J = 0.9$ eV at temperature $T = 3020$ K. Red empty dots indicates the calculations with $H_U = 0$ and $H_J \neq 0$, black filled dots indicates the calculations with $H_U = 0$ and $H_J = 0$. (a) Total occupation number of the 3d orbitals $\langle n_{3d} \rangle$ versus chemical potential μ. (b) Square of the total magnetic moment at the 3d orbitals $\langle (M_{3d})^2 \rangle$ versus chemical potential μ. (c) Expectation value of H_J versus chemical potential μ.

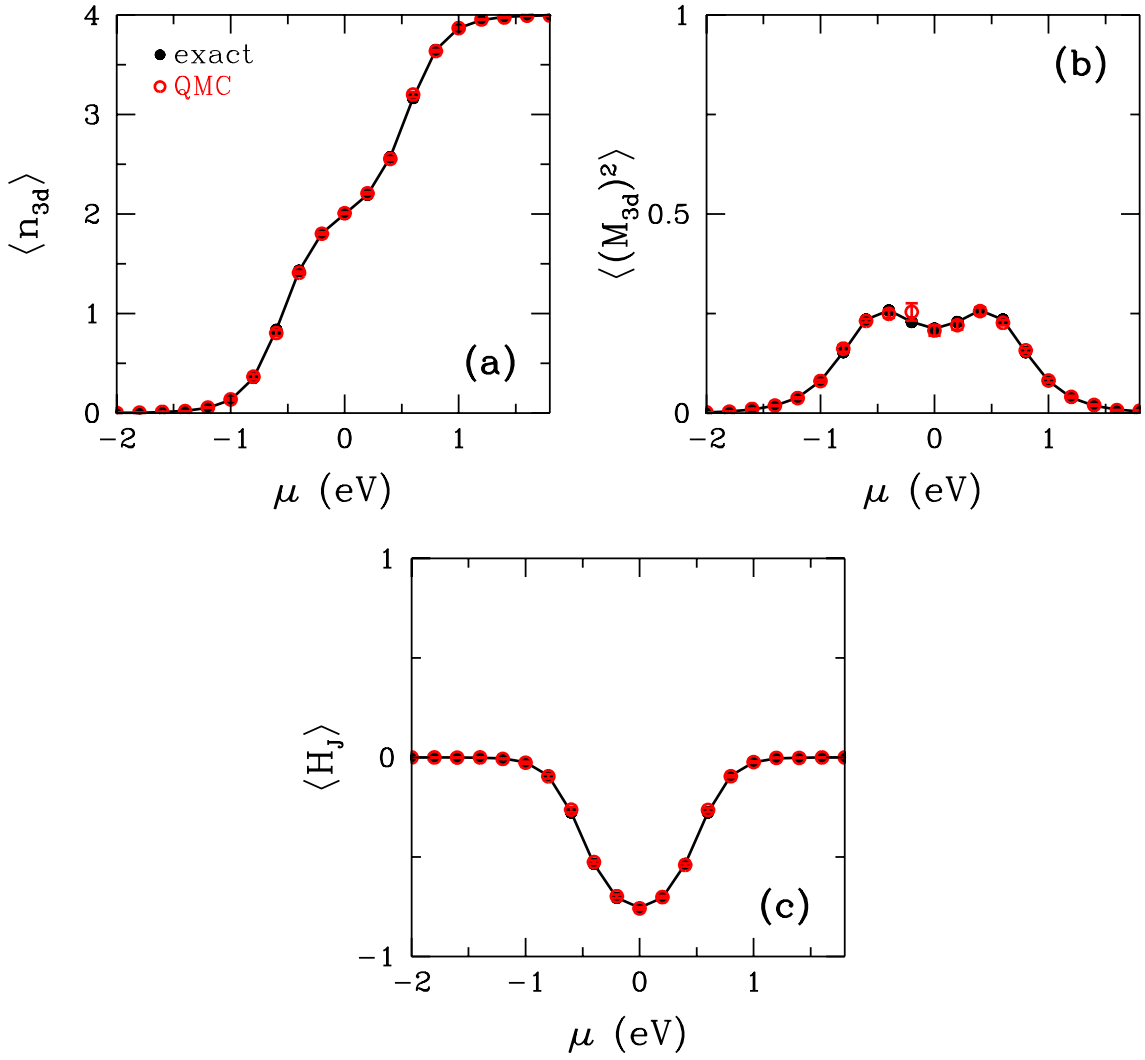

Figure 6.2. Exact diagonalization vs QMC comparison results plotted as a function of chemical potential μ, for theoretical 2-impurity orbitals of energies $\varepsilon_1 = 0$ eV and $\varepsilon_2 = 0$ eV at temperature $T = 3020$ K. In these calculations $H_U = 0$ and $H_J \neq 0$. The transverse components of Hund's coupling $J = 0.9$ eV. In QMC simulations $\Delta\tau = 0.06$ and $L = 64$. The free parameter $\gamma - \beta J = 0.3$. 2000 warm up and 5000 measurement sweeps were taken for QMC simulations. Red empty dots for calculations with the QMC simulations, black filled dots for the exact diagonalization results. (a) Total occupation number of the 3d orbitals $\langle n_{3d} \rangle$ versus chemical potential μ. (b) Square of the total magnetic moment at the 3d orbitals $\langle (M_{3d})^2 \rangle$ versus chemical potential μ. (c) Expectation value of H_J versus chemical potential μ.

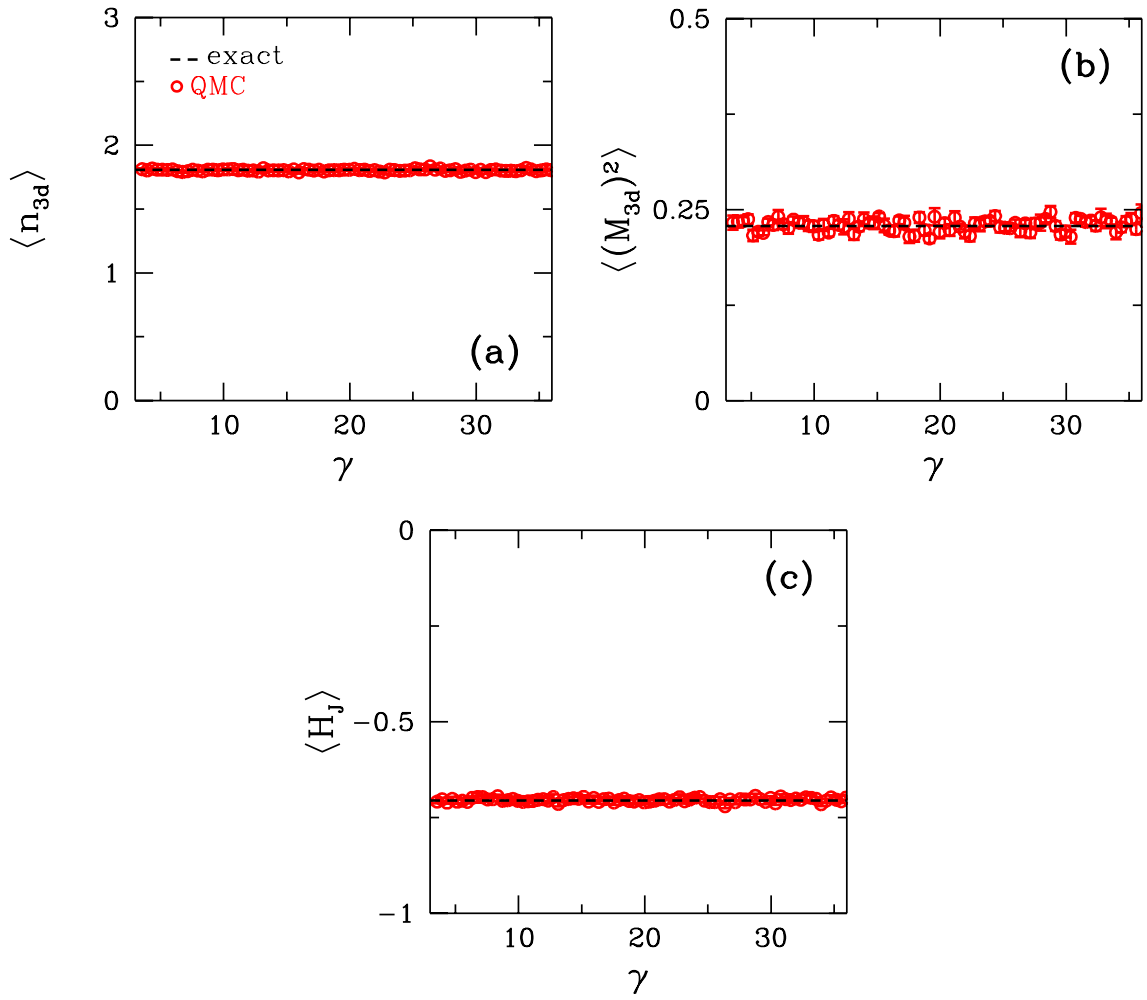

Figure 6.3. Exact diagonalization vs QMC comparison results plotted as a function of the free expansion parameter γ, for theoretical 2-impurity orbitals of energies $\varepsilon_1 = 0$ eV and $\varepsilon_2 = 0$ eV at temperature $T = 3020$ K. In these calculations $H_U = 0$ and $H_J \neq 0$. The transverse components of Hund's coupling $J = 0.9$ eV. In QMC simulations $\Delta\tau = 0.06$ and $L = 64$. The chemical potential is constant as $\mu = -0.2$. 5000 warm up and 10000 measurement sweeps were taken for QMC simulations. Red empty dots for calculations with the QMC simulations, black dashed line for the exact diagonalization result. (a) Total occupation number of the 3d orbitals $\langle n_{3d} \rangle$ versus free expansion parameter γ. (b) Square of the total magnetic moment at the 3d orbitals $\langle (M_{3d})^2 \rangle$ versus free expansion parameter γ. (c) Expectation value of H_J versus free expansion parameter γ.

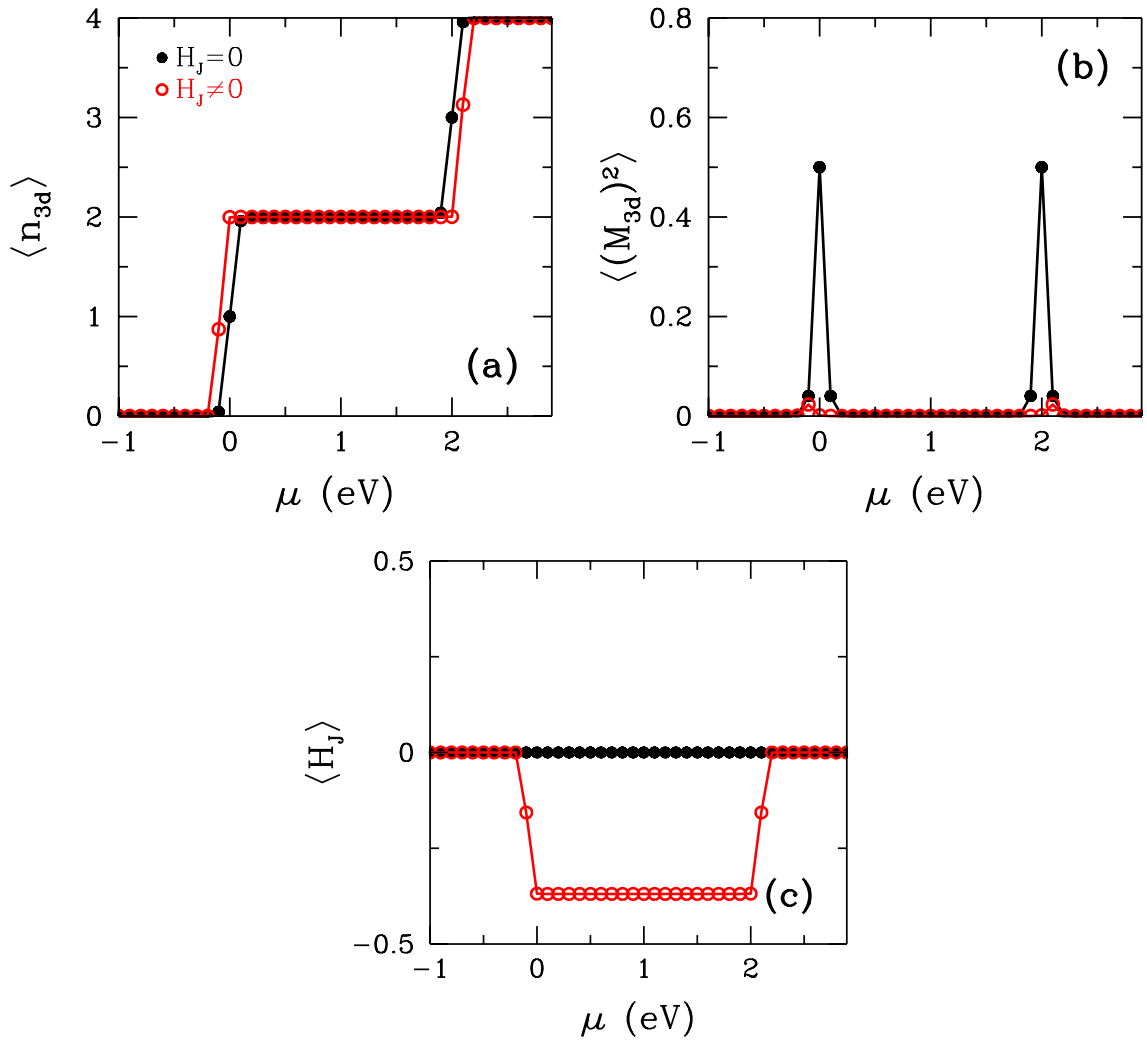

Figure 6.4. Exact diagonalization results plotted as a function of chemical potential μ, for theoretical 2-impurity orbitals of non-degenerate energy levels, and no hybridization between the host and the impurity. $\varepsilon_1 = 0$ eV and $\varepsilon_2 = 2$ eV. Coulomb interaction between the 3d orbitals $U = 0$ eV and Hund's coupling $J = 0.9$ eV at temperature $T = 300$ K. Red empty dots indicates the calculations with $H_U = 0$ and $H_J \neq 0$, black filled dots indicates the calculations with $H_U = 0$ and $H_J = 0$. (a) Total occupation number of the 3d orbitals $\langle n_{3d} \rangle$ versus chemical potential μ. (b) Square of the total magnetic moment at the 3d orbitals $\langle (M_{3d})^2 \rangle$ versus chemical potential μ. (c) Expectation value of H_J versus chemical potential μ.

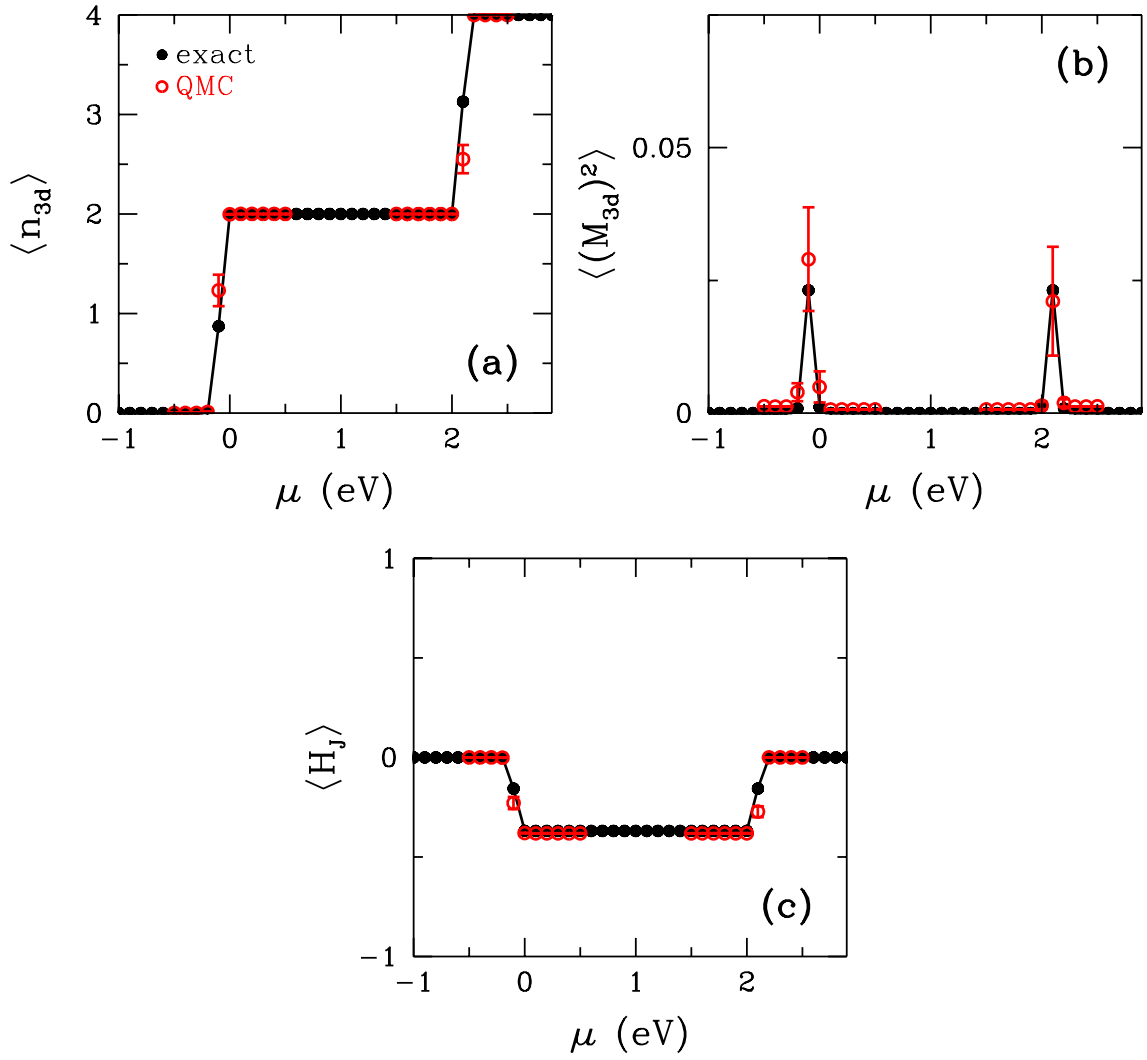

Figure 6.5. Exact diagonalization vs QMC comparison results plotted as a function of chemical potential μ, for theoretical 2-impurity orbitals of energies $\varepsilon_1 = 0$ eV and $\varepsilon_2 = 2$ eV at temperature $T = 300$ K. In these calculations $H_U = 0$ and $H_J \neq 0$. The transverse components of Hund's coupling $J = 0.9$ eV. In QMC simulations $\Delta\tau = 0.13063$ and $L = 296$. The free parameter $\gamma - \beta J = 0.3$. 5000 warm up and 5000 measurement sweeps and 32 cpu per point were taken in QMC simulations. Red empty dots for calculations with the QMC simulations, black filled dots for the exact diagonalization results. (a) Total occupation number of the 3d orbitals $\langle n_{3d} \rangle$ versus chemical potential μ. (b) Square of the total magnetic moment at the 3d orbitals $\langle (M_{3d})^2 \rangle$ versus chemical potential μ. (c) Expectation value of H_J versus chemical potential μ.

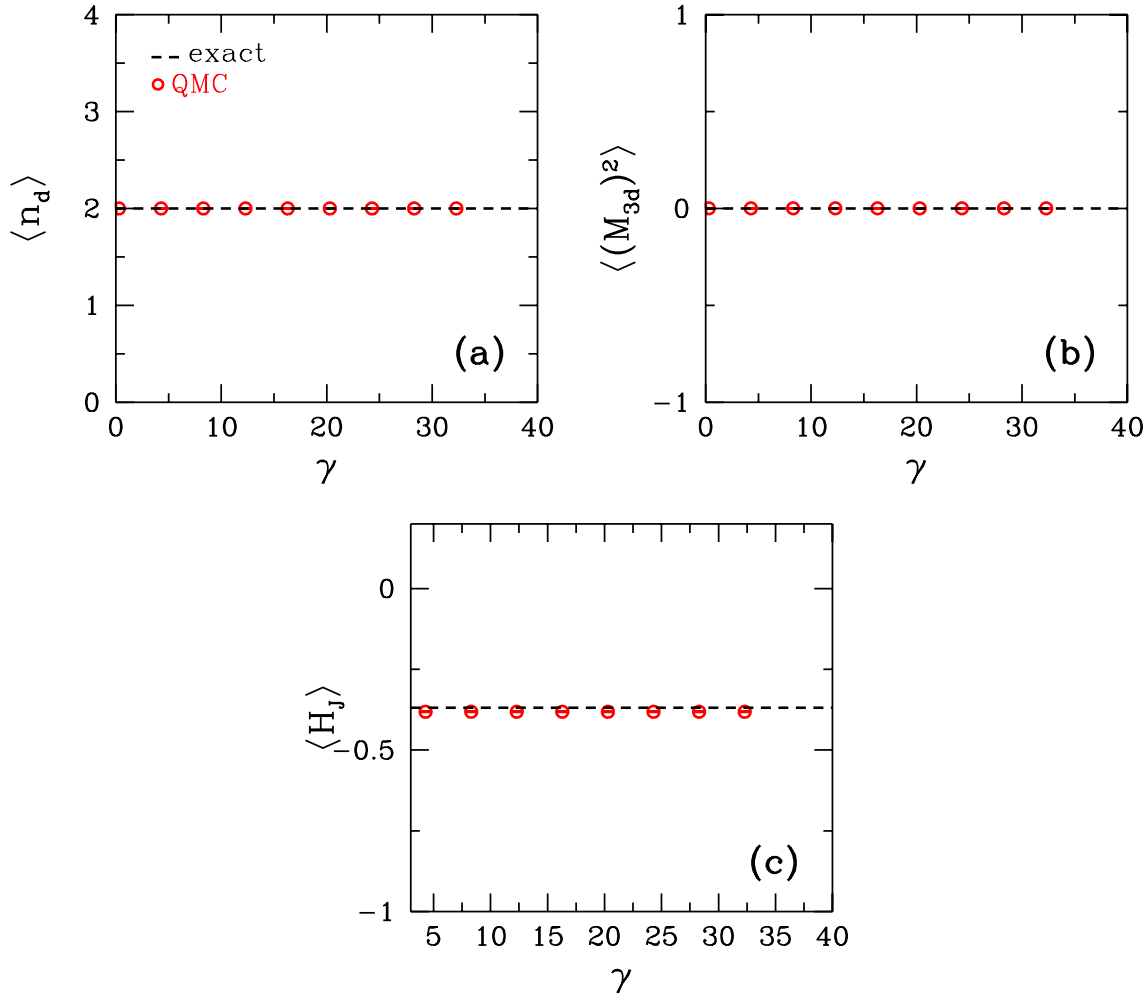

Figure 6.6. Exact diagonalization vs QMC comparison results plotted as a function of the free expansion parameter γ, for theoretical 2-impurity orbitals of energies $\varepsilon_1 = 0$ eV and $\varepsilon_2 = 2$ eV at temperature $T = 300$ K. In these calculations $H_U = 0$ and $H_J \neq 0$. The transverse components of Hund's coupling $J = 0.9$ eV. In QMC simulations $\Delta\tau = 0.13063$ and $L = 296$. The chemical potential is constant as $\mu = 1.0$ eV. 5000 warm up and 5000 measurement sweeps and 32 cpu per point were taken in QMC simulations. Red empty dots for calculations with the QMC simulations, black dashed line for the exact diagonalization result. (a) Total occupation number of the 3d orbitals $\langle n_{3d} \rangle$ versus free expansion parameter γ. (b) Square of the total magnetic moment at the 3d orbitals $\langle (M_{3d})^2 \rangle$ versus free expansion parameter γ. (c) Expectation value of H_J versus free expansion parameter γ.

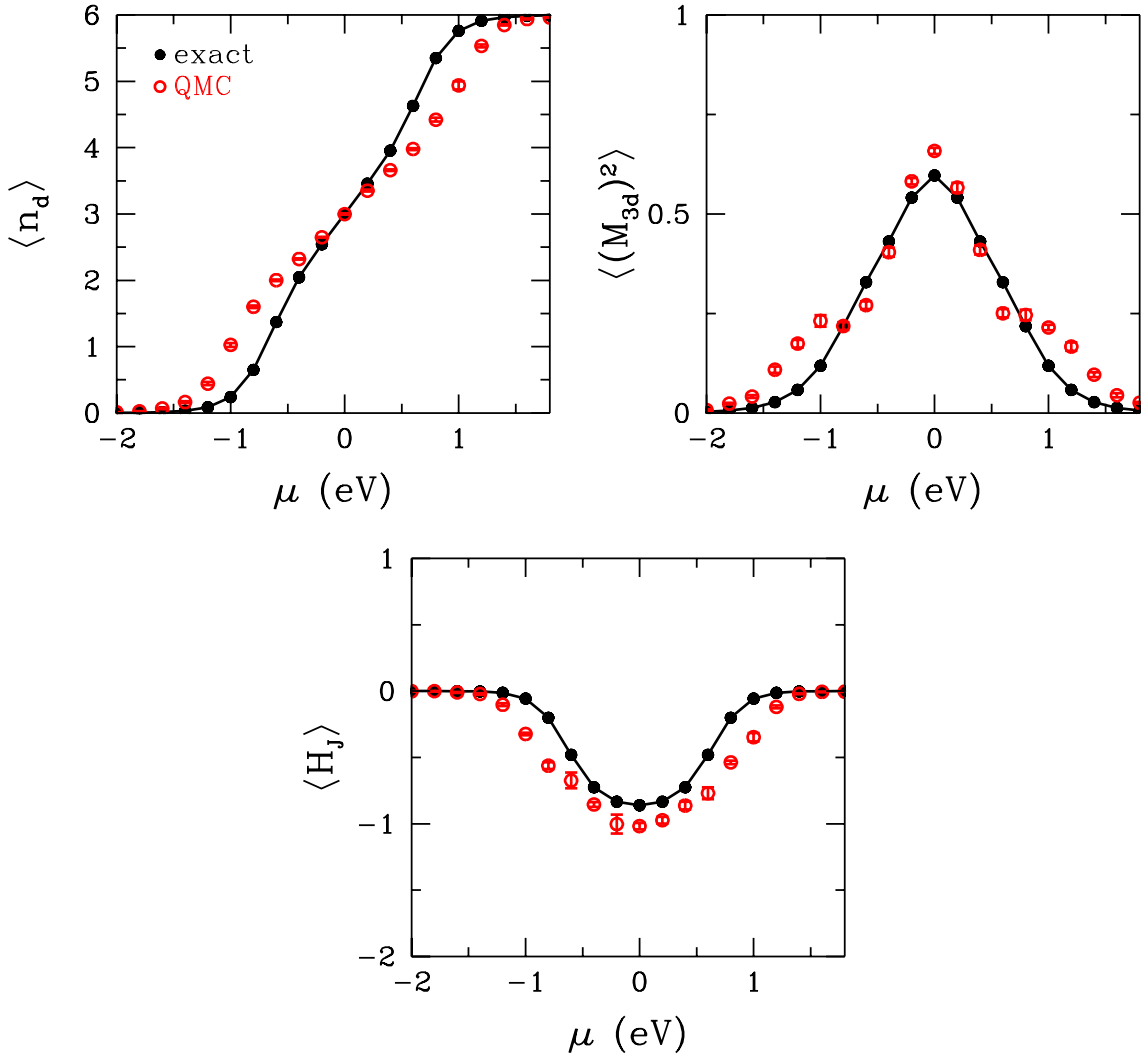

Figure 6.7. Exact diagonalization vs QMC comparison results plotted as a function of chemical potential μ, for theoretical 3-impurity orbitals of energies $\varepsilon_\nu = 0$ eV for all at temperature $T = 3020$ K. In these calculations $H_U = 0$ and $H_J \neq 0$. The transverse components of Hund's coupling $J = 0.9$ eV. In QMC simulations $\Delta\tau = 0.06$ and $L = 64$. The free parameter $\gamma - \beta J = 0.3$. 5000 warm up and 10000 measurement sweeps were taken in QMC simulations. Red empty dots for calculations with the QMC simulations, black filled dots for the exact diagonalization results. (a) Total occupation number of the 3d orbitals $\langle n_{3d} \rangle$ versus chemical potential μ. (b) Square of the total magnetic moment at the 3d orbitals $\langle (M_{3d})^2 \rangle$ versus chemical potential μ. (c) Expectation value of H_J versus chemical potential μ.

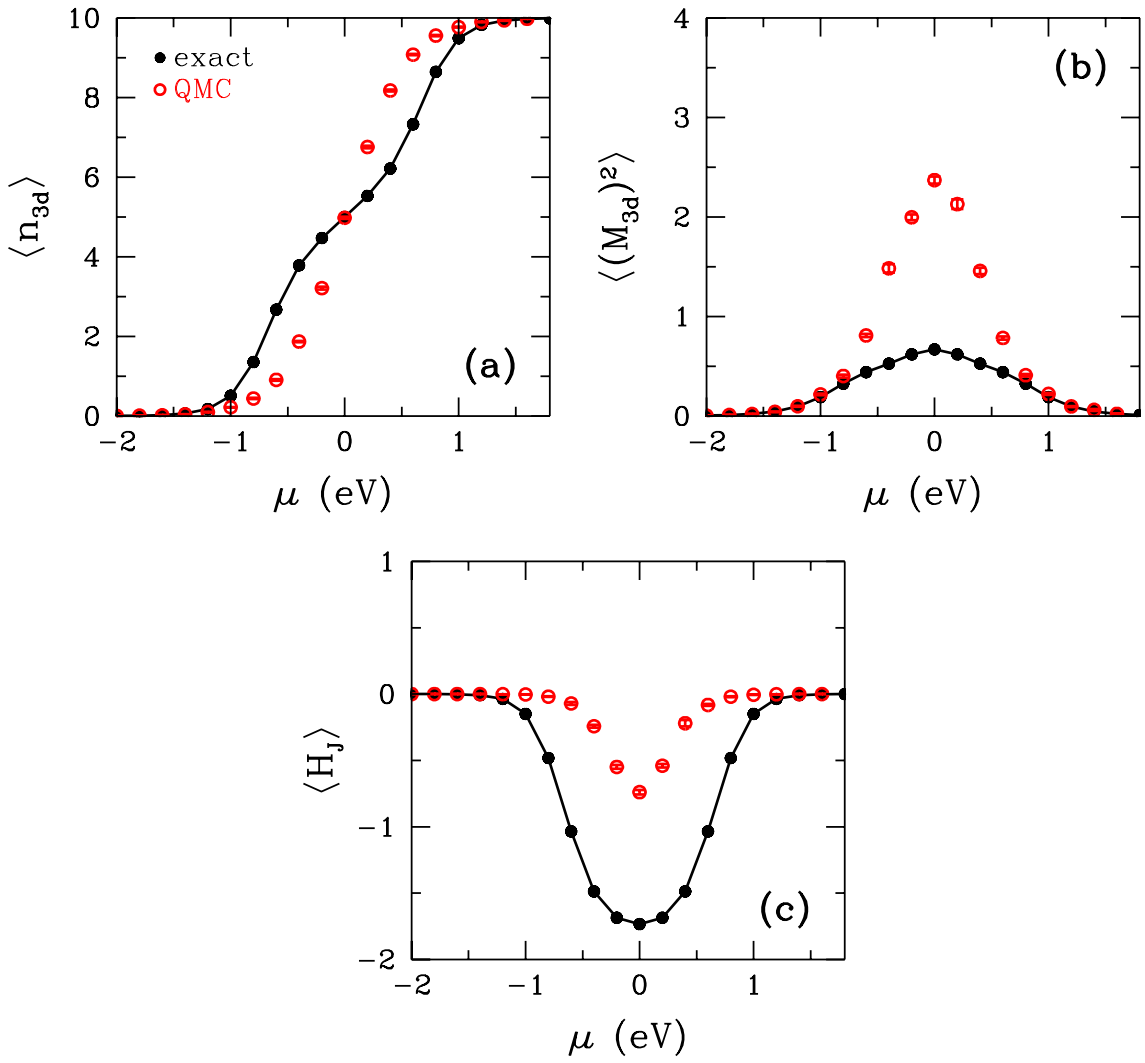

Figure 6.8. Exact diagonalization vs QMC comparison results plotted as a function of chemical potential μ, for theoretical 5-impurity orbitals of energies $\varepsilon_\nu = 0$ eV for all at temperature $T = 3020$ K. In these calculations $H_U = 0$ and $H_J \neq 0$. The transverse components of Hund's coupling $J = 0.9$ eV. In QMC simulations $\Delta\tau = 0.06$ and $L = 64$. The free parameter $\gamma - \beta J = 0.3$. 100 warm up and 100 measurement sweeps were taken at 10 processors for each point on the graph in QMC simulations. Red empty dots for calculations with the QMC simulations, black filled dots for the exact diagonalization results. (a) Total occupation number of the 3d orbitals $\langle n_{3d} \rangle$ versus chemical potential μ. (b) Square of the total magnetic moment at the 3d orbitals $\langle (M_{3d})^2 \rangle$ versus chemical potential μ. (c) Expectation value of H_J versus chemical potential μ.

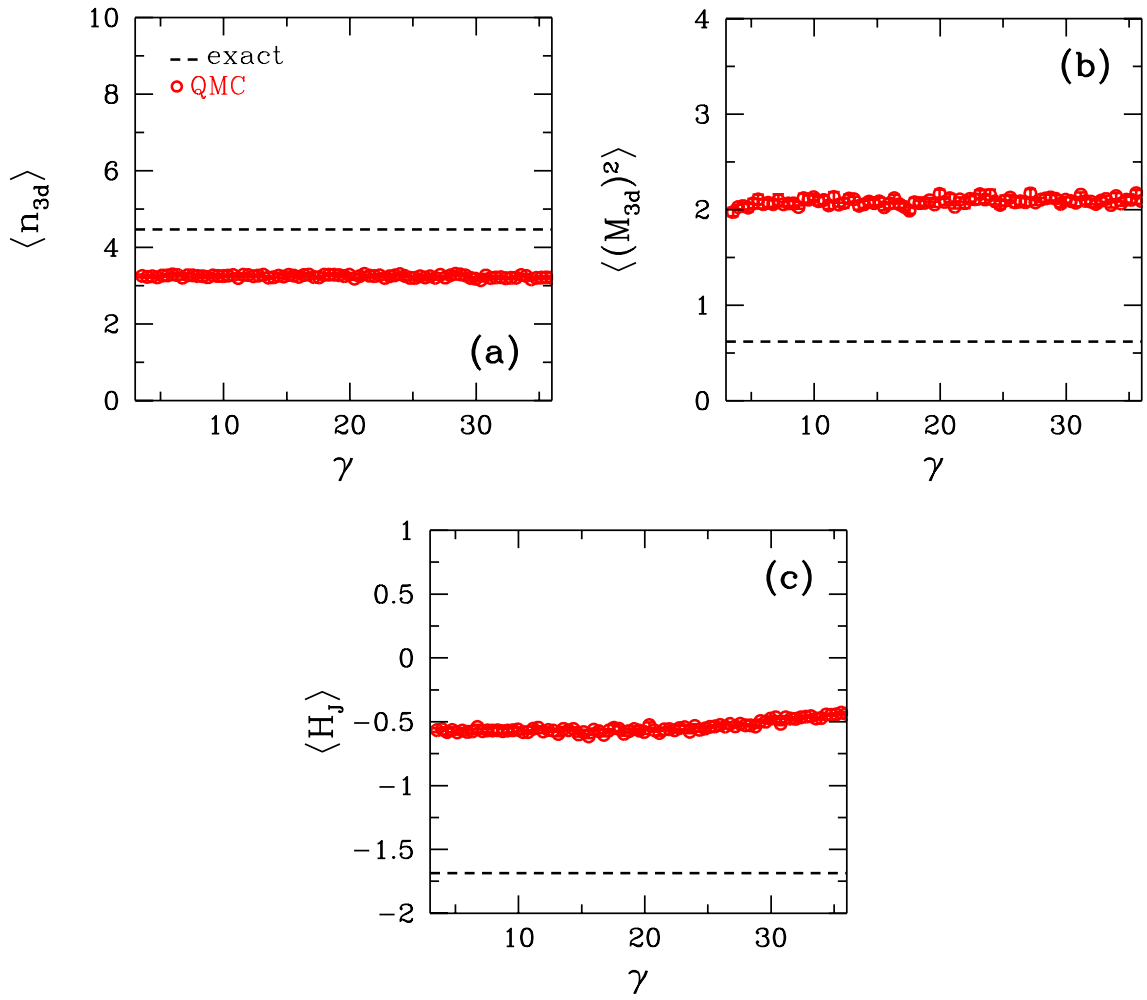

Figure 6.9. Exact diagonalization vs QMC comparison results plotted as a function of the free expansion parameter γ, for theoretical 5-impurity orbitals of energies $\varepsilon_\nu = 0$ eV for all at temperature $T = 3020$ K. In these calculations $H_U = 0$ and $H_J \neq 0$. The transverse components of Hund's coupling $J = 0.9$ eV. In QMC simulations $\Delta\tau = 0.12$ and $L = 32$. The chemical potential is constant as $\mu = -0.2$. 100 warm up and 100 measurement sweeps were taken at 10 processors for each point on the graph in QMC simulations. Red empty dots for calculations with the QMC simulations, black black dashed line for the exact diagonalization result. (a) Total occupation number of the 3d orbitals $\langle n_{3d} \rangle$ versus free expansion parameter γ. (b) Square of the total magnetic moment at the 3d orbitals $\langle (M_{3d})^2 \rangle$ versus free expansion parameter γ. (c) Expectation value of H_J versus free expansion parameter γ.

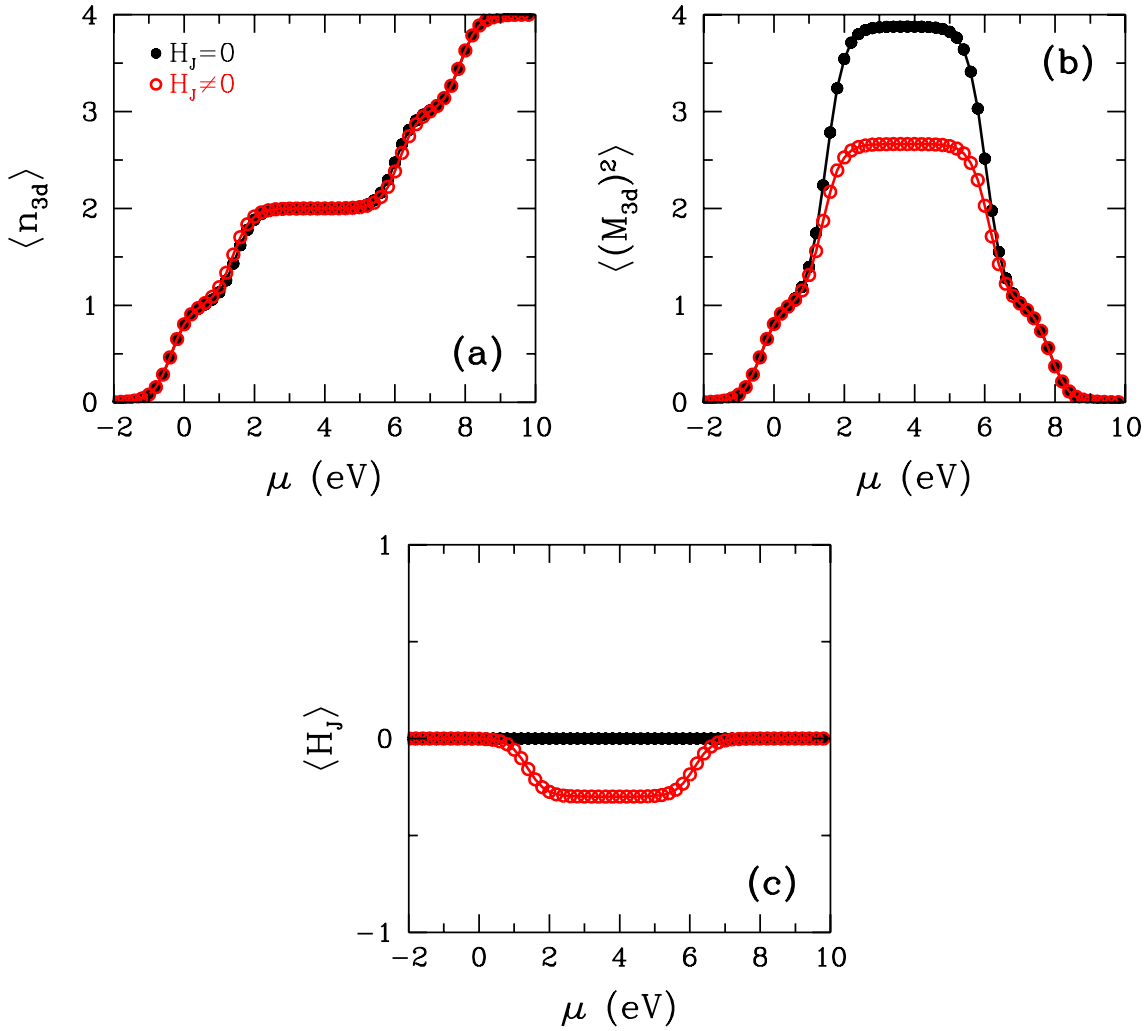

Figure 6.10. Exact diagonalization results plotted as a function of chemical potential μ, for theoretical 2-impurity orbitals of degenerate energy levels, and no hybridization between the host and the impurity. $\varepsilon_1 = 0$ eV and $\varepsilon_2 = 0$ eV. Coulomb interaction between the 3d orbitals $U = 4$ eV and Hund's coupling $J = 0.9$ eV at temperature $T = 3020$ K. Red empty dots indicates the calculations with $H_J \neq 0$, black filled dots indicates the calculations with $H_J = 0$. (a) Total occupation number of the 3d orbitals $\langle n_{3d} \rangle$ versus chemical potential μ. (b) Square of the total magnetic moment at the 3d orbitals $\langle (M_{3d})^2 \rangle$ versus chemical potential μ. (c) Expectation value of H_J versus chemical potential μ.

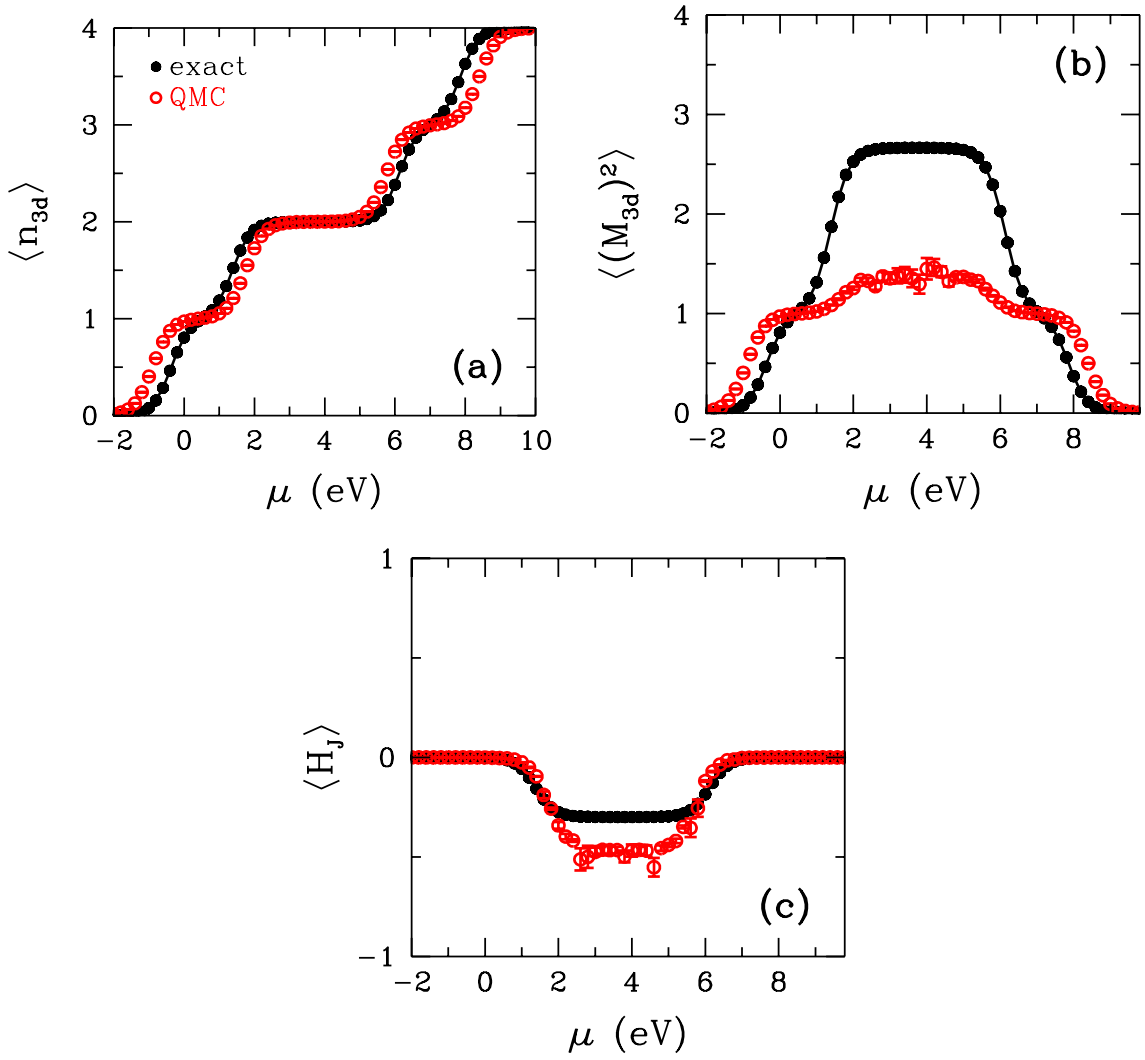

Figure 6.11. Exact diagonalization vs QMC comparison results plotted as a function of chemical potential μ, for theoretical 2-impurity orbitals of energies $\varepsilon_1 = 0$ eV and $\varepsilon_2 = 0$ eV at temperature $T = 3020$ K. In these calculations $H_U \neq 0$ and $H_J \neq 0$. The transverse components of Hund's coupling $J = 0.9$ eV and Coulomb interaction between the 3d orbitals $U = 4$ eV. In QMC simulations $\Delta\tau = 0.12$ and $L = 32$. The free parameter $\gamma - \beta J = 0.3$. 10000 warm up and 50000 measurement sweeps were taken at 30 processors for each point on the graph in QMC simulations. Red empty dots for calculations with the QMC simulations, black filled dots for the exact diagonalization results. (a) Total occupation number of the 3d orbitals $\langle n_{3d} \rangle$ versus chemical potential μ. (b) Square of the total magnetic moment at the 3d orbitals $\langle (M_{3d})^2 \rangle$ versus chemical potential μ. (c) Expectation value of H_J versus chemical potential μ.

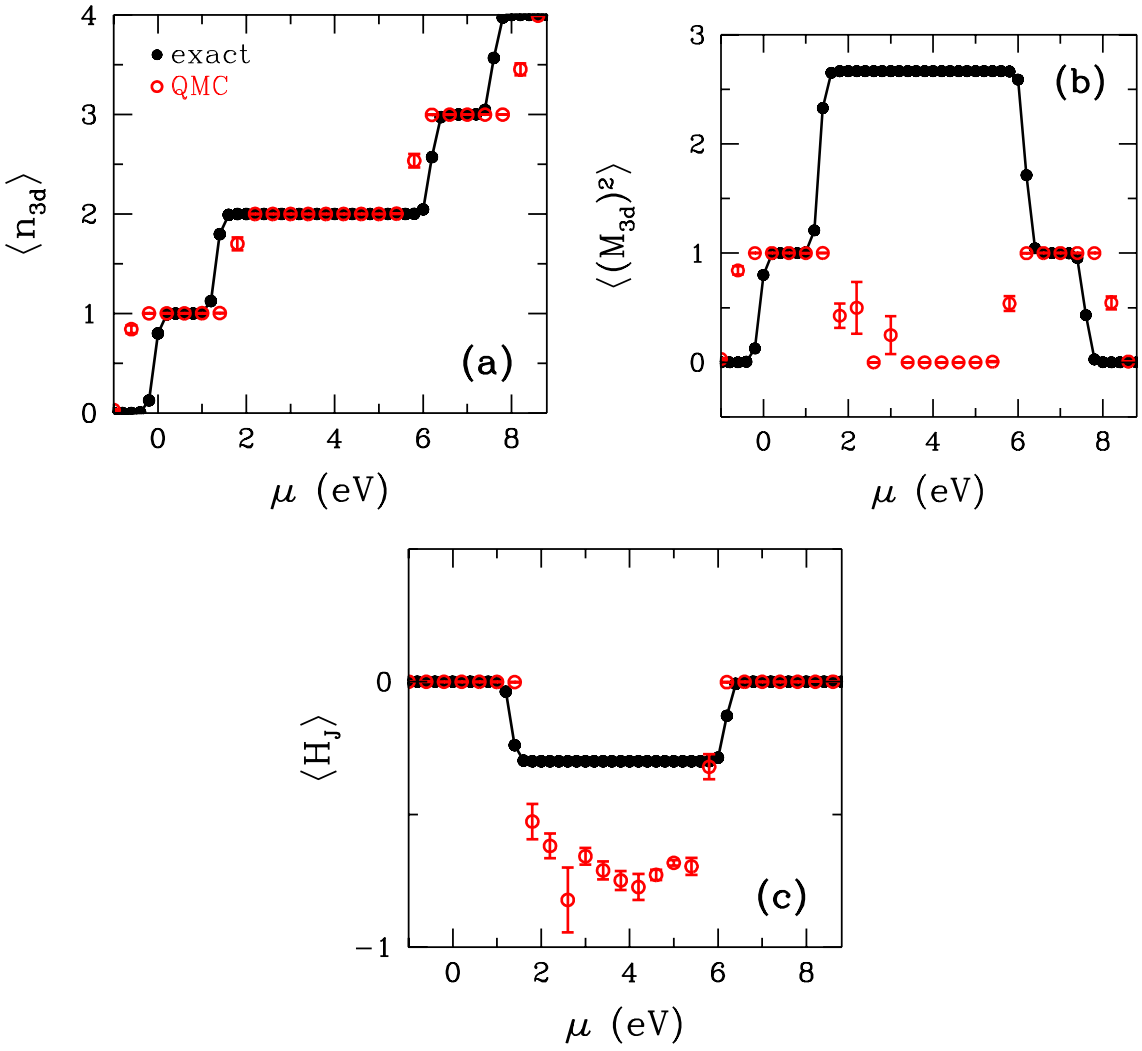

Figure 6.12. Exact diagonalization vs QMC comparison results plotted as a function of chemical potential μ, for theoretical 2-impurity orbitals of energies $\varepsilon_1 = 0$ eV and $\varepsilon_2 = 0$ eV at temperature $T = 700$ K. In these calculations $H_U \neq 0$ and $H_J \neq 0$. The transverse components of Hund's coupling $J = 0.9$ eV and Coulomb interaction between the 3d orbitals $U = 4$ eV. In QMC simulations $\Delta\tau = 0.13810$ and $L = 120$. The free parameter $\gamma - \beta J = 0.3$. 1000 warm up and 4000 measurement sweeps were taken at 32 processors for each point on the graph in QMC simulations. Red empty dots for calculations with the QMC simulations, black filled dots for the exact diagonalization results. (a) Total occupation number of the 3d orbitals $\langle n_{3d} \rangle$ versus chemical potential μ. (b) Square of the total magnetic moment at the 3d orbitals $\langle (M_{3d})^2 \rangle$ versus chemical potential μ. (c) Expectation value of H_J versus chemical potential μ.

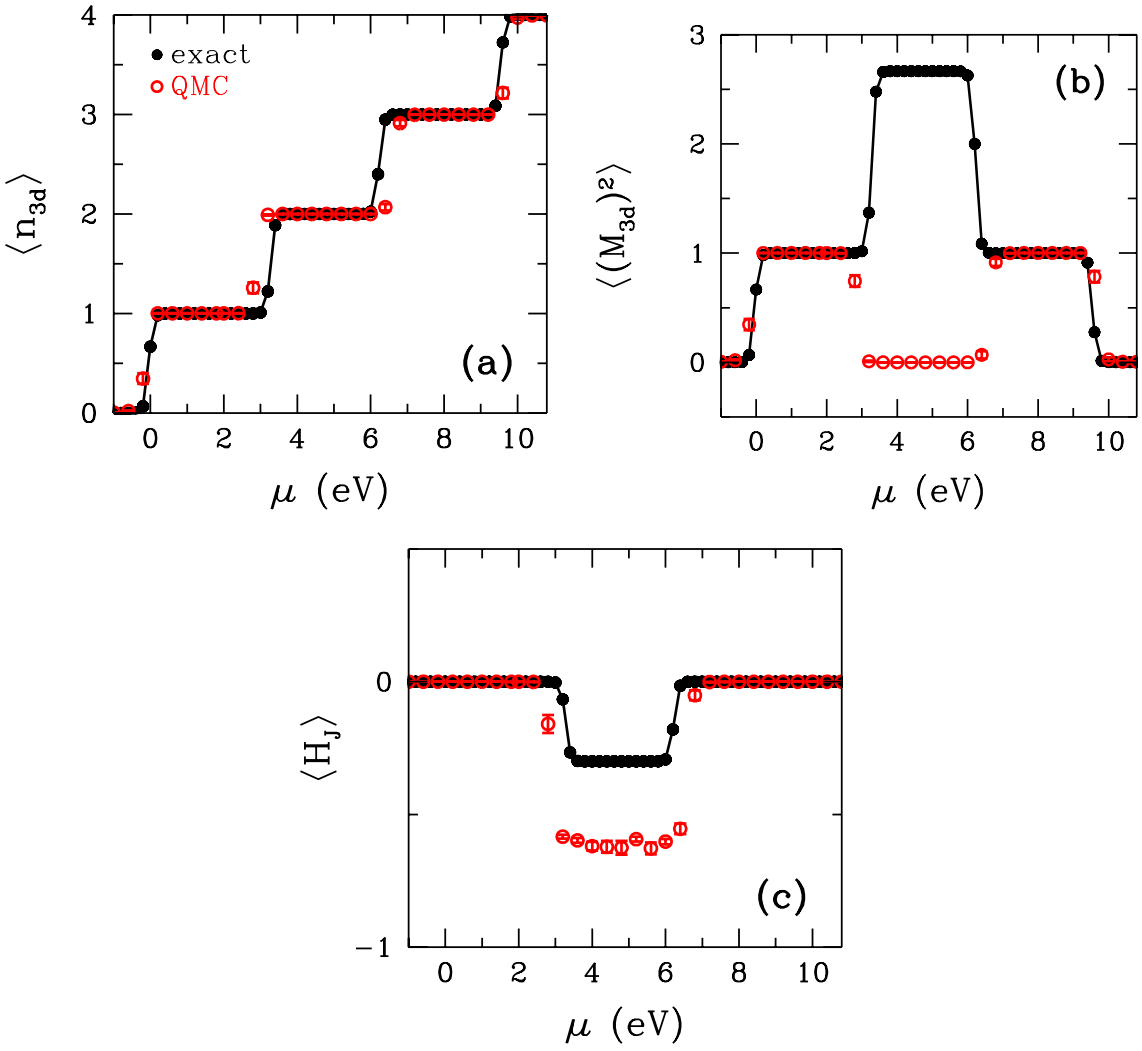

Figure 6.13. Exact diagonalization vs QMC comparison results plotted as a function of chemical potential μ, for theoretical 2-impurity orbitals of energies $\varepsilon_1 = 0$ eV and $\varepsilon_2 = 2$ eV at temperature $T = 700$ K. In these calculations $H_U \neq 0$ and $H_J \neq 0$. The transverse components of Hund's coupling $J = 0.9$ eV. In QMC simulations $\Delta\tau = 0.13810$ and $L = 120$. The free parameter $\gamma - \beta J = 0.3$. 1000 warm up and 4000 measurement sweeps were taken at 32 processors for each point on the graph in QMC simulations. Red empty dots for calculations with the QMC simulations, black filled dots for the exact diagonalization results. (a) Total occupation number of the 3d orbitals $\langle n_{3d} \rangle$ versus chemical potential μ. (b) Square of the total magnetic moment at the 3d orbitals $\langle (M_{3d})^2 \rangle$ versus chemical potential μ. (c) Expectation value of H_J versus chemical potential μ.

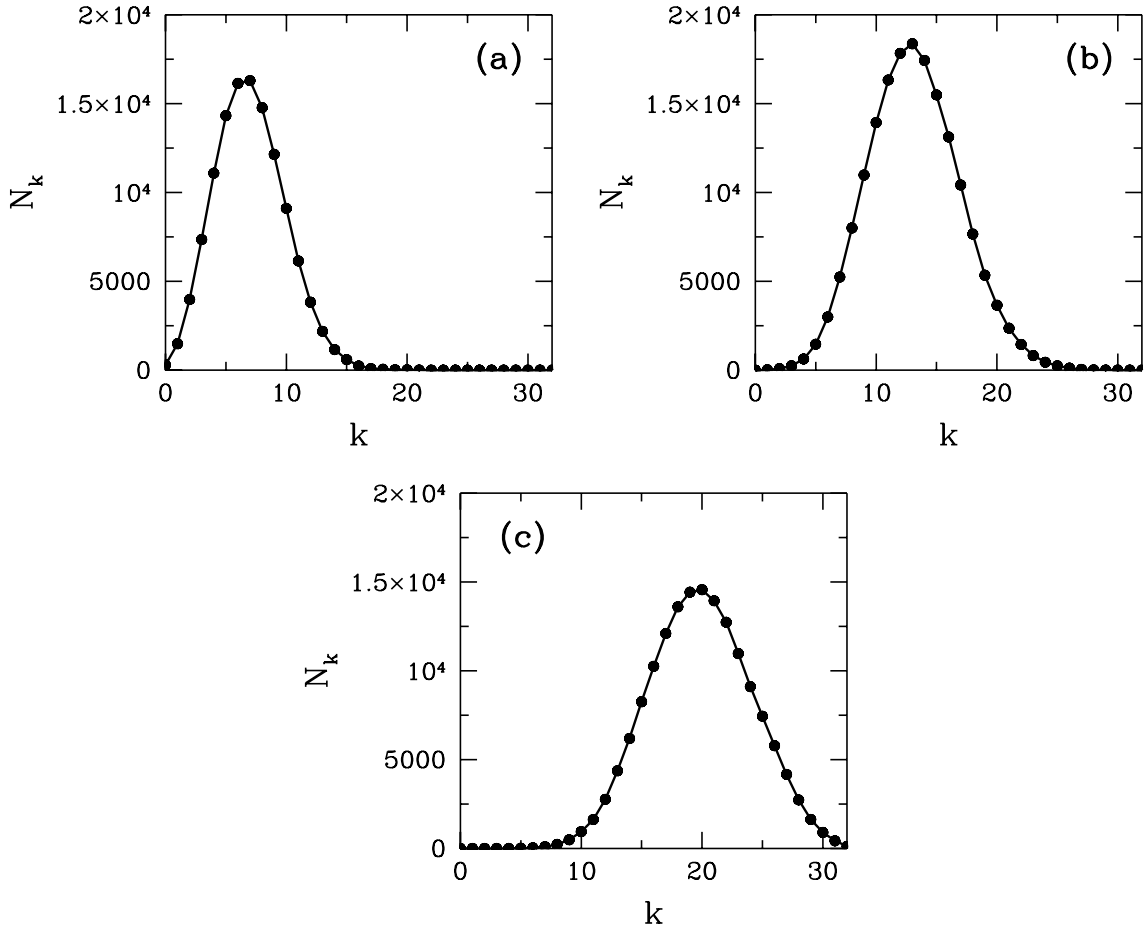

Figure 6.14. Histograms of the expansion orders from the QMC simulations for typical parameters for theoretical 2-impurity orbitals of degenerate energies $\varepsilon_1 = 0$ eV and $\varepsilon_2 = 0$ eV at temperature $T = 3020$ K. $H_U = 0$, $H_J \neq 0$ and $J = 0.9$ eV. $\Delta\tau = 0.12$ and $L = 32$. 5000 warm up and 10000 measurement sweeps. a) The free parameter $\gamma - \beta J = 0.3$. The average expansion order $\langle k \rangle \approx 6$. b) The free parameter $\gamma - \beta J = 7$. The average expansion order $\langle k \rangle \approx 13$. c) The free parameter $\gamma - \beta J = 15$. The average expansion order $\langle k \rangle \approx 20$.

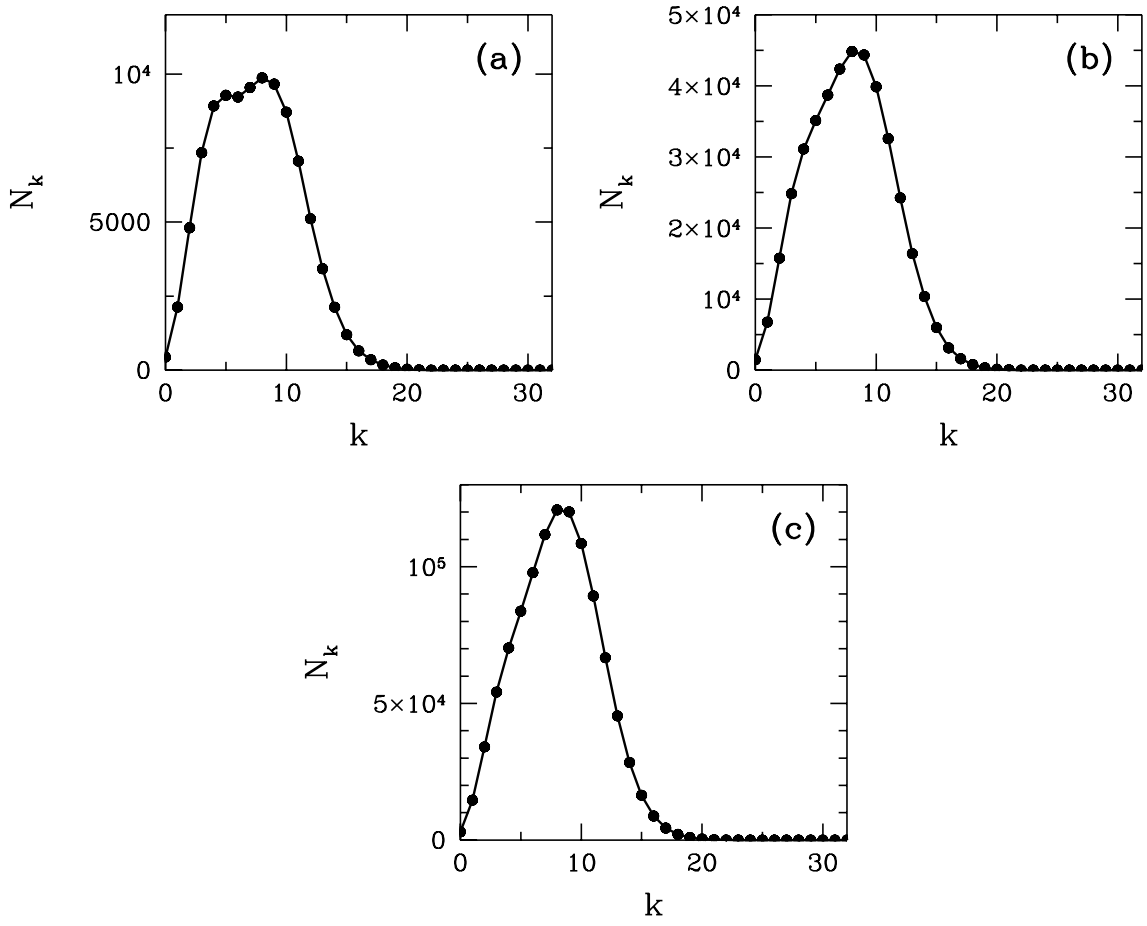

Figure 6.15. Histograms of the expansion orders from the QMC simulations for typical parameters for theoretical 2-impurity orbitals of degenerate energies $\varepsilon_1 = 0$ eV and $\varepsilon_2 = 0$ eV at temperature $T = 3020$ K. $H_U \neq 0$, $H_J \neq 0$ and $U = 4$ eV, $J = 0.9$ eV. $\Delta\tau = 0.12$ and $L = 32$. The free parameter $\gamma - \beta J = 0.3$. a) 5000 warm up and 10000 measurement sweeps. The average expansion order $\langle k \rangle \approx 6$. b) 10000 warm up and 50000 measurement sweeps. The average expansion order $\langle k \rangle \approx 7$. c) 50000 warm up and 100000 measurement sweeps. The average expansion order $\langle k \rangle \approx 7$.

6.2. Tests of the QMC Algorithm for Series Expansion of $U' - J$ Term

Here, we have constructed a Hamiltonian which only includes the z-component of the Hund's coupling.

$$H = H_0 + H_U + H_{U'-J} \tag{6.4}$$

where

$$\begin{aligned} H_U &= \sum_{\nu} \left[U n_{\nu\uparrow} n_{\nu\downarrow} - \frac{U}{2}(n_{\nu\uparrow} + n_{\nu\downarrow}) \right] + \sum_{\nu>\nu',\sigma} \left[U' n_{\nu\sigma} n_{\nu',-\sigma} - \frac{U'}{2}(n_{\nu\sigma} + n_{\nu',-\sigma}) \right] \\ H_{U'-J} &= \sum_{\nu>\nu',\sigma} \left[(U'-J) n_{\nu\sigma} n_{\nu'\sigma} - \frac{(U'-J)}{2}(n_{\nu\sigma} + n_{\nu'\sigma}) \right] \end{aligned} \tag{6.5}$$

We expanded the Boltzmann factor with respect to $H_{U'-J}$

$$\begin{aligned} e^{-\beta(H_0+H_U)+(\gamma-\beta H_J)} &= e^{-\beta(H_0+H_U)} \\ &+ \sum_{k=1}^{\infty} \int_0^1 d\tau_k \cdots \int_0^{\tau_2} d\tau_1 \\ &\times \prod_{i=1}^{k} \left[e^{-\tau_i \beta(H_0+H_U)} (\gamma - \beta H_{U'-J}) e^{\tau_i \beta(H_0+H_U)} \right] e^{-\beta(H_0+H_U)} \end{aligned} \tag{6.6}$$

After this, we follow the same derivations what we developed in the study except for the Rombouts' transformation. For $U' - J$ terms, we have used a decoupling formula similar to the transformation in Gull et al. (2008).

$$\begin{aligned} 1 - \frac{\beta(U'-J)}{\gamma} \sum_{\nu>\nu'} \sum_{\sigma} \left[n_{\nu\sigma} n_{\nu'\sigma} - \frac{1}{2}(n_{\nu\sigma} + n_{\nu'\sigma}) \right] = \\ \frac{1}{4} \frac{1}{N_{pair}} \sum_{\nu>\nu'} \sum_{\sigma} \sum_{S^{U'-J}_{\nu\nu',\sigma}=\pm 1} e^{\lambda_{U'-J} S^{U'-J}_{\nu\nu',\sigma} (n_{\nu\sigma} - n_{\nu'\sigma})} \end{aligned} \tag{6.7}$$

where

$$\cosh(\lambda_{U'-J}) = 1 + \frac{N_{pair}\beta(U' - J)}{\gamma} \tag{6.8}$$

We have carried out tests for this Hamiltonian for 2-orbital case to check the compatibility of the Hubbard-Stratonovich transformation and the Rombouts' transformation.

Figure 6.16 shows the QMC results and exact diagonalization comparison for $U = 4$ eV, $U = 2.2$ eV and $U' - J = 1.3$ eV, $\Delta\tau = 0.12$ and $L = 32$ at $T = 3020$ K. The free parameter $\gamma = 0.3$. In these simulations 5000 warm up and 10000 measurement sweeps were taken at 20 processors for each point on the graph. The QMC results match the exact diagonalization calculations with small errors. These error are actually the statistical errors and can be corrected with more Monte Carlo samples.

We have carried out calculations in more realistic temperatures with same parameters. In figure 6.17, $U = 4$ eV, $U = 2.2$ eV and $U' - J = 1.3$ eV, $\Delta\tau = 0.13063$ and $L = 296$ at $T = 300$ K. The free parameter $\gamma = 0.3$. For QMC results, 1000 warm up and 1000 measurement sweeps were taken at 32 processors for each point on the graph. At $T = 300$ K, the matrices are bigger, thus the run times of the simulations are higher than the simulations at high temperatures. Therefore, we only carried out QMC simulations at the chemical potential values which have critical jumps in the figures. We saw some points in figures 6.17 which do not match the exact calculations. These points have statistical error and can be corrected by taking more Monte Carlo samples.

In figure 6.18, the QMC results are plotted as a function of the free parameter γ. The parameters are $U = 4$ eV, $U = 2.2$ eV and $U' - J = 1.3$ eV, $\Delta\tau = 0.13063$, $L = 296$ at $T = 300$ K and constant chemical potential value $\mu = 7eV$. 1000 warm up and 1000 measurement sweeps were taken at 32 processors for each point on the graph. The QMC results are independent of the free parameter γ as expected. These results lead to the fact that Hubbard-Stratonovich transformation and Rombouts' transformation are compatible when the transformed terms are diagonal in the occupation number basis.

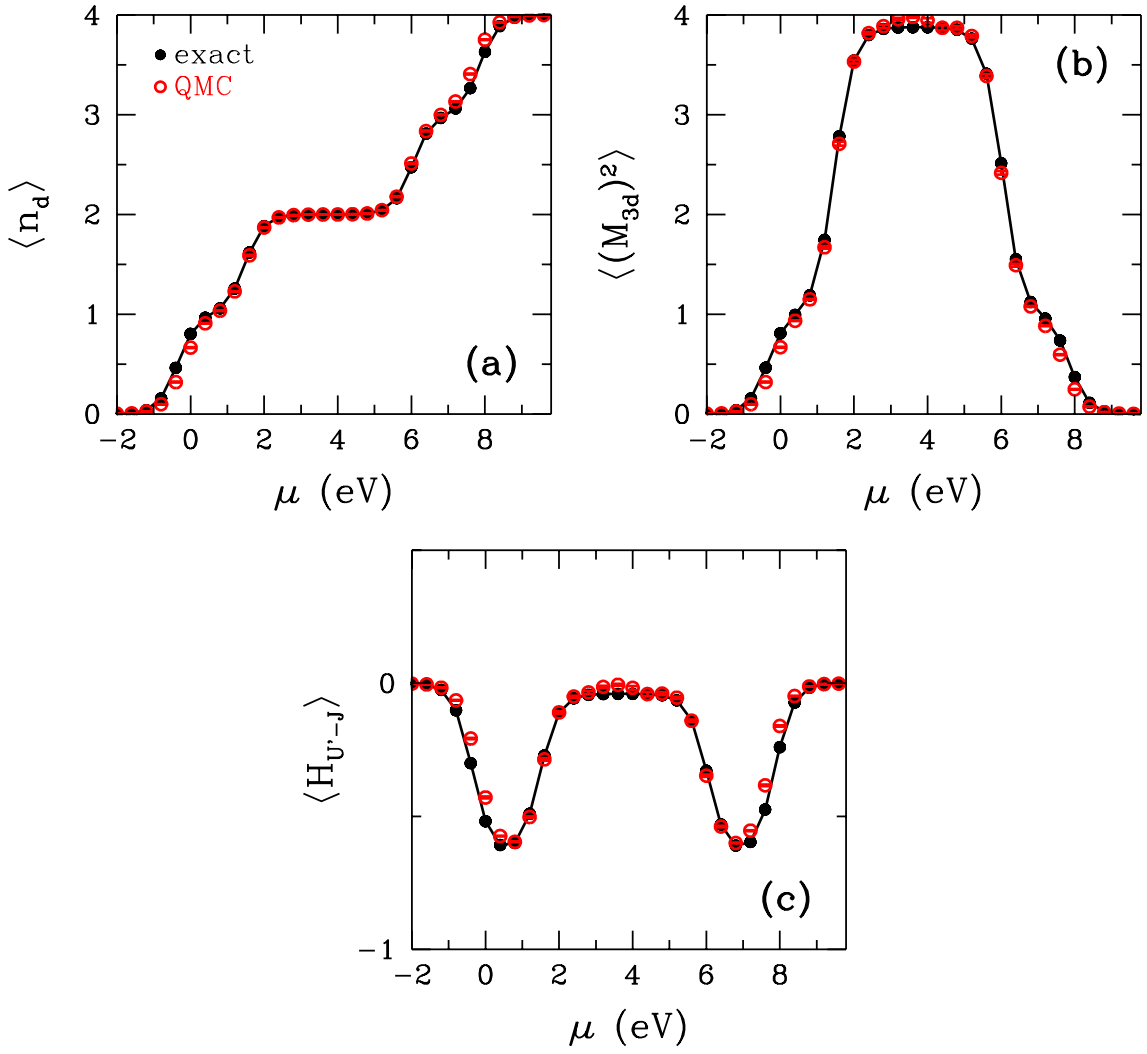

Figure 6.16. QMC results for the series expansion to the $U' - J$ vs exact diagonalization comparison plotted as a function of chemical potential μ, for theoretical 2-impurity orbitals of energies $\varepsilon_1 = 0$ eV and $\varepsilon_2 = 0$ eV at temperature $T = 3020$ K. In these calculations $H_U \neq 0$ and $H_{U'-J} \neq 0$. $U = 4$ eV, $U = 2.2$ eV and $U' - J = 1.3$ eV. In QMC simulations $\Delta\tau = 0.12$ and $L = 32$. The free parameter $\gamma = 0.3$. 5000 warm up and 10000 measurement sweeps were taken at 20 processors for each point on the graph in QMC simulations. Red empty dots for calculations with the QMC simulations, black filled dots for the exact diagonalization results. (a) Total occupation number of the 3d orbitals $\langle n_{3d} \rangle$ versus chemical potential μ. (b) Square of the total magnetic moment at the 3d orbitals $\langle (M_{3d})^2 \rangle$ versus chemical potential μ. (c) Expectation value of H_J versus chemical potential μ.

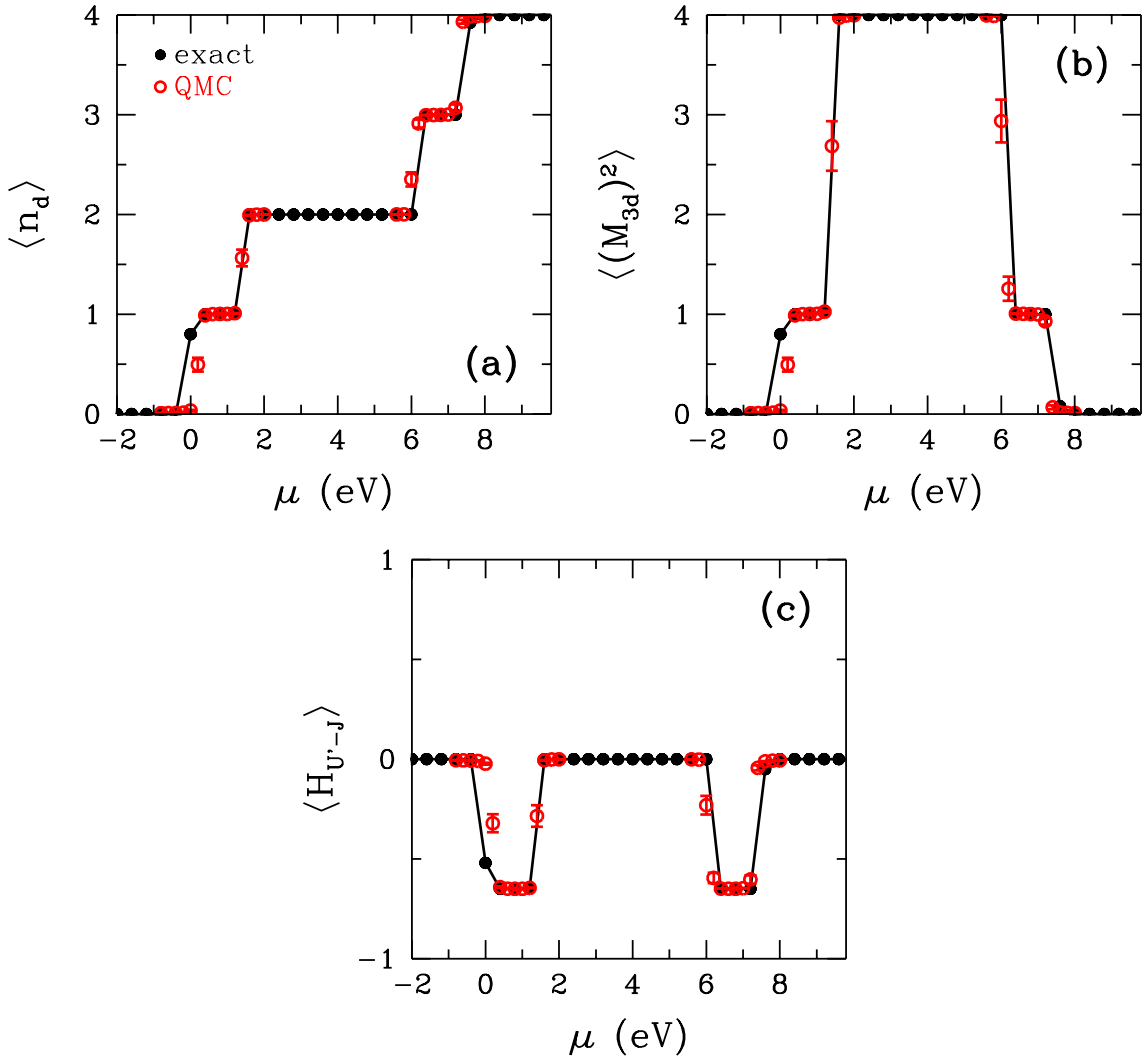

Figure 6.17. QMC results for the series expansion to the $U' - J$ vs exact diagonalization comparison plotted as a function of chemical potential μ, for theoretical 2-impurity orbitals of energies $\varepsilon_1 = 0$ eV and $\varepsilon_2 = 0$ eV at temperature $T = 300$ K. In these calculations $H_U \neq 0$ and $H_{U'-J} \neq 0$. $U = 4$ eV, $U = 2.2$ eV and $U' - J = 1.3$ eV. In QMC simulations $\Delta\tau = 0.13063$ and $L = 296$. The free parameter $\gamma = 0.3$. 1000 warm up and 1000 measurement sweeps were taken at 32 processors for each point on the graph in QMC simulations. Red empty dots for calculations with the QMC simulations, black filled dots for the exact diagonalization results. (a) Total occupation number of the 3d orbitals $\langle n_{3d} \rangle$ versus chemical potential μ. (b) Square of the total magnetic moment at the 3d orbitals $\langle (M_{3d})^2 \rangle$ versus chemical potential μ. (c) Expectation value of H_J versus chemical potential μ.

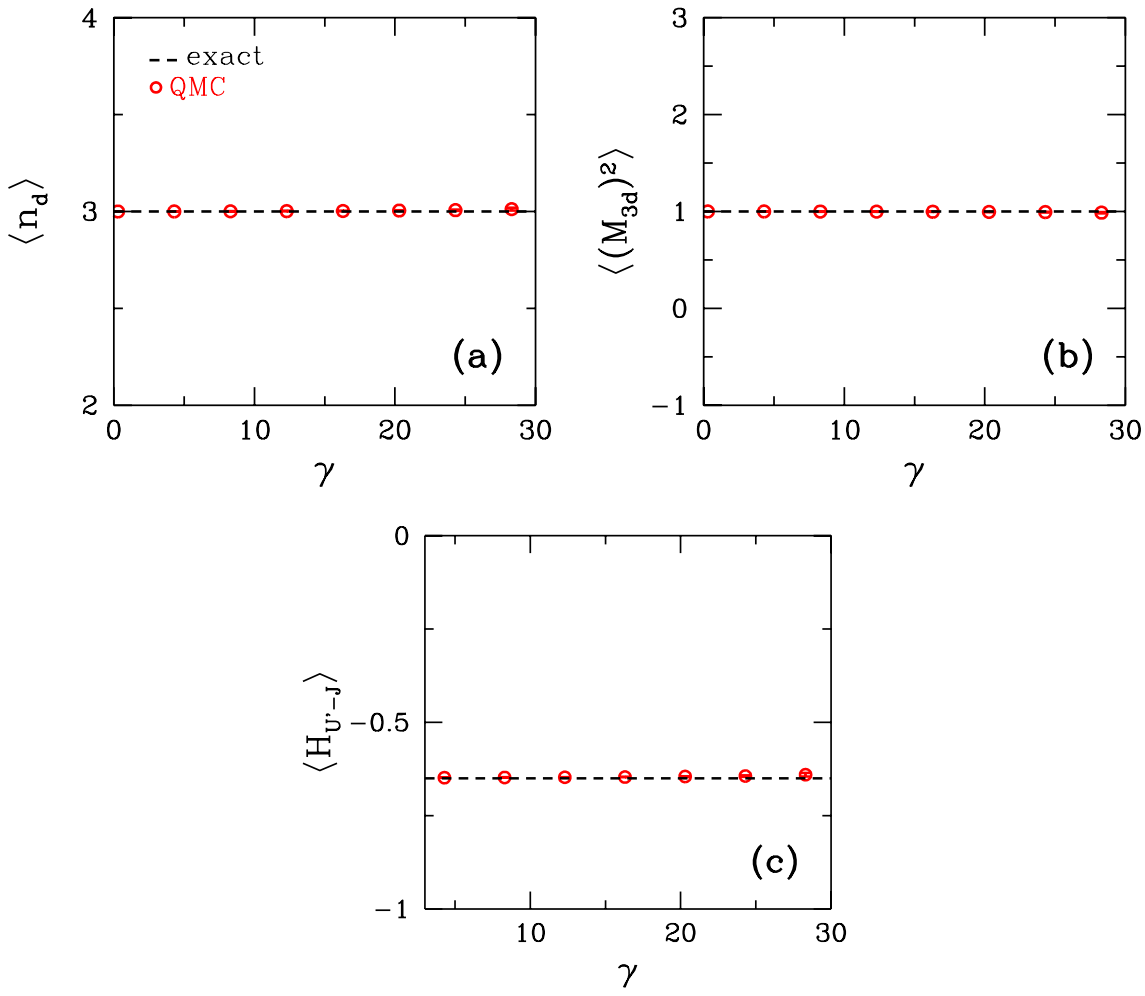

Figure 6.18. QMC results for the series expansion to the $U' - J$ vs exact diagonalization comparison plotted as a function of the free parameter γ, for theoretical 2-impurity orbitals of energies $\varepsilon_1 = 0$ eV and $\varepsilon_2 = 0$ eV at temperature $T = 300$ K. In these calculations $H_U \neq 0$ and $H_{U'-J} \neq 0$. $U = 4$ eV, $U = 2.2$ eV and $U' - J = 1.3$ eV. In QMC simulations $\Delta\tau = 0.13063$ and $L = 296$. The chemical potential is constant as $\mu = 7$ eV. 1000 warm up and 1000 measurement sweeps were taken at 32 processors for each point on the graph in QMC simulations. Red empty dots for calculations with the QMC simulations, black filled dots for the exact diagonalization results. (a) Total occupation number of the 3d orbitals $\langle n_{3d} \rangle$ versus chemical potential μ. (b) Square of the total magnetic moment at the 3d orbitals $\langle (M_{3d})^2 \rangle$ versus chemical potential μ. (c) Expectation value of H_J versus chemical potential μ.

CHAPTER 7

CONCLUSIONS

In this thesis, we have implemented a quantum Monte Carlo method to solve the multi-orbital Anderson impurity model including the SU(2) invariant Hund's coupling. The QMC method involves a series expansion to the partition function and Trotter decomposition in order to apply the renowned Hirsch-Fye QMC algorithm with the spin-flip and pair hopping terms. The detailed derivations was carried out, and the QMC program was written to simulate the deoxy and oxyheme molecules. On the other hand, we have developed an exact diagonalization program to solve the SU(2) invariant Hamiltonian in the atomic limit.

To form an insight about the effect of transverse components of the Hund's coupling, the hybridization matrix elements between the Fe(3d) orbitals of hemoglobin molecules and the remaining host orbitals are neglected. This allowed us to diagonalize the Hamiltonian in the atomic limit. The exact diagonalization calculations revealed that the transverse Hund's coupling terms affect the system for certain points, and suppress the tendency to ferromagnetic regime of the longitudinal Hund's terms, decreasing the total magnetic moments before the dramatic jumps for hemoglobin molecules. Additionally, calculations with the theoretical two and five orbital systems showed that the effect of the spin-flip and the pair-hopping terms can be more increased which resulted in more decrement in the total magnetization.

We have compared the QMC measurements and the exact diagonalization calculations with zero hybridization to ensure the accuracy of the simulations. In QMC measurements, the results have matched to exact diagonalization results for spin-flip and pair-hopping terms in two orbital systems when the Coulomb interactions are neglected. We have observed that the free expansion parameter γ does not affect the results as expected since it is just a constant with respect to electron creation/annihilation operators. The increment of γ increases the average expansion order k, while it is decreasing the strength of the decoupled H_J. Therefore, the results are not dependent on the free parameter γ. However, smaller values of γ is safer because we have cut off the expansion order at L and average expansion order should much smaller than that L. For two orbital systems, the expectation value of H_J was overestimated in QMC measurements when Coulomb interactions are taken into account, thus the results do not match to the exact ones. Although

the behaviors of the QMC results and the exact results are very similar, the magnetization values are decreased more than expected. When we examine the distribution of the expansion orders which are sampled in the QMC simulations, the normal behavior is broken if H_U terms are taken into account along with the H_J terms. These results suggests that the diagonal terms transformed by Hubbard-Stratonovich transformation and the off-diagonal terms decoupled with Rombouts' transformation may be incompatible to use in QMC simulations or calculating the partition functions. The second suggestion is that the transition probabilities in the Monte Carlo steps may be chosen inaccurately which leads errors in the QMC results. However, when we used Rombouts' transformation on $U' - J$ part of the Hamiltonian, the decoupling gives diagonal terms with respect to the occupation number basis. The results from the series expansion of $U' - J$ terms showed that the Hubbard-Stratonovich transformation and Rombouts' transformation can be used together when the terms which are decoupled are diagonal.

All in all, we have found that the effect of spin-flip and pair-hopping terms cannot be neglected from the exact diagonalization results. The calculations with the multi-orbital Anderson impurity model including SU(2) invariant Hund's coupling in order to obtain the electronic properties of the metalloproteins can give more realistic results. The QMC algorithm was derived for general interactions, any number of impurity orbitals, especially for metalloproteins. The first steps have been taken for the QMC studies of the SU(2) invariant Anderson impurity models on metalloproteins and similar materials.

REFERENCES

Anderson, P. W. (1961, Oct). Localized magnetic states in metals. *Phys. Rev. 124*, 41–53.

Ceperley, D., G. V. Chester, and M. H. Kalos (1977, Oct). Monte carlo simulation of a many-fermion study. *Phys. Rev. B 16*, 3081–3099.

Ceperley, D. M. (1995, Apr). Path integrals in the theory of condensed helium. *Rev. Mod. Phys. 67*, 279–355.

Foulkes, W. M. C., L. Mitas, R. J. Needs, and G. Rajagopal (2001, Jan). Quantum monte carlo simulations of solids. *Rev. Mod. Phys. 73*, 33–83.

Gull, E., A. J. Millis, A. I. Lichtenstein, A. N. Rubtsov, M. Troyer, and P. Werner (2011, May). Continuous-time monte carlo methods for quantum impurity models. *Rev. Mod. Phys. 83*, 349–404.

Gull, E., P. Werner, O. Parcollet, and M. Troyer (2008). Continuous-time auxiliary-field monte carlo for quantum impurity models. *EPL (Europhysics Letters) 82*(5), 57003.

Haldane, F. D. M. and P. W. Anderson (1976, Mar). Simple model of multiple charge states of transition-metal impurities in semiconductors. *Phys. Rev. B 13*, 2553–2559.

Han, J. E. (2004, Aug). Spin-triplet s-wave local pairing induced by hund's rule coupling. *Phys. Rev. B 70*, 054513.

Held, K. and D. Vollhardt (1998, Oct). Microscopic conditions favoring itinerant ferromagnetism: Hund's rule coupling and orbital degeneracy. *The European Physical Journal B - Condensed Matter and Complex Systems 5*(3), 473–478.

Hirsch, J. E. (1983, Oct). Discrete hubbard-stratonovich transformation for fermion lattice models. *Phys. Rev. B 28*, 4059–4061.

Hirsch, J. E. and R. M. Fye (1986, Jun). Monte carlo method for magnetic impurities in metals. *Phys. Rev. Lett. 56*, 2521–2524.

Hubbard, J. (1963). Electron correlations in narrow energy bands. *Proceedings of the Royal Society of London A: Mathematical, Physical and Engineering Sciences 276*(1365), 238–257.

Jungwirth, T., J. Sinova, A. H. MacDonald, B. L. Gallagher, V. Novák, K. W. Edmonds,

A. W. Rushforth, R. P. Campion, C. T. Foxon, L. Eaves, E. Olejník, J. Mašek, S.-R. E. Yang, J. Wunderlich, C. Gould, L. W. Molenkamp, T. Dietl, and H. Ohno (2007, Sep). Character of states near the fermi level in (ga,mn)as: Impurity to valence band crossover. *Phys. Rev. B 76*, 125206.

Kandemir, Z., S. Mayda, and N. Bulut (2016, May). Electronic structure and correlations of vitamin b12 studied within the haldane-anderson impurity model. *The European Physical Journal B 89*(5), 113.

Mayda, S., Z. Kandemir, and N. Bulut (2017, Nov). Electronic structure of cyanocobalamin: Dft+qmc study. *Journal of Superconductivity and Novel Magnetism 30*(11), 3301–3308.

McMillan, W. L. (1965, Apr). Ground state of liquid he^4. *Phys. Rev. 138*, A442–A451.

Motome, Y. and M. Imada (1997). A quantum monte carlo method and its applications to multi-orbital hubbard models. *Journal of the Physical Society of Japan 66*(7), 1872–1875.

Ohno, H., H. Munekata, T. Penney, S. von Molnár, and L. L. Chang (1992, Apr). Magnetotransport properties of p-type (in,mn)as diluted magnetic iii-v semiconductors. *Phys. Rev. Lett. 68*, 2664–2667.

Ohno, H., A. Shen, F. Matsukura, A. Oiwa, A. Endo, S. Katsumoto, and Y. Iye (1996). (ga,mn)as: A new diluted magnetic semiconductor based on gaas. *Applied Physics Letters 69*(3), 363–365.

Pauling, L. and C. D. Coryell (1936). The magnetic properties and structure of hemoglobin, oxyhemoglobin and carbonmonoxyhemoglobin. *Proceedings of the National Academy of Sciences 22*(4), 210–216.

Rombouts, S., K. Heyde, and N. Jachowicz (1998). A discrete hubbard-stratonovich decomposition for general, fermionic two-body interactions. *Physics Letters A 242*(4), 271 – 276.

Rombouts, S. M. A., K. Heyde, and N. Jachowicz (1999, May). Quantum monte carlo method for fermions, free of discretization errors. *Phys. Rev. Lett. 82*, 4155–4159.

Sakai, S., R. Arita, and H. Aoki (2004, Nov). Numerical algorithm for the double-orbital hubbard model: Hund-coupled pairing symmetry in the doped case. *Phys. Rev. B 70*, 172504.

Sakai, S., R. Arita, K. Held, and H. Aoki (2006, Oct). Quantum monte carlo study for multiorbital systems with preserved spin and orbital rotational symmetries. *Phys. Rev. B 74*, 155102.

Sandvik, A. W. and J. Kurkijärvi (1991, Mar). Quantum monte carlo simulation method for spin systems. *Phys. Rev. B 43*, 5950–5961.

Tomoda, Y., N. Bulut, and S. Maekawa (2009). Inter-impurity and impurityâhost magnetic correlations in semiconductors with low-density transitionâmetal impurities. *Physica B: Condensed Matter 404*(8), 1159 – 1168.

APPENDIX A

SERIES EXPANSION

Interaction representation: Operators and wavefunctions have time dependence. Hamiltonian consists of kinetic part and a potential part.

$$H = H_0 + V \tag{A.1}$$

The imaginary time variable is defined as

$$\tau = it \tag{A.2}$$

The partition function is

$$\begin{aligned} Z &= Tr\left(e^{-\beta H}\right) \\ &= Tr\left[\left(e^{-\beta H}e^{\beta H_0}\right)e^{-\beta H_0}\right] \end{aligned} \tag{A.3}$$

Let us define an operator $U(\tau)$.

$$U(\tau) = e^{-\tau H}e^{\tau H_0} \tag{A.4}$$

Time evolution of this operator is

$$\begin{aligned} \frac{\partial}{\partial\tau}U(\tau) &= e^{-\tau H}(H_0 - H)e^{\tau H_0} \\ &= -e^{-\tau H}Ve^{\tau H_0} \\ &= -U(\tau)V(\tau) \end{aligned} \tag{A.5}$$

where

$$V(\tau) = e^{-\tau H_0} V e^{\tau H_0} \tag{A.6}$$

Taking τ integral on both sides

$$\begin{aligned} U(\tau) &= 1 - \int_0^\tau d\tau_1 U(\tau_1) V(\tau_1) \\ &= \sum_{k=0}^{\infty} (-1)^k \int_0^\tau d\tau_1 \cdots \int_0^{\tau_{k-1}} d\tau_k V(\tau_k) \cdots V(\tau_1) \\ &= \sum_{k=0}^{\infty} (-1)^k \int_0^\tau d\tau_k \cdots \int_0^{\tau_2} d\tau_1 \prod_{i=1}^{k} V(\tau_i) \end{aligned} \tag{A.7}$$

where we have changed the order of the integrals. Thus, the Boltzmann operator becomes

$$e^{-\beta H} = \left[1 + \sum_{k=1}^{\infty} (-1)^k \int_0^\beta d\tau_k \cdots \int_0^{\tau_2} d\tau_1 \prod_{i=1}^{k} V(\tau_i) \right] e^{-\beta H_0} \tag{A.8}$$

In τ integrals substitute τ_i with $\tau_i \beta$. This substitution changes the limits of the integrals.

$$\begin{aligned} e^{-\beta H} &= e^{-\beta H_0} + \sum_{k=1}^{\infty} (-1)^k \beta^k \int_0^1 d\tau_k \cdots \int_0^{\tau_2} d\tau_1 \prod_{i=1}^{k} \left[e^{-\tau_i \beta H_0} V e^{\tau_i \beta H_0} \right] e^{-\beta H_0} \\ &= e^{-\beta H_0} + \sum_{k=1}^{\infty} \int_0^1 d\tau_k \cdots \int_0^{\tau_2} d\tau_1 \prod_{i=1}^{k} \left[e^{-\tau_i \beta H_0} (-\beta V) e^{\tau_i \beta H_0} \right] e^{-\beta H_0} \end{aligned} \tag{A.9}$$

APPENDIX B

DERIVATION OF EXPANSION WEIGHTS

The Hamiltonian is denifed as

$$H = H_0 + H_U + H_J \tag{B.1}$$

and the series expansion of the Boltzmann operator is

$$\begin{aligned} e^{-\beta(H_0+H_U)+(\gamma-\beta H_J)} &= e^{-\beta(H_0+H_U)} \\ &+ \sum_{k=1}^{\infty} \int_0^1 d\tau_k \cdots \int_0^{\tau_2} d\tau_1 \\ &\times \prod_{i=1}^{k} \left[e^{-\tau_i \beta(H_0+H_U)} (\gamma - \beta H_J) e^{\tau_i \beta(H_0+H_U)} \right] e^{-\beta(H_0+H_U)} \end{aligned} \tag{B.2}$$

Discretize it for numerical calculations

$$\begin{aligned} e^{\gamma-\beta H} &= e^{-\beta(H_0+H_U)} \\ &+ \sum_{k=1}^{\infty} L^{-k} \sum_{j_k=1}^{L} \cdots \sum_{j_1=1}^{j_2} \\ &\times \prod_{i=1}^{k} \left[e^{-j_i \Delta\tau(H_0+H_U)} (\gamma - \beta H_J) e^{j_i \Delta\tau(H_0+H_U)} \right] e^{-\beta(H_0+H_U)} + O(\Delta\tau) \end{aligned} \tag{B.3}$$

$$\Delta\tau = \beta \Big/ L \tag{B.4}$$

Firstly, the k summation in equation B.3 is cut off at L with the condition $\langle k \rangle \ll L$. Originally the summation goes to infinity. It cannot be expanded to infinite order. If we cut of it at L, k_{max} should be much smaller than L.

Secondly, in order to reduce the computation time and the number of configurations, we need to do some alterations when we sample from the terms of the expansion. The terms having consecutive $\gamma - \beta H_J$ at the same imaginary-time interval should be changed into approximate terms consisting one $\gamma - \beta H_J$ per imaginary-time interval. For example, $\cdots e^{-\beta(H_0+H_U)}(\gamma - \beta H_J)(\gamma - \beta H_J)\cdots$ should be replaced by $\cdots(\gamma - \beta H_J)e^{-\beta(H_0+H_U)}(\gamma - \beta H_J)\cdots$.

If we expand equation B.3, there are some terms which have equal time variables. For example; for $k = 2 \rightarrow j_1 = 2, j_2 = 2$ or for $k = 5 \rightarrow j_5 = 3, j_4 = 3, j_3 = 2, j_2 = 1, j_1 = 1$. For terms like these, we have to be careful about the fact that originally imaginary-time variables hold the relation $\cdots t_i < t_{i+1} < t_{i+2}\cdots$. For that reason, we should correct the volumes of the integrals depending on the number of consecutive $\gamma - \beta H_J$. Thus, the correction of the volumes of the integrals for ℓ consecutive $\gamma - \beta H_J$ is

$$\frac{1}{\ell!} \tag{B.5}$$

Let us define

$$\chi \equiv \gamma - \beta H_J \tag{B.6}$$

After these changes the Boltzmann operator can be written as

$$e^{\gamma-\beta H} = \sum_{r_1,r_2,\cdots,r_L=0,1} F(k; r_1, r_2, \cdots, r_L) \prod_{i=1}^{L} \left[e^{-\Delta\tau(H_0+H_U)}\chi_{r_i}\right] + O(\Delta\tau) \tag{B.7}$$

where $k = \sum_{i=1}^{L} r_i$ and $\chi_0 = 1$. F is a positive weight factor.

B.1. Derivation on the example of L=8

We now show that how F terms arise on an example of $L = 8$ by expanding the sum of equation B.7.

B.1.1. k=1

$$8^{-1}\sum_{j_1=1}^{8} e^{-j_1\Delta\tau(H_0+H_U)}\chi e^{j_1\Delta\tau(H_0+H_U)}e^{-\beta(H_0+H_U)} =$$
$$8^{-1}\sum_{j_1=1}^{8} e^{-j_1\Delta\tau(H_0+H_U)}\chi e^{j_1\Delta\tau(H_0+H_U)}\left[\prod_{i=1}^{8} e^{-\Delta\tau(H_0+H_U)}\right] \tag{B.8}$$

$$\begin{aligned} j_1 = 1 &\longrightarrow 8^{-1}e^{-\Delta\tau(H_0+H_U)}\chi e^{\Delta\tau(H_0+H_U)}e^{-\beta(H_0+H_U)} \\ j_1 = 2 &\longrightarrow 8^{-1}e^{-\Delta\tau(H_0+H_U)}e^{-\Delta\tau(H_0+H_U)}\chi e^{\Delta\tau(H_0+H_U)}e^{\Delta\tau(H_0+H_U)}e^{-\beta(H_0+H_U)} \\ &\vdots \end{aligned}$$

We drop L^{-1} terms and change the notation for simplicity;

$$\begin{aligned} e^{-\Delta\tau(H_0+H_U)} &\equiv h \\ \chi &\equiv x \end{aligned}$$

Expanding the terms for $k = 1$ gives us

$$\begin{aligned} j_1 = 1 &\longrightarrow hx\frac{1}{h}hhhhhhhh = hxhhhhhhh \\ j_1 = 2 &\longrightarrow hhxhhhhhh \\ &\vdots \\ j_1 = 8 &\longrightarrow hhhhhhhhx \end{aligned}$$

For these terms there are no consecutive χ's. There is no need for correction. The treatment of configurations is the following.

hx	h	h	h	h	h	h	h	$\longrightarrow$	configuration
ℓ_1	ℓ_2	ℓ_3	ℓ_4	ℓ_5	ℓ_6	ℓ_7	ℓ_8	$\longrightarrow$	imaginary-time interval
F(1;1,	0,	0,	0,	0,	0,	0,	0)	$\longrightarrow$	F term

All substrings having j times x, $j-1$ times h and consecutive x will be replaced by $\cdots xhxhx\cdots$. For example, $\cdots xxh\cdots$ and $\cdots xhx\cdots$ are approximately same terms, and should be corrected by 1 for xhx and $1/2!$ for xxh. Weight for this is $1+\frac{1}{2!}=\frac{3}{2}$.

B.1.2. k=2

$$8^{-2}\sum_{j_2=1}^{8}\sum_{j_1=1}^{j_2}\left[e^{-j_1\Delta\tau(H_0+H_U)}\chi e^{j_1\Delta\tau(H_0+H_U)}\right]\left[e^{-j_2\Delta\tau(H_0+H_U)}\chi e^{j_2\Delta\tau(H_0+H_U)}\right]e^{-\beta(H_0+H_U)} \tag{B.9}$$

Weight factors of the pairings below are

$$\begin{aligned}
&\textbf{a)}F(2;1,1,0,0,0,0,0,0)=(1+\frac{1}{2!})8^{-2}=\frac{3}{2}8^{-2}\\
&\textbf{b)}F(2;0,1,1,0,0,0,0,0)=(1+\frac{1}{2!})8^{-2}=\frac{3}{2}8^{-2}\\
&\qquad\vdots\\
&\textbf{g)}F(2;0,0,0,0,0,0,1,1)=(1+\frac{1}{2!}+\frac{1}{2!})8^{-2}=2\cdot 8^{-2}
\end{aligned} \tag{B.10}$$

It is seen that we have to be careful when the consecutive χ's are located at the end of the strings.

j_2	j_1	$\longrightarrow$	configuration			j_2	j_1	$\longrightarrow$	configuration
1	1	$\longrightarrow$	$h\underline{xx}hhhhhh$	**a**		6	3	$\longrightarrow$	$hhhxhhhxhh$
2	1	$\longrightarrow$	$h\underline{xhx}hhhhhh$	**a**		6	4	$\longrightarrow$	$hhhhxhhxhh$
2	2	$\longrightarrow$	$hh\underline{xx}hhhhhh$	**b**	**e**	6	5	$\longrightarrow$	$hhhhh\underline{xhx}hh$
3	1	$\longrightarrow$	$hxhhxhhhhh$		**f**	6	6	$\longrightarrow$	$hhhhhh\underline{xx}hh$
3	2	$\longrightarrow$	$hh\underline{xhx}hhhhh$	**b**		7	1	$\longrightarrow$	$hxhhhhhhxh$
3	3	$\longrightarrow$	$hhh\underline{xx}hhhhh$	**c**		7	2	$\longrightarrow$	$hhxhhhhhxh$
4	1	$\longrightarrow$	$hxhhhxhhhh$			7	3	$\longrightarrow$	$hhhxhhhhxh$
4	2	$\longrightarrow$	$hhxhhxhhhh$			7	4	$\longrightarrow$	$hhhhxhhhxh$
4	3	$\longrightarrow$	$hhh\underline{xhx}hhhh$	**c**		7	5	$\longrightarrow$	$hhhhhxhhxh$
4	4	$\longrightarrow$	$hhhh\underline{xx}hhhh$	**d**	**f**	7	6	$\longrightarrow$	$hhhhhh\underline{xhx}h$
5	1	$\longrightarrow$	$hxhhhhxhhh$		**g**	7	7	$\longrightarrow$	$hhhhhhh\underline{xx}h$
5	2	$\longrightarrow$	$hhxhhhxhhh$			8	1	$\longrightarrow$	$hxhhhhhhhx$
5	3	$\longrightarrow$	$hhhxhhxhhh$			8	2	$\longrightarrow$	$hhxhhhhhhx$
5	4	$\longrightarrow$	$hhhh\underline{xhx}hhh$	**d**		8	3	$\longrightarrow$	$hhhxhhhhhx$
5	5	$\longrightarrow$	$hhhhh\underline{xx}hhh$	**e**		8	4	$\longrightarrow$	$hhhhxhhhhx$
6	1	$\longrightarrow$	$hxhhhhhxhh$			8	5	$\longrightarrow$	$hhhhhxhhhx$
6	2	$\longrightarrow$	$hxxhhhhhhh$			8	6	$\longrightarrow$	$hhhhhhxhhx$
					g	8	7	$\longrightarrow$	$hhhhhhh\underline{xhx}$
					g	8	8	$\longrightarrow$	$hhhhhhh\underline{hxx}$

B.1.3. k=3

$$
\begin{aligned}
8^{-3} \sum_{j_3=1}^{8} \sum_{j_2=1}^{j_3} \sum_{j_1=1}^{j_2} & \left[e^{-j_1 \Delta\tau (H_0+H_U)} \chi e^{j_1 \Delta\tau (H_0+H_U)} \right] \\
& \times \left[e^{-j_2 \Delta\tau (H_0+H_U)} \chi e^{j_2 \Delta\tau (H_0+H_U)} \right] \left[e^{-j_3 \Delta\tau (H_0+H_U)} \chi e^{j_3 \Delta\tau (H_0+H_U)} \right] \\
& \times e^{-\beta (H_0+H_U)}
\end{aligned} \tag{B.11}
$$

j_3	j_2	j_1	$\longrightarrow$	configuration			j_3	j_2	j_1	$\longrightarrow$	configuration
1	1	1	$\longrightarrow$	$h\underline{xxx}hhhhhh$	**a**	**c**	3	3	1	$\longrightarrow$	$hxhh\underline{xxh}hhhh$
2	1	1	$\longrightarrow$	$h\underline{xxhxh}hhhhh$	**a**	**b**	3	3	2	$\longrightarrow$	$hh\underline{xhxxh}hhhh$
2	2	1	$\longrightarrow$	$h\underline{xhxxh}hhhhh$	**a**		3	3	3	$\longrightarrow$	$hhhxxxhhhhh$
2	2	2	$\longrightarrow$	$hh\underline{xxxhh}hhhh$	**b**		4	1	1	$\longrightarrow$	$hxxhhhxhhhh$
3	1	1	$\longrightarrow$	$h\underline{xxhhx}hhhhh$	**a**		4	2	1	$\longrightarrow$	$hxhxhhxhhhh$
3	2	1	$\longrightarrow$	$h\underline{xhxhx}hhhhh$	**a**	**b**	4	2	2	$\longrightarrow$	$hh\underline{xxhhx}hhhh$
3	2	2	$\longrightarrow$	$hh\underline{xxhxh}hhhh$	**b**	**c**	4	3	1	$\longrightarrow$	$hxhh\underline{xhx}hhhh$
	$\vdots$					**b**	4	3	2	$\longrightarrow$	$hh\underline{xhxhx}hhhh$
	$\vdots$									$\vdots$	
7	7	7	$\longrightarrow$	$hhhhhhhxxxh$	**d**	**d**	8	7	7	$\longrightarrow$	$hhhhhhhxxhx$
	$\vdots$									$\vdots$	
8	6	6	$\longrightarrow$	$hhhhhhxxhhx$	**d**	**d**	8	8	6	$\longrightarrow$	$hhhhhhxhhxx$
	$\vdots$					**d**	8	8	7	$\longrightarrow$	$hhhhhhhxhxx$
8	7	6	$\longrightarrow$	$hhhhhhxhxhx$	**d**	**d**	8	8	8	$\longrightarrow$	$hhhhhhhhxxx$

Weight factors of these pairings are

$$\begin{aligned}
&\textbf{a)} F(3;1,1,1,0,0,0,0,0) = (1+\frac{1}{2!}+\frac{1}{2!}+\frac{1}{2!}+\frac{1}{3!})8^{-3} \\
&\textbf{b)} F(3;0,1,1,1,0,0,0,0) = (1+\frac{1}{2!}+\frac{1}{2!}+\frac{1}{2!}+\frac{1}{3!})8^{-3} \\
&\textbf{c)} F(3;1,0,1,1,0,0,0,0) = (1+\frac{1}{2!})8^{-3} \\
&\textbf{d)} F(3;0,0,0,0,0,1,1,1) = (1+\frac{1}{2!}+\frac{1}{2!}+\frac{1}{2!}+\frac{1}{2!}+\frac{1}{3!}+\frac{1}{3!})8^{-3}
\end{aligned} \tag{B.12}$$

Here, it is also seen that when the consecutive χ's are located at the end of the string, the weight factors are changing.

B.2. Recursive Formulas

There are recursive formulas in order to find those weights, F, easily. We show that how these recursive formulas can be derived on two example. These formulas do not generate L^{-k} part of the weights. Suppose there are i times h and j times x in a substring. Recursive formulas come from leaving out $\cdots hxxxxx\cdots$ string from that

substring, each time decreasing x.

B.2.1. xhx substring (i=1, j=2)

Generates xhx and xxh. Weight of that configuration is $1 + \frac{1}{2!}$.

$\longrightarrow$ Start from "xhx".
Drop one "$\cdots hxxxxx \cdots$" string with $j - 1$ x from that substring.
$j - 1 = 2 - 1 = 1$, thus, drop one "hx".
The remaning is "x". It has a weight of $\frac{1}{1!} \cdot \frac{1}{1!} = 1$.
The first $\frac{1}{1!}$ comes from leaving out 1 "hx", correction for
one consecutive χ.
The other one comes from correction of volume of the integral
for one consecutive χ.

$\longrightarrow$ Again start from "xhx".
Drop one "h" (j-2=2-2=0).
The remaining is "xx". It has a weight of $\frac{1}{0!} \cdot \frac{1}{2!}$.
$1/0!$ comes from leaving out one "h", correction for zero χ.
$1/2!$ comes from correction for 2 consecutive χ's.

$\longrightarrow$ Sum the results.
The weight of xhx is $1 + \frac{1}{2!} = \frac{3}{2}$.

B.2.2. xhxhx substring (i=2, j=3)

Generates $xxxhh$, $xxhxh$, $xhxxh$, $xxhhx$, $xhxhx$. Weight of that configuration is $1 + \frac{1}{2!} + \frac{1}{2!} + \frac{1}{2!} + \frac{1}{3!}$.

$\longrightarrow$ Start from "$xhxhx$".
Drop one "hx" (j-2=3-2=1) and multiply remaining with $1/1!$.
Remaining is "xhx" (i=1, j=2).
Drop one "hx" and drop one "h".
Remaining is "x" and "xx".
Weight is $\frac{1}{1!}\left(\frac{1}{1!}\frac{1}{1!} + \frac{1}{0!}\frac{1}{2!}\right)$.
Thus, 1 and $1/2!$ are generated.

$\longrightarrow$ Again start from "$xhxhx$".
Drop one "h" (j-3=3-3=0) and multiply remaining with $1/0!$.
Remaining is "$xhxx$" (i=1, j=3).

$\longrightarrow$ Now start from "$xhxx$".
Drop one "hxx" (j-1=3-1=2) and multiply remaining with $1/2!$.
Remaining is "x". Weight is $\frac{1}{0!}\frac{1}{2!}\frac{1}{1!}$.

$\longrightarrow$ Again start from "$xhxx$".
Drop one "hx" (j-1=2-1=1) and multiply remaining with $1/1!$.
Remaining is "xx". Weight is $\frac{1}{0!}\frac{1}{1!}\frac{1}{2!}$.

$\longrightarrow$ Again start from "$xhxx$".
Drop one "h" (j-1=1-1=0) and multiply remaining with $1/0!$.
Remaining is "xxx". Weight is $\frac{1}{0!}\frac{1}{0!}\frac{1}{3!}$.
Thus, $1/2!$, $1/2!$, $1/3!$ are generated.

$\longrightarrow$ Sum the results.
the weight of $xhxhx$ is $1 + \frac{1}{2!} + \frac{1}{2!} + \frac{1}{2!} + \frac{1}{3!}$.

B.2.3. Introducing Recursive Formulas

From the results we can introduce the recursive formulas. For j consecutive x, we had

$$b(0, j) = \frac{1}{j!} \quad \text{for} \quad 0 \leq j \leq L \tag{B.13}$$

The recursive formula using $b(0, j)$ and the results from the examples is

$$b(i, j) = \sum_{k=i}^{j} \frac{1}{(j-k)!} b(i-1, k) \quad \text{for} \quad 1 \leq i \leq j \leq L \tag{B.14}$$

Therefore, for $\cdots xhxhxhx \cdots$ substring, i times x and $i-1$ times h;

$$a_i = b(i-1, i) \quad \text{for} \quad 1 \leq i \leq L \tag{B.15}$$

For the terms in which x is located at the last time slice, $\cdots xhxhx$, i times x and $i-1$ times h; it is enough just to change the lower limit of the summation in equation B.14 to 0. It generates the remaining terms.

$$d(0,j) = \frac{1}{j!} \quad \text{for} \quad 0 \leq j \leq L \tag{B.16}$$

$$d(i,j) = \sum_{k=0}^{j} \frac{1}{(j-k)!} d(i-1,k) \quad \text{for} \quad 1 \leq i \leq L-1 \quad \text{and} \quad 0 \leq j \leq L \tag{B.17}$$

Therefore, for $\cdots xhxhxhx$ substring, i times x and $i-1$ times h;

$$c_i = d(i-1,i) \quad \text{for} \quad 1 \leq i \leq L \tag{B.18}$$

Here is some examples for L=8;

$$\begin{aligned} F(2;1,1,0,0,0,0,0,0) &= a_2 8^{-2} \\ F(3;0,1,1,1,0,0,0,0) &= a_3 8^{-3} \\ F(3;0,0,0,0,0,1,1,1) &= c_3 8^{-3} \\ F(5;1,1,0,0,0,1,1,1) &= a_2 c_3 8^{-5} \end{aligned} \tag{B.19}$$

APPENDIX C

DECOUPLING OF THE SPIN-FLIP AND THE PAIR-HOPPING TERMS

$$\gamma^{\nu\nu'} - \beta H_J^{\nu\nu'} = \frac{\gamma^{\nu\nu'} - \beta J}{8} \sum_{q,t_\uparrow,t_\downarrow} \prod_\sigma e^{\lambda_4 \left[\sigma q f_\sigma^{\nu\nu'} + t_\sigma g_\sigma^{\nu\nu'}\right]} \tag{C.1}$$

where

$$H_J^{\nu\nu'} = J f_\uparrow^{\nu\nu'} f_\downarrow^{\nu\nu'} \tag{C.2}$$

$$f_\sigma^{\nu\nu'} = c_{\nu\sigma}^\dagger c_{\nu'\sigma} + c_{\nu'\sigma}^\dagger c_{\nu\sigma} \tag{C.3}$$

$$g_\sigma^{\nu\nu'} = (n_{\nu\sigma} + n_{\nu'\sigma} - 1) \tag{C.4}$$

$$\lambda_4 = \frac{1}{2} \ln \frac{1+\kappa}{1-\kappa} \tag{C.5}$$

$$\kappa = \sqrt{\frac{\beta J}{\gamma^{\nu\nu'}}} < 1 \tag{C.6}$$

$$n_{\nu\sigma} = c_{\nu\sigma}^\dagger c_{\nu\sigma} \tag{C.7}$$

$$\{q, t_\uparrow, t_\downarrow\} = \pm 1 \tag{C.8}$$

Let us derive equation C.1 starting from some identities. We can find these identities simply applying the operators to a trial wavefunction $|\nu\nu'\rangle$.

$$f_\sigma^{\nu\nu'} = \begin{cases} 1 & if \quad n_{\nu\sigma} = 1, n_{\nu'\sigma} = 0 \quad or \quad n_{\nu\sigma} = 0, n_{\nu'\sigma} = 1 \\ 0 & if \quad n_{\nu\sigma} = 1, n_{\nu'\sigma} = 1 \quad or \quad n_{\nu\sigma} = 0, n_{\nu'\sigma} = 0 \end{cases} \tag{C.9}$$

$$g_\sigma^{\nu\nu'} = \begin{cases} 1 & if \quad n_{\nu\sigma} = 1, n_{\nu'\sigma} = 1 \\ 0 & if \quad n_{\nu\sigma} = 1, n_{\nu'\sigma} = 0 \quad or \quad n_{\nu\sigma} = 0, n_{\nu'\sigma} = 1 \\ -1 & if \quad n_{\nu\sigma} = 0, n_{\nu'\sigma} = 0 \end{cases} \tag{C.10}$$

From equations C.9 and C.10 we can find the product of $f_\sigma^{\nu\nu'} \cdot g_\sigma^{\nu\nu'}$. We see that

$$\begin{aligned} &\text{If} \quad f_\sigma^{\nu\nu'} = 1 \quad \longrightarrow \quad g_\sigma^{\nu\nu'} = 0 \\ &\text{If} \quad g_\sigma^{\nu\nu'} = \pm 1 \quad \longrightarrow \quad f_\sigma^{\nu\nu'} = 0 \end{aligned}$$

For all cases

$$f_\sigma^{\nu\nu'} \cdot g_\sigma^{\nu\nu'} = 0 \tag{C.11}$$

The square of $f_\sigma^{\nu\nu'}$ operator is

$$\begin{aligned} f_\sigma^{\nu\nu'} \cdot f_\sigma^{\nu\nu'} &= c_{\nu\sigma}^\dagger c_{\nu'\sigma} c_{\nu\sigma}^\dagger c_{\nu'\sigma} + c_{\nu'\sigma}^\dagger c_{\nu\sigma} c_{\nu'\sigma}^\dagger c_{\nu\sigma} + c_{\nu\sigma}^\dagger c_{\nu'\sigma} c_{\nu'\sigma}^\dagger c_{\nu\sigma} + c_{\nu'\sigma}^\dagger c_{\nu\sigma} c_{\nu\sigma}^\dagger c_{\nu'\sigma} \\ &= c_{\nu\sigma}^\dagger c_{\nu'\sigma} + c_{\nu'\sigma}^\dagger c_{\nu\sigma} \end{aligned}$$

$$\begin{aligned} \implies \quad & (f_\sigma^{\nu\nu'})^{2n} = (f_\sigma^{\nu\nu'})^2 = (f_\sigma^{\nu\nu'})^4 = \cdots \\ & (f_\sigma^{\nu\nu'})^{2n-1} = (f_\sigma^{\nu\nu'})^1 = (f_\sigma^{\nu\nu'})^3 = \cdots \end{aligned} \tag{C.12}$$

The square of $g_\sigma^{\nu\nu'}$ operator is

$$\begin{aligned} g_\sigma^{\nu\nu'} \cdot g_\sigma^{\nu\nu'} &= (n_{\nu\sigma} + n_{\nu'\sigma} - 1)(n_{\nu\sigma} + n_{\nu'\sigma} - 1) \\ &= |g_\sigma^{\nu\nu'}| \end{aligned}$$

$$\begin{aligned}\implies \quad & (g_\sigma^{\nu\nu'})^{2n} = |g_\sigma^{\nu\nu'}| = (g_\sigma^{\nu\nu'})^2 = (g_\sigma^{\nu\nu'})^4 = \cdots \\ & (g_\sigma^{\nu\nu'})^{2n-1} = g_\sigma^{\nu\nu'} = (g_\sigma^{\nu\nu'})^3 = (g_\sigma^{\nu\nu'})^5 = \cdots \end{aligned} \tag{C.13}$$

And the last identity $(f_\sigma^{\nu\nu'})^2 + |g_\sigma^{\nu\nu'}|$.

$$(f_\sigma^{\nu\nu'})^2 = \begin{cases} 1 \quad if \quad n_{\nu\sigma} = 1, n_{\nu'\sigma} = 0 \quad or \quad n_{\nu\sigma} = 0, n_{\nu'\sigma} = 1 \\ 0 \quad if \quad n_{\nu\sigma} = 1, n_{\nu'\sigma} = 1 \quad or \quad n_{\nu\sigma} = 0, n_{\nu'\sigma} = 0 \end{cases}$$

$$|g_\sigma^{\nu\nu'}| = \begin{cases} 1 \quad if \quad n_{\nu\sigma} = 1, n_{\nu'\sigma} = 1 \quad or \quad n_{\nu\sigma} = 0, n_{\nu'\sigma} = 0 \\ 0 \quad if \quad n_{\nu\sigma} = 1, n_{\nu'\sigma} = 0 \quad or \quad n_{\nu\sigma} = 0, n_{\nu'\sigma} = 1 \end{cases}$$

For all cases

$$(f_\sigma^{\nu\nu'})^2 + |g_\sigma^{\nu\nu'}| = 1 \tag{C.14}$$

We can expand $\prod_\sigma e^{\lambda_4\left[\sigma q f_\sigma^{\nu\nu'} + t_\sigma g_\sigma^{\nu\nu'}\right]}$ in series using equations C.9, C.10, C.11, C.12, C.13, C.14.

$$\begin{aligned} & e^{\lambda_4\left[q f_\uparrow^{\nu\nu'} + t_\uparrow g_\uparrow^{\nu\nu'}\right]} e^{\lambda_4\left[-q f_\downarrow^{\nu\nu'} + t_\downarrow g_\downarrow^{\nu\nu'}\right]} = \\ & \left\{1 + \lambda_4\left(q f_\uparrow^{\nu\nu'} + t_\uparrow g_\uparrow^{\nu\nu'}\right) + \frac{1}{2!}(\lambda_4)^2\left(q f_\uparrow^{\nu\nu'} + t_\uparrow g_\uparrow^{\nu\nu'}\right)^2 + \cdots\right\} \\ & \times \left\{1 + \lambda_4\left(-q f_\downarrow^{\nu\nu'} + t_\downarrow g_\downarrow^{\nu\nu'}\right) + \frac{1}{2!}(\lambda_4)^2\left(-q f_\downarrow^{\nu\nu'} + t_\downarrow g_\downarrow^{\nu\nu'}\right)^2 + \cdots\right\} \end{aligned} \tag{C.15}$$

By using equation C.11

$$
\begin{aligned}
& e^{\lambda_4\left[qf_{\uparrow}^{\nu\nu'}+t_{\uparrow}g_{\uparrow}^{\nu\nu'}\right]}e^{\lambda_4\left[-qf_{\downarrow}^{\nu\nu'}+t_{\downarrow}g_{\downarrow}^{\nu\nu'}\right]} = \\
& \left\{1+\lambda_4\left(qf_{\uparrow}^{\nu\nu'}+t_{\uparrow}g_{\uparrow}^{\nu\nu'}\right)+\frac{1}{2!}(\lambda_4)^2\left[(f_{\uparrow}^{\nu\nu'})^2+(g_{\uparrow}^{\nu\nu'})^2\right]+\cdots\right\} \\
& \times\left\{1+\lambda_4\left(-qf_{\downarrow}^{\nu\nu'}+t_{\downarrow}g_{\downarrow}^{\nu\nu'}\right)+\frac{1}{2!}(\lambda_4)^2\left[(f_{\downarrow}^{\nu\nu'})^2+(g_{\downarrow}^{\nu\nu'})^2\right]+\cdots\right\}
\end{aligned}
\tag{C.16}
$$

$$
\begin{aligned}
& e^{\lambda_4\left[qf_{\uparrow}^{\nu\nu'}+t_{\uparrow}g_{\uparrow}^{\nu\nu'}\right]}e^{\lambda_4\left[-qf_{\downarrow}^{\nu\nu'}+t_{\downarrow}g_{\downarrow}^{\nu\nu'}\right]} = \\
& \left\{1+\lambda_4\left(qf_{\uparrow}^{\nu\nu'}+t_{\uparrow}g_{\uparrow}^{\nu\nu'}\right)+\frac{1}{2!}(\lambda_4)^2\left[(f_{\uparrow}^{\nu\nu'})^2+|g_{\uparrow}^{\nu\nu'}|\right]+\cdots\right\} \\
& \times\left\{1+\lambda_4\left(-qf_{\downarrow}^{\nu\nu'}+t_{\downarrow}g_{\downarrow}^{\nu\nu'}\right)+\frac{1}{2!}(\lambda_4)^2\left[(f_{\downarrow}^{\nu\nu'})^2+|g_{\downarrow}^{\nu\nu'}|\right]+\cdots\right\}
\end{aligned}
\tag{C.17}
$$

To group the same terms into parentheses

$$
\begin{aligned}
& \sum_{q,t_{\uparrow},t_{\downarrow}} e^{\lambda_4\left[qf_{\uparrow}^{\nu\nu'}+t_{\uparrow}g_{\uparrow}^{\nu\nu'}\right]}e^{\lambda_4\left[-qf_{\downarrow}^{\nu\nu'}+t_{\downarrow}g_{\downarrow}^{\nu\nu'}\right]} = \\
& \quad \sum_{q,t_{\uparrow},t_{\downarrow}} \left\{\left(qf_{\uparrow}^{\nu\nu'}+t_{\uparrow}g_{\uparrow}^{\nu\nu'}\right)\left(\lambda_4+\frac{1}{3!}(\lambda_4)^3+\cdots\right)\right. \\
& \quad \left.+\left[(f_{\uparrow}^{\nu\nu'})^2+|g_{\uparrow}^{\nu\nu'}|\right]\left(1+\lambda_4+\frac{1}{2!}(\lambda_4)^2+\cdots\right)\right\} \\
& \quad \times\left\{\left(-qf_{\downarrow}^{\nu\nu'}+t_{\downarrow}g_{\downarrow}^{\nu\nu'}\right)\left(\lambda_4+\frac{1}{3!}(\lambda_4)^3+\cdots\right)\right. \\
& \quad \left.+\left[(f_{\downarrow}^{\nu\nu'})^2+|g_{\downarrow}^{\nu\nu'}|\right]\left(1+\lambda_4+\frac{1}{2!}(\lambda_4)^2+\cdots\right)\right\}
\end{aligned}
\tag{C.18}
$$

By using equation C.14

$$
\begin{aligned}
& \sum_{q,t_{\uparrow},t_{\downarrow}} e^{\lambda_4\left[qf_{\uparrow}^{\nu\nu'}+t_{\uparrow}g_{\uparrow}^{\nu\nu'}\right]}e^{\lambda_4\left[-qf_{\downarrow}^{\nu\nu'}+t_{\downarrow}g_{\downarrow}^{\nu\nu'}\right]} = \\
& \quad \sum_{q,t_{\uparrow},t_{\downarrow}} \left\{\left(qf_{\uparrow}^{\nu\nu'}+t_{\uparrow}g_{\uparrow}^{\nu\nu'}\right)\sinh(\lambda_4)+\cosh(\lambda_4)\right\} \\
& \quad \times\left\{\left(-qf_{\downarrow}^{\nu\nu'}+t_{\downarrow}g_{\downarrow}^{\nu\nu'}\right)\sinh(\lambda_4)+\cosh(\lambda_4)\right\}
\end{aligned}
\tag{C.19}
$$

$$\sum_{q,t_\uparrow,t_\downarrow} e^{\lambda_4\left[qf_\uparrow^{\nu\nu'}+t_\uparrow g_\uparrow^{\nu\nu'}\right]} e^{\lambda_4\left[-qf_\downarrow^{\nu\nu'}+t_\downarrow g_\downarrow^{\nu\nu'}\right]} =$$
$$\sum_{q,t_\uparrow,t_\downarrow} \Big[\sinh(\lambda_4)\cosh(\lambda_4)\left(qf_\uparrow^{\nu\nu'} - qf_\downarrow^{\nu\nu'} + t_\uparrow g_\uparrow^{\nu\nu'} + t_\downarrow g_\downarrow^{\nu\nu'}\right) + \cosh^2(\lambda_4)$$
$$+ \sinh^2(\lambda_4)\left(-f_\uparrow^{\nu\nu'}f_\downarrow^{\nu\nu'} + qt_\downarrow f_\uparrow^{\nu\nu'}g_\downarrow^{\nu\nu'} - qt_\uparrow g_\uparrow^{\nu\nu'}f_\downarrow^{\nu\nu'} + t_\uparrow t_\downarrow g_\uparrow g_\downarrow\right)\Big] \tag{C.20}$$

After expand the summation in equation C.20, and multiply with $\frac{\gamma^{\nu\nu'}-\beta J}{8}$, we have equation C.1 expanded. Notice that in the summation there are 2^3 elements.

$$\frac{\gamma^{\nu\nu'}-\beta J}{8}\sum_{q,t_\uparrow,t_\downarrow}\prod_\sigma e^{\lambda_4\left[\sigma q f_\sigma^{\nu\nu'}+t_\sigma g_\sigma^{\nu\nu'}\right]} = \left(\gamma^{\nu\nu'}-\beta J\right)\left(\cosh^2(\lambda_4) - f_\uparrow^{\nu\nu'}f_\downarrow^{\nu\nu'}\sinh^2(\lambda_4)\right)$$
$$= \gamma^{\nu\nu'} - \beta H_J^{\nu\nu'} \tag{C.21}$$

$$\gamma^{\nu\nu'} - \beta J f_\uparrow^{\nu\nu'}f_\downarrow^{\nu\nu'} = \left(\gamma^{\nu\nu'}-\beta J\right)\left(\cosh^2(\lambda_4) - f_\uparrow^{\nu\nu'}f_\downarrow^{\nu\nu'}\sinh^2(\lambda_4)\right)$$
$$= \left(\gamma^{\nu\nu'}-\beta J\right)\left(1+\sinh^2(\lambda_4) - f_\uparrow^{\nu\nu'}f_\downarrow^{\nu\nu'}\sinh^2(\lambda_4)\right) \tag{C.22}$$

If we solve this equation

$$\Longrightarrow \begin{cases} f_\uparrow^{\nu\nu'}f_\downarrow^{\nu\nu'}\left[\beta J - \left(\gamma^{\nu\nu'}-\beta J\right)\sinh^2(\lambda_4)\right] = 0 \\ -\gamma^{\nu\nu'} + \left(\gamma^{\nu\nu'}-\beta J\right) + \left(\gamma^{\nu\nu'}-\beta J\right)\sinh^2(\lambda_4) = 0 \end{cases} \tag{C.23}$$

For the decomposition to be valid, the solution of λ_4 is

$$\sinh^2(\lambda_4) = \frac{\beta J}{\gamma^{\nu\nu'}-\beta J} \tag{C.24}$$

Let us define $\kappa = \sqrt{\frac{\beta J}{\gamma^{\nu\nu'}}}$.

$$\lambda_4 = \operatorname{arcsinh}\left(\frac{\kappa}{\sqrt{1-\kappa^2}}\right) \tag{C.25}$$

Using the identity $\operatorname{arcsinh}(x) = \ln(x + \sqrt{x^2+1})$;

$$\begin{aligned}
\operatorname{arcsinh}\left(\frac{\kappa}{\sqrt{1-\kappa^2}}\right) &= \ln\left(\frac{\kappa}{\sqrt{1-\kappa^2}} + \sqrt{\frac{\kappa^2}{1-\kappa^2}+1}\right) \\
&= \ln\left(\frac{\kappa}{\sqrt{1-\kappa^2}} + \frac{1}{\sqrt{1-\kappa^2}}\right) && \text{(C.26)} \\
&= \ln\left(\frac{1+\kappa}{\sqrt{1-\kappa^2}}\right) && \text{(C.27)} \\
&= \ln\left[\frac{(1+\kappa)^2}{1-\kappa^2}\right]^2 && \text{(C.28)} \\
&= \frac{1}{2}\ln\left[\frac{(1+\kappa)(1+\kappa)}{(1+\kappa)(1-\kappa)}\right] && \text{(C.29)}
\end{aligned}$$

$$\implies \lambda_4 = \frac{1}{2}\ln\left(\frac{1+\kappa}{1-\kappa}\right) \qquad \text{(C.30)}$$

$$\kappa = \sqrt{\frac{\beta J}{\gamma^{\nu\nu'}}} \quad \text{and} \quad \kappa < 1 \qquad \text{(C.31)}$$

APPENDIX D

TRACE OF THE EXPONENTIAL OPERATORS

Trace of the quadratic operators in the Boltzmann factor is very important to formulate the algorithm. In this chapter, we will use a compact notation for simplicity. Recall that the partition function is

$$\begin{aligned} Z &= \mathrm{Tr} e^{\beta H} \\ &= \sum_{\{r_\ell\}} \widetilde{F}(\{r_\ell\}) \sum_{\{\widetilde{S}_\ell\}} \sum_{\alpha} \sum_{\{P_\ell^\alpha\}} \mathrm{Tr} \prod_{\sigma} \prod_{\ell} D_\sigma(\ell) \end{aligned} \tag{D.1}$$

where

$$D_\sigma(\ell) = e^{-\Delta\tau \sum_{\nu,\nu'} c^\dagger_{\nu\sigma} [H_0]_{\nu,\nu'} c_{\nu'\sigma}} e^{\sum_{\nu,\nu'} c^\dagger_{\nu\sigma} [W_\sigma(\ell)]_{\nu,\nu'} c_{\nu'\sigma}} e^{\sum_{\nu,\nu'} c^\dagger_{\nu\sigma} [T^\alpha_\sigma(\ell)]_{\nu,\nu'} c_{\nu'\sigma}} \tag{D.2}$$

The operators H_0, $W_\sigma(\ell)$ and $T^\alpha_\sigma(\ell)$ are quadratic with respect to electron creation / annihilation operators, and they are defined in chapter 4 along with the weight terms, $\widetilde{F}(\{r_\ell\})$. Actually, this operators depend on the configurations $\{r_\ell\}, \{\widetilde{S}_\ell\}, \{\alpha\}, \{P^\alpha_\ell\}$, however we do not write them to simplify the notation. In the rest of the chapter, the spin indices σ, and the orbital indices α for H_J term will be dropped. The summation indices, $\nu\nu'$, are changed into ij. Therefore, the matrices will be seen as

$$D(\ell) = e^{-\Delta\tau \sum_{i,j} c^\dagger_i [H_0]_{i,j} c_j} e^{\sum_{i,j} c^\dagger_i [W(\ell)]_{i,j} c_j} e^{\sum_{i,j} c^\dagger_i [T(\ell)]_{i,j} c_j} \tag{D.3}$$

The configuration space consists of $\{r_\ell\}, \{\widetilde{S}_\ell\}, \{\alpha\}, \{P^\alpha_\ell\}$. Thus, a given configuration will be given as

$$\{\zeta\} \equiv \left\{ \{r_\ell\}, \{\widetilde{S}_\ell\}, \{\alpha\}, \{P^\alpha_\ell\} \right\} \tag{D.4}$$

D.1. Trace Over Fermionic Degrees of Freedom

For a given configuration $\{\zeta\}$, the partition function is

$$Z_{\{\zeta\}} = \mathrm{Tr} \prod_{\ell} e^{-\Delta\tau \sum_{i,j} c_i^\dagger [H_0]_{i,j} c_j} e^{\sum_{i,j} c_i^\dagger [W(\ell)]_{i,j} c_j} e^{\sum_{i,j} c_i^\dagger [T(\ell)]_{i,j} c_j} \tag{D.5}$$

Suppose $\lambda_\phi = e^{-p_\phi}$ are the eigenvalues of the matrix $\prod_\ell e^{-\Delta\tau H_0} e^{W(\ell)} e^{T(\ell)}$. Therefore, the product of the exponential operators in the partition function can be rewritten in the diagonal basis as

$$\begin{aligned} \prod_{\ell} e^{-\Delta\tau \sum_{i,j} c_i^\dagger [H_0]_{i,j} c_j} e^{\sum_{i,j} c_i^\dagger [W(\ell)]_{i,j} c_j} e^{\sum_{i,j} c_i^\dagger [T(\ell)]_{i,j} c_j} &= e^{-\sum_\phi c_\phi^\dagger p_\phi c_\phi} \\ &= \prod_{\phi} e^{-c_\phi^\dagger p_\phi c_\phi} \end{aligned} \tag{D.6}$$

We can take the trace in this diagonal basis easily. There are two possibilities for all ϕ states since we are in the diagonal basis. There is zero or one electron for the trace over $c_\phi^\dagger c_\phi$.

$$\mathrm{Tr} \prod_{\phi} e^{-c_\phi^\dagger p_\phi c_\phi} = \prod_{\phi} \left(1 + e^{-p_\phi}\right) \tag{D.7}$$

This equation simply the multiplication of the eigenvalues, thus it can be written as determinant of the original matrices.

$$\prod_{\phi} \left(1 + e^{-p_\phi}\right) = \det \left[1 + \prod_{\ell} e^{-\Delta\tau H_0} e^{W(\ell)} e^{T(\ell)}\right] \tag{D.8}$$

Thus, the partition function is

$$Z_{\{\zeta\}} = \det \left[1 + \prod_{\ell} B_\ell\right] \tag{D.9}$$

where

$$B_\ell = e^{-\Delta\tau H_0} e^{W(\ell)} e^{T(\ell)} \tag{D.10}$$

D.2. Calculation of the Green's Function from M^{-1}

We can further simplify the equation D.9 by introducing M matrices.

$$\det\left[I + B_L B_{L-1} \cdots B_1\right] = \det M \tag{D.11}$$

where

$$M = \begin{bmatrix} I & 0 & \cdots & & & B_L \\ -B_1 & I & 0 & & & 0 \\ 0 & -B_2 & I & & & \vdots \\ \vdots & \vdots & \vdots & \ddots & & \vdots \\ & & & & I & 0 \\ 0 & 0 & \cdots & 0 & -B_{L-1} & I \end{bmatrix}_{N_d \cdot L \times N_d \cdot L} \tag{D.12}$$

Here we changed the sequence in the product of the B_ℓ matrices since it simplify the programming part of the algorithm, and I is identity matrix.. In this section, the equal time Green's functions will be derived. For a given configuration the single particle equal time Green's function is calculated in the following way,

$$\begin{aligned} G_{xy,\{\zeta\}} &= \langle c_x c_y^\dagger \rangle_{\{\zeta\}} \\ &= \frac{\mathrm{Tr} c_x c_y^\dagger \prod_\ell D(\ell)}{\mathrm{Tr} \prod_\ell D(\ell)} \end{aligned} \tag{D.13}$$

where

$$D(\ell) = e^{-\Delta\tau \sum_{i,j} c_i^\dagger [H_0]_{i,j} c_j} e^{\sum_{i,j} c_i^\dagger [W(\ell)]_{i,j} c_j} e^{\sum_{i,j} c_i^\dagger [T(\ell)]_{i,j} c_j} \tag{D.14}$$

Here the Green's function defined with plus sign, as in Hirsch-Fye paper. We should use the diagonal basis, ϕ, in order to evaluate the trace. The transformation is the following,

$$c_x = \sum_\phi \langle x|\phi\rangle c_\phi \tag{D.15}$$

$$c_x^\dagger = \sum_\phi \langle \phi|x\rangle c_\phi^\dagger \tag{D.16}$$

Using these, the Green's function becomes

$$\langle c_x c_y^\dagger \rangle_{\{\zeta\}} = \sum_{\phi,\phi'} \langle x|\phi\rangle \langle \phi'|y\rangle \frac{\mathrm{Tr} c_\phi c_{\phi'}^\dagger \prod_{\phi''} e^{-c_{\phi''}^\dagger p_{\phi''} c_{\phi''}}}{\mathrm{Tr} \prod_{\phi''} e^{-c_{\phi''}^\dagger p_{\phi''} c_{\phi''}}} \tag{D.17}$$

Since the trace is in the diagonal basis, the only contribution comes from $c_\phi c_\phi^\dagger$. Thus the summation over ϕ' is eliminated.

$$\langle c_x c_y^\dagger \rangle_{\{\zeta\}} = \sum_{\phi} \langle x|\phi\rangle \langle \phi|y\rangle \frac{\mathrm{Tr} c_\phi c_{\phi}^\dagger \prod_{\phi''} e^{-c_{\phi''}^\dagger p_{\phi''} c_{\phi''}}}{\mathrm{Tr} \prod_{\phi''} e^{-c_{\phi''}^\dagger p_{\phi''} c_{\phi''}}} \tag{D.18}$$

The operator $c_{\phi''}^\dagger c_{\phi''}$ is the number operator. There are two possibilities in all states for number operator as 0 or 1.

$$\mathrm{Tr} \prod_\phi e^{-c_{\phi''}^\dagger p_{\phi''} c_{\phi''}} = \prod_{\phi''} \left(1 + e^{-p_{\phi''}}\right) \tag{D.19}$$

However, in the numerator the term $c_\phi c_\phi^\dagger$ cancels ϕ terms in this multiplication, because of the following,

$$\begin{aligned}\mathrm{Tr} c_\phi c_\phi^\dagger e^{-p_\phi c_\phi^\dagger c_\phi} &= \langle n_\phi = 0 | c_\phi c_\phi^\dagger e^{-p_\phi c_\phi^\dagger c_\phi} | n_\phi = 0 \rangle + \langle n_\phi = 1 | c_\phi c_\phi^\dagger e^{-p_\phi c_\phi^\dagger c_\phi} | n_\phi = 1 \rangle \\ &= 1 + 0 \\ &= 1 \end{aligned} \tag{D.20}$$

where

$$n_\phi = c_\phi^\dagger c_\phi \tag{D.21}$$

Therefore, all terms except ϕ term in the denominator are canceled.

The Green's function becomes

$$\begin{aligned}\langle c_x c_y^\dagger \rangle_{\{\zeta\}} &= \sum_\phi \langle x | \phi \rangle \langle \phi | y \rangle \frac{1}{1 + e^{-p_\phi}} \\ &= \sum_\phi \langle x | \phi \rangle \frac{1}{1 + e^{-p_\phi}} \langle \phi | y \rangle \end{aligned} \tag{D.22}$$

Recall that e^{-p_ϕ} are the eigenvalues of the matrix $\prod_\ell e^{-\Delta\tau H_0} e^{W(\ell)} e^{T(\ell)}$. Equation D.22, without the inner products, is the inverse of this matrix represented in the diagonal basis.

$$\begin{aligned}\sum_\phi |\phi\rangle \frac{1}{1 + e^{-p_\phi}} \langle \phi| &= \left[1 + \prod_\ell e^{-\Delta\tau H_0} e^{W(\ell)} e^{T(\ell)} \right]^{-1} \\ &= \left[I + B_L B_{L-1} \cdots B_1 \right]^{-1} \end{aligned} \tag{D.23}$$

Thus, the single particle equal-time Green's function becomes,

$$G_{xy,\{\zeta\}} = \langle c_x c_y^\dagger \rangle_{\{\zeta\}} = \left[I + B_L B_{L-1} \cdots B_1 \right]^{-1}_{xy} \tag{D.24}$$

Here the matrices $G_{\{\zeta\}}$ and $\left[I + B_L B_{L-1} \cdots B_1 \right]^{-1}$ are $N_d \times N_d$ matrices. We know that

$[I + B_L B_{L-1} \cdots B_1]$ can be written as the M matrices which are $N_d \cdot L \times N_d \cdot L$. Thus, in the changed notation, the Green's functions represented in the $N_d \cdot L \times N_d \cdot L$ matrices is

$$G^{\{\zeta\}}_{x,y}(\ell, \ell') = \langle T c_x(\ell) c^\dagger_y(\ell') \rangle_{\{\zeta\}} = [M]^{-1}_{x\ell, y\ell'} \tag{D.25}$$

where

$$M = \begin{bmatrix} I & 0 & \cdots & & & B_L \\ -B_1 & I & 0 & & & 0 \\ 0 & -B_2 & I & & & \vdots \\ \vdots & \vdots & \vdots & \ddots & & \vdots \\ & & & & I & 0 \\ 0 & 0 & \cdots & 0 & -B_{L-1} & I \end{bmatrix}_{N_d \cdot L \times N_d \cdot L} \tag{D.26}$$

and

$$B_\ell = e^{-\Delta\tau H_0} e^{W(\ell)} e^{T(\ell)} \tag{D.27}$$

Calculations of the unequal-time Green's functions or equal-time Green's function in different time slices can be evaluated in the same steps with this appendix.

APPENDIX E

FAST UPDATE SCHEME

There are 5 types of change in the updates. First, turning on 3 auxiliary field variables at imaginary-time slice ℓ and impurity sites η, η' for H_J term which indicates $r_\ell = 0 \rightarrow r'_\ell = 1$. Second, turning off 3 auxiliary field variables at imaginary-time slice ℓ and impurity sites η, η' for H_J term which indicates $r_\ell = 1 \rightarrow r'_\ell = 0$. Third, single spin flip at imaginary-time slice ℓ and impurity sites η, η' for H_J term which are $q_\ell^{\eta\eta'}$, $t_{\uparrow\ell}^{\eta\eta'}$ and $t_{\downarrow\ell}^{\eta\eta'}$. Forth kind of change occurs for the intra-orbital and inter-orbital interactions when H_J term is turned on. Fifth is for the intra-orbital and inter-orbital interactions when H_J term is turned off. However, all these changes occurs only for one imaginary-time slices.

In this appendix the $\eta\eta'$ indices are dropped from the auxiliary field variables $q_\ell^{\eta\eta'}$, $t_{\uparrow\ell}^{\eta\eta'}$ and $t_{\downarrow\ell}^{\eta\eta'}$. In equation 5.41 the matrix multiplication $\Lambda_\sigma^{-1}\Lambda'_\sigma$ has all elements zero except the diagonal elements and all diagonal elements are 1 excluding the imaginary-time slice part that the change occurs. Let us look at the matrix forms in order to see that clearly.

$$\Lambda'_\sigma = \begin{bmatrix} \Lambda_\sigma(1) & & & & & 0 \\ & \Lambda_\sigma(2) & & & & \\ & & \ddots & & & \\ & & & \Lambda'_\sigma(\ell) & & \\ & & & & \ddots & \\ 0 & & & & & \Lambda_\sigma(L) \end{bmatrix} \tag{E.1}$$

and

$$\Lambda_\sigma^{-1} = \begin{bmatrix} [\Lambda_\sigma(1)]^{-1} & & & & & 0 \\ & [\Lambda_\sigma(2)]^{-1} & & & & \\ & & \ddots & & & \\ & & & [\Lambda_\sigma(\ell)]^{-1} & & \\ & & & & \ddots & \\ 0 & & & & & [\Lambda_\sigma(L)]^{-1} \end{bmatrix} \tag{E.2}$$

Here Λ is a $N_d \cdot L \times N_d \cdot L$ matrix, and there are $N_d \times N_d$ matrices in the diagonal elements which are denoted as $\Lambda(\ell)$. $\Lambda(\ell)$ can be written as

$$[\Lambda(\ell)]_{i,j} = [\Lambda]_{i\ell,j\ell} \tag{E.3}$$

The product of these two matrices is following.

$$\Lambda_\sigma^{-1}\Lambda'_\sigma = \begin{bmatrix} I & & & & & 0 \\ & I & & & & \\ & & \ddots & & & \\ & & & [\Lambda_\sigma(\ell)]^{-1}\Lambda'_\sigma(\ell) & & \\ & & & & \ddots & \\ 0 & & & & & I \end{bmatrix} \tag{E.4}$$

That's why we will only focus imaginary-time slice ℓ part of these matrix products in the

following sections of this chapter. We can see that clearly from this equation $(\Lambda_\sigma^{-1}\Lambda'_\sigma - I)$;

$$\left(\Lambda_\sigma^{-1}\Lambda'_\sigma - I\right) = \begin{bmatrix} 0 & & & & 0 \\ & 0 & & & \\ & & \ddots & & \\ & & & \left\{[\Lambda_\sigma(\ell)]^{-1}\,\Lambda'_\sigma(\ell) - I\right\}_{N_d \times N_d} & \\ & & & & \ddots \\ 0 & & & & 0 \end{bmatrix} \tag{E.5}$$

E.1. General Expression for Updates with Four Non-zero Elements

Equation 5.41 is used for updating the Green's functions. For this equation the form of $(\Lambda_\sigma^{-1}\Lambda'_\sigma - I)$ is important and it varies for all single spin-flip operations. There are cases with 4 non-zero elements and 5 non-zero elements. In this section we derive the expression for 4 non-zero elements. This expression is used for a spin-flip operation that affects 4 elements of the matrix.

$$(G^\sigma)' = G^\sigma + (G^\sigma - I)\left(\Lambda_\sigma^{-1}\Lambda'_\sigma - I\right) A_\sigma^{-1} G^\sigma \tag{E.6}$$

where

$$A_\sigma = I + (I - G^\sigma)\left(\Lambda_\sigma^{-1}\Lambda'_\sigma - I\right) \tag{E.7}$$

The form of $\left\{\left[\Lambda_\sigma(\ell)\right]^{-1}\Lambda'_\sigma(\ell)-I\right\}_{N_d\times N_d}$ with 4 non-zero elements is following;

$$\left[\Lambda_\sigma(\ell)\right]^{-1}\Lambda'_\sigma(\ell)-I=\begin{bmatrix} 0 & & & & 0\\ & \ddots & \boldsymbol{\eta',\eta'} & \boldsymbol{\eta',\eta} & \\ & & \bullet & \bullet & \\ & & 0 & & \\ & & \bullet & \bullet & \\ & & \boldsymbol{\eta,\eta'} & \boldsymbol{\eta,\eta} & \ddots \\ 0 & & & & 0 \end{bmatrix} \tag{E.8}$$

All elements except the dots are zero. The form of $N_d\cdot L\times N_d\cdot L$ matrix $(\Lambda_\sigma^{-1}\Lambda'_\sigma-I)$ is the same;

$$\Lambda_\sigma^{-1}\Lambda'_\sigma-I=\begin{bmatrix} 0 & & & & 0\\ & \ddots & \boldsymbol{\eta'\ell,\eta'\ell} & \boldsymbol{\eta'\ell,\eta\ell} & \\ & & \bullet & \bullet & \\ & & 0 & & \\ & & \bullet & \bullet & \\ & & \boldsymbol{\eta\ell,\eta'\ell} & \boldsymbol{\eta\ell,\eta\ell} & \ddots \\ 0 & & & & 0 \end{bmatrix} \tag{E.9}$$

The matrix representation of this matrix is

$$\begin{aligned}\left(\Lambda_\sigma^{-1}\Lambda'_\sigma-I\right)_{\nu_1\ell_1,\nu_2\ell_2}=\delta_{\ell,\ell_1}\delta_{\ell,\ell_2}\Big\{&\delta_{\eta',\nu_1}\delta_{\eta',\nu_2}\left(\Lambda_\sigma^{-1}\Lambda'_\sigma-I\right)_{\eta'\ell,\eta'\ell}\\ &+\delta_{\eta,\nu_1}\delta_{\eta,\nu_2}\left(\Lambda_\sigma^{-1}\Lambda'_\sigma-I\right)_{\eta\ell,\eta\ell}\\ &+\delta_{\eta',\nu_1}\delta_{\eta,\nu_2}\left(\Lambda_\sigma^{-1}\Lambda'_\sigma-I\right)_{\eta'\ell,\eta\ell}\\ &+\delta_{\eta,\nu_1}\delta_{\eta',\nu_2}\left(\Lambda_\sigma^{-1}\Lambda'_\sigma-I\right)_{\eta\ell,\eta'\ell}\Big\}\end{aligned} \tag{E.10}$$

The matrix representation of equation E.6 is

$$\left(G^{\sigma}_{\nu_1,\nu_2}(\ell_1,\ell_2)\right)' = G^{\sigma}_{\nu_1,\nu_2}(\ell_1,\ell_2) + \sum_{\ell_3,\ell_4,\ell_5}\sum_{\nu_3,\nu_4,\nu_5} \left(G^{\sigma}-I\right)_{\nu_1\ell_1,\nu_3\ell_3}\left(\Lambda_{\sigma}^{-1}\Lambda_{\sigma}'-I\right)_{\nu_3\ell_3,\nu_4\ell_4}\left(A_{\sigma}^{-1}\right)_{\nu_4\ell_4,\nu_5\ell_5} G^{\sigma}_{\nu_5,\nu_2}(\ell_5,\ell_2) \tag{E.11}$$

After equation E.10 is inserted in equation E.11, equation E.11 becomes

$$\begin{aligned}\left(G^{\sigma}_{\nu_1,\nu_2}(\ell_1,\ell_2)\right)' = G^{\sigma}_{\nu_1,\nu_2}(\ell_1,\ell_2) &+ \left(G^{\sigma}-I\right)_{\nu_1\ell_1,\eta'\ell}\left(\Lambda_{\sigma}^{-1}\Lambda_{\sigma}'-I\right)_{\eta'\ell,\eta'\ell}\sum_{\ell_5,\nu_5}\left(A_{\sigma}^{-1}\right)_{\eta'\ell,\nu_5\ell_5} G^{\sigma}_{\nu_5,\nu_2}(\ell_5,\ell_2)\\ &+ \left(G^{\sigma}-I\right)_{\nu_1\ell_1,\eta\ell}\left(\Lambda_{\sigma}^{-1}\Lambda_{\sigma}'-I\right)_{\eta\ell,\eta\ell}\sum_{\ell_5,\nu_5}\left(A_{\sigma}^{-1}\right)_{\eta\ell,\nu_5\ell_5} G^{\sigma}_{\nu_5,\nu_2}(\ell_5,\ell_2)\\ &+ \left(G^{\sigma}-I\right)_{\nu_1\ell_1,\eta'\ell}\left(\Lambda_{\sigma}^{-1}\Lambda_{\sigma}'-I\right)_{\eta'\ell,\eta\ell}\sum_{\ell_5,\nu_5}\left(A_{\sigma}^{-1}\right)_{\eta\ell,\nu_5\ell_5} G^{\sigma}_{\nu_5,\nu_2}(\ell_5,\ell_2)\\ &+ \left(G^{\sigma}-I\right)_{\nu_1\ell_1,\eta\ell}\left(\Lambda_{\sigma}^{-1}\Lambda_{\sigma}'-I\right)_{\eta\ell,\eta'\ell}\sum_{\ell_5,\nu_5}\left(A_{\sigma}^{-1}\right)_{\eta'\ell,\nu_5\ell_5} G^{\sigma}_{\nu_5,\nu_2}(\ell_5,\ell_2)\end{aligned} \tag{E.12}$$

From this equation it is seen that we only need 4 elements of A_{σ}^{-1}; $(\eta\ell,\eta\ell)$, $(\eta'\ell,\eta'\ell)$, $(\eta'\ell,\eta\ell)$ and $(\eta\ell,\eta'\ell)$ elements.
Now let us calculate A_{σ}^{-1} using equation E.7 and E.10;

$$A_{\sigma} = I + \left(I-G^{\sigma}\right)\left(\Lambda_{\sigma}^{-1}\Lambda_{\sigma}'-I\right) \tag{E.13}$$

$$A_\sigma = I + \begin{bmatrix} \cdots & \cdot & \cdot & \cdots & \cdot & \cdot & \cdots \\ \cdot & \cdot & \cdot & \cdot & \cdot & \cdot & \cdot \\ \vdots & \cdot & \ddots & \cdot & \cdot & \cdot & \vdots \\ \cdot & \cdot & \cdot & \cdot & \cdot & \cdot & \cdot \\ \vdots & \cdot & \cdot & \ddots & \cdot & \cdot & \vdots \\ \cdot & \cdot & \cdot & \cdot & \cdot & \cdot & \cdot \\ \vdots & \cdot & \cdot & \cdot & \ddots & \cdot & \vdots \\ \cdot & \cdot & \cdot & \cdot & \cdot & \cdot & \cdot \\ \cdots & \cdot & \cdot & \cdots & \cdot & \cdot & \cdots \end{bmatrix} \begin{bmatrix} 0 & & & & & & 0 \\ & \ddots & & & & & \\ & & \bullet & & & \bullet & \\ & & & \ddots & & & \\ & & & & 0 & & \\ & & & & & \ddots & \\ & & \bullet & & & \bullet & \\ & & & & & & \ddots \\ 0 & & & & & & 0 \end{bmatrix} \tag{E.14}$$

$$A_\sigma = \begin{bmatrix} 1 & & & & & & 0 \\ & \ddots & & & & & \\ & & \bullet & & & \bullet & \\ & & & \ddots & & & \\ & & & & 1 & & \\ & & & & & \ddots & \\ & & \bullet & & & \bullet & \\ & & & & & & \ddots \\ 0 & & & & & & 1 \end{bmatrix} \tag{E.15}$$

Here all elements in the diagonal are 1 except the big dots, vertical lines indicates the non-zero elements, and all other elements are zero. The representation of A_σ is

$$(A_\sigma)_{\nu_1\ell_1,\nu_2\ell_2} = \delta_{\nu_1,\nu_2}\delta_{\ell_1,\ell_2} + \sum_{\nu_3,\ell_3} (I - G^\sigma)_{\nu_1\ell_1,\nu_3\ell_3} \left(\Lambda_\sigma^{-1}\Lambda'_\sigma - I\right)_{\nu_3\ell_3,\nu_2\ell_2} \tag{E.16}$$

If we insert equation E.10 into E.16, A_σ becomes

$$\begin{aligned}(A_\sigma)_{\nu_1\ell_1,\nu_2\ell_2} = \delta_{\nu_1,\nu_2}\delta_{\ell_1,\ell_2} &+ \delta_{\eta',\nu_2}\delta_{\ell,\ell_2}(I-G^\sigma)_{\nu_1\ell_1,\eta'\ell}\left(\Lambda_\sigma^{-1}\Lambda'_\sigma - I\right)_{\eta'\ell,\eta'\ell} \\ &+ \delta_{\eta,\nu_2}\delta_{\ell,\ell_2}(I-G^\sigma)_{\nu_1\ell_1,\eta\ell}\left(\Lambda_\sigma^{-1}\Lambda'_\sigma - I\right)_{\eta\ell,\eta\ell} \\ &+ \delta_{\eta,\nu_2}\delta_{\ell,\ell_2}(I-G^\sigma)_{\nu_1\ell_1,\eta'\ell}\left(\Lambda_\sigma^{-1}\Lambda'_\sigma - I\right)_{\eta'\ell,\eta\ell} \\ &+ \delta_{\eta',\nu_2}\delta_{\ell,\ell_2}(I-G^\sigma)_{\nu_1\ell_1,\eta\ell}\left(\Lambda_\sigma^{-1}\Lambda'_\sigma - I\right)_{\eta\ell,\eta'\ell} \qquad \text{(E.17)}\end{aligned}$$

Let us look at the form of A_σ^{-1}.

$$A_\sigma \cdot A_\sigma^{-1} = I \qquad \text{(E.18)}$$

The matrix form of this is following;

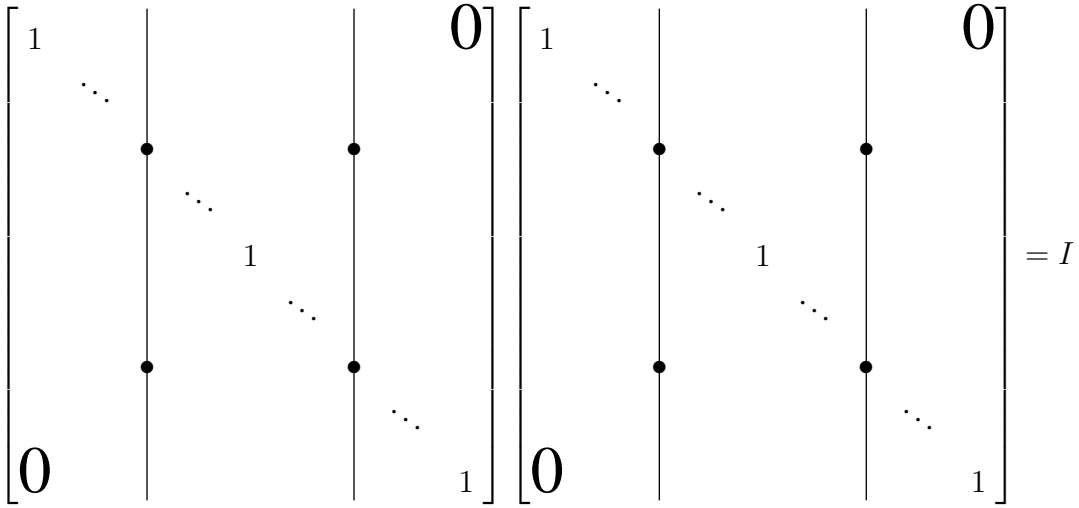

(E.19)

A_σ $\qquad\qquad$ A_σ^{-1}

It is seen from equation E.12 that we only need 4 elements of A_σ^{-1} which are indicated as big dots. Thanks to the form of A_σ^{-1}, we can work on only 2×2 part of A_σ and take the

inverse. Let us define 2×2 matrix $\widetilde{A}$ as

$$\widetilde{A} = \begin{bmatrix} (A_\sigma)_{\eta'\ell,\eta'\ell} & (A_\sigma)_{\eta'\ell,\eta\ell} \\ \\ (A_\sigma)_{\eta\ell,\eta'\ell} & (A_\sigma)_{\eta\ell,\eta\ell} \end{bmatrix} \tag{E.20}$$

The inverse of $\widetilde{A}$ is following;

$$\widetilde{A}^{-1} = \frac{1}{\det \widetilde{A}} \begin{bmatrix} (A_\sigma)_{\eta\ell,\eta\ell} & -(A_\sigma)_{\eta'\ell,\eta\ell} \\ \\ -(A_\sigma)_{\eta\ell,\eta'\ell} & (A_\sigma)_{\eta'\ell,\eta'\ell} \end{bmatrix} \tag{E.21}$$

where

$$\det \widetilde{A} = (A_\sigma)_{\eta'\ell,\eta'\ell} (A_\sigma)_{\eta\ell,\eta\ell} - (A_\sigma)_{\eta'\ell,\eta\ell} (A_\sigma)_{\eta\ell,\eta'\ell} \tag{E.22}$$

In addition to that, $\det \widetilde{A}$ is equal to $\det A_\sigma$ thanks to the form of A_σ.

$$\det \widetilde{A} = \det A_\sigma \tag{E.23}$$

Therefore, the elements which we need of A_σ^{-1} are the following;

$$\left(A_\sigma^{-1}\right)_{\eta'\ell,\eta'\ell} = \frac{(A_\sigma)_{\eta\ell,\eta\ell}}{\det A_\sigma} \tag{E.24}$$

$$\left(A_\sigma^{-1}\right)_{\eta'\ell,\eta\ell} = -\frac{(A_\sigma)_{\eta'\ell,\eta\ell}}{\det A_\sigma} \tag{E.25}$$

$$\left(A_\sigma^{-1}\right)_{\eta\ell,\eta'\ell} = -\frac{(A_\sigma)_{\eta\ell,\eta'\ell}}{\det A_\sigma} \tag{E.26}$$

$$\left(A_\sigma^{-1}\right)_{\eta\ell,\eta\ell} = \frac{(A_\sigma)_{\eta'\ell,\eta'\ell}}{\det A_\sigma} \tag{E.27}$$

Finally, after these findings equation E.12 becomes "General Expression for Updates with $(\Lambda_\sigma^{-1}\Lambda'_\sigma - I)$ Having Four Non-zero Elements";

$$
\begin{aligned}
\left(G^\sigma_{\nu_1,\nu_2}(\ell_1,\ell_2)\right)' = {} & G^\sigma_{\nu_1,\nu_2}(\ell_1,\ell_2) \\
& + \Big[(G^\sigma - I)_{\nu_1\ell_1,\eta'\ell}\left(\Lambda_\sigma^{-1}\Lambda'_\sigma - I\right)_{\eta'\ell,\eta'\ell} \\
& \quad + (G^\sigma - I)_{\nu_1\ell_1,\eta\ell}\left(\Lambda_\sigma^{-1}\Lambda'_\sigma - I\right)_{\eta\ell,\eta'\ell}\Big] \\
& \times \left[\frac{(A_\sigma)_{\eta\ell,\eta\ell}}{\det A_\sigma}G^\sigma_{\eta',\nu_2}(\ell,\ell_2) - \frac{(A_\sigma)_{\eta'\ell,\eta\ell}}{\det A_\sigma}G^\sigma_{\eta,\nu_2}(\ell,\ell_2)\right] \\
& + \Big[(G^\sigma - I)_{\nu_1\ell_1,\eta\ell}\left(\Lambda_\sigma^{-1}\Lambda'_\sigma - I\right)_{\eta\ell,\eta\ell} \\
& \quad + (G^\sigma - I)_{\nu_1\ell_1,\eta'\ell}\left(\Lambda_\sigma^{-1}\Lambda'_\sigma - I\right)_{\eta'\ell,\eta\ell}\Big] \\
& \times \left[-\frac{(A_\sigma)_{\eta\ell,\eta'\ell}}{\det A_\sigma}G^\sigma_{\eta',\nu_2}(\ell,\ell_2) + \frac{(A_\sigma)_{\eta'\ell,\eta'\ell}}{\det A_\sigma}G^\sigma_{\eta,\nu_2}(\ell,\ell_2)\right]
\end{aligned}
\tag{E.28}
$$

where

$$
\begin{aligned}
(A_\sigma)_{\eta'\ell,\eta'\ell} &= 1 + \left[1 - G^\sigma_{\eta',\eta'}(\ell,\ell)\right]\left(\Lambda_\sigma^{-1}\Lambda'_\sigma - I\right)_{\eta'\ell,\eta'\ell} - G^\sigma_{\eta',\eta}(\ell,\ell)\left(\Lambda_\sigma^{-1}\Lambda'_\sigma - I\right)_{\eta\ell,\eta'\ell} \\
(A_\sigma)_{\eta'\ell,\eta\ell} &= -G^\sigma_{\eta',\eta}(\ell,\ell)\left(\Lambda_\sigma^{-1}\Lambda'_\sigma - I\right)_{\eta\ell,\eta\ell} + \left[1 - G^\sigma_{\eta',\eta'}(\ell,\ell)\right]\left(\Lambda_\sigma^{-1}\Lambda'_\sigma - I\right)_{\eta'\ell,\eta\ell} \\
(A_\sigma)_{\eta\ell,\eta'\ell} &= -G^\sigma_{\eta,\eta'}(\ell,\ell)\left(\Lambda_\sigma^{-1}\Lambda'_\sigma - I\right)_{\eta'\ell,\eta'\ell} + \left[1 - G^\sigma_{\eta,\eta}(\ell,\ell)\right]\left(\Lambda_\sigma^{-1}\Lambda'_\sigma - I\right)_{\eta\ell,\eta'\ell} \\
(A_\sigma)_{\eta\ell,\eta\ell} &= 1 + \left[1 - G^\sigma_{\eta,\eta}(\ell,\ell)\right]\left(\Lambda_\sigma^{-1}\Lambda'_\sigma - I\right)_{\eta\ell,\eta\ell} - G^\sigma_{\eta,\eta'}(\ell,\ell)\left(\Lambda_\sigma^{-1}\Lambda'_\sigma - I\right)_{\eta'\ell,\eta\ell}
\end{aligned}
\tag{E.29}
$$

and

$$
\det A_\sigma = (A_\sigma)_{\eta'\ell,\eta'\ell}(A_\sigma)_{\eta\ell,\eta\ell} - (A_\sigma)_{\eta'\ell,\eta\ell}(A_\sigma)_{\eta\ell,\eta'\ell} \tag{E.30}
$$

Equations E.28, E.29 and E.30 are the general expressions for the updates when an arbitrary spin variable changes at an orbital on which H_J is turned on and when $N_d \cdot L \times N_d \cdot L$ matrix $(\Lambda_\sigma^{-1}\Lambda'_\sigma - I)$ has 4 non-zero elements.

E.2. General Expression for Updates with Two Non-zero Elements

When there are 2 elements of $(\Lambda_\sigma^{-1}\Lambda'_\sigma - I)$ is non-zero, the update is the same as the update derived in section E.1 except that we just exclude the off-diagonal terms of the non-zero elements. Therefore, the update of the Green's function when $(\Lambda_\sigma^{-1}\Lambda'_\sigma - I)$ has two non-zero elements is

$$\begin{aligned}\left(G^\sigma_{\nu_1,\nu_2}(\ell_1,\ell_2)\right)' = G^\sigma_{\nu_1,\nu_2}(\ell_1,\ell_2) \\ + (G^\sigma - I)_{\nu_1\ell_1,\eta'\ell}\left(\Lambda_\sigma^{-1}\Lambda'_\sigma - I\right)_{\eta'\ell,\eta'\ell} \\ \times\left[\frac{(A_\sigma)_{\eta\ell,\eta\ell}}{\det A_\sigma}G^\sigma_{\eta',\nu_2}(\ell,\ell_2) - \frac{(A_\sigma)_{\eta'\ell,\eta\ell}}{\det A_\sigma}G^\sigma_{\eta,\nu_2}(\ell,\ell_2)\right] \\ + (G^\sigma - I)_{\nu_1\ell_1,\eta\ell}\left(\Lambda_\sigma^{-1}\Lambda'_\sigma - I\right)_{\eta\ell,\eta\ell} \\ \times\left[-\frac{(A_\sigma)_{\eta\ell,\eta'\ell}}{\det A_\sigma}G^\sigma_{\eta',\nu_2}(\ell,\ell_2) + \frac{(A_\sigma)_{\eta'\ell,\eta'\ell}}{\det A_\sigma}G^\sigma_{\eta,\nu_2}(\ell,\ell_2)\right]\end{aligned} \tag{E.31}$$

where

$$\begin{aligned}(A_\sigma)_{\eta'\ell,\eta'\ell} &= 1 + \left[1 - G^\sigma_{\eta',\eta'}(\ell,\ell)\right]\left(\Lambda_\sigma^{-1}\Lambda'_\sigma - I\right)_{\eta'\ell,\eta'\ell} \\ (A_\sigma)_{\eta'\ell,\eta\ell} &= -G^\sigma_{\eta',\eta}(\ell,\ell)\left(\Lambda_\sigma^{-1}\Lambda'_\sigma - I\right)_{\eta\ell,\eta\ell} \\ (A_\sigma)_{\eta\ell,\eta'\ell} &= -G^\sigma_{\eta,\eta'}(\ell,\ell)\left(\Lambda_\sigma^{-1}\Lambda'_\sigma - I\right)_{\eta'\ell,\eta'\ell} \\ (A_\sigma)_{\eta\ell,\eta\ell} &= 1 + \left[1 - G^\sigma_{\eta,\eta}(\ell,\ell)\right]\left(\Lambda_\sigma^{-1}\Lambda'_\sigma - I\right)_{\eta\ell,\eta\ell}\end{aligned} \tag{E.32}$$

and

$$\det A_\sigma = (A_\sigma)_{\eta'\ell,\eta'\ell}(A_\sigma)_{\eta\ell,\eta\ell} - (A_\sigma)_{\eta'\ell,\eta\ell}(A_\sigma)_{\eta\ell,\eta'\ell} \tag{E.33}$$

Equations E.31, E.32 and E.33 are the general expressions for the updates when an arbitrary spin variable changes at an orbital on which H_J is turned on and when $N_d\cdot L \times N_d\cdot L$ matrix $(\Lambda_\sigma^{-1}\Lambda'_\sigma - I)$ has 2 non-zero elements.

E.3. General Expression for Updates with Five Non-zero Elements

In this section we derive the expression in section E.1 for 5 non-zero elements. This expression is used for a spin-flip operation that affects 5 elements of the matrix. The form of $\left\{\left[\Lambda_\sigma(\ell)\right]^{-1}\Lambda'_\sigma(\ell) - I\right\}_{N_d\times N_d}$ with 5 non-zero elements is following;

$$\left[\Lambda_\sigma(\ell)\right]^{-1}\Lambda'_\sigma(\ell) - I = \begin{bmatrix} 0 & & & & & & 0 \\ & \ddots & \boldsymbol{\eta',\eta'}\downarrow & & \boldsymbol{\eta',\eta}\downarrow & & \\ & & \bullet & & \bullet & & \\ & & & \ddots & & & \\ & & \bullet & & \bullet & & \\ & & \boldsymbol{\eta,\eta'}\uparrow & & \boldsymbol{\eta,\eta}\uparrow & \ddots & \\ & & & & & \bullet & \\ & & & & & \boldsymbol{\nu,\nu}\uparrow & \ddots \\ 0 & & & & & & 0 \end{bmatrix} \tag{E.34}$$

In this example, $\nu > \eta$ and $\nu > \eta'$ but it can be the opposite case. In our derivation, however, we derive it for a general case. Thus, it does not matter wherever ν is. All elements except the dots are zero. The form of $N_d \cdot L \times N_d \cdot L$ matrix $(\Lambda_\sigma^{-1}\Lambda'_\sigma - I)$ is the same;

$$\Lambda_\sigma^{-1}\Lambda'_\sigma - I = \begin{bmatrix} 0 & & & & & & 0 \\ & \ddots & \boldsymbol{\eta',\eta'}\downarrow & & \boldsymbol{\eta',\eta}\downarrow & & \\ & & \bullet & & \bullet & & \\ & & & \ddots & & & \\ & & \bullet & & \bullet & & \\ & & \boldsymbol{\eta,\eta'}\uparrow & & \boldsymbol{\eta,\eta}\uparrow & \ddots & \\ & & & & & \bullet & \\ & & & & & \boldsymbol{\nu,\nu}\uparrow & \ddots \\ 0 & & & & & & 0 \end{bmatrix} \tag{E.35}$$

The matrix representation of this matrix is not very different from equation E.10.

$$\begin{aligned}\left(\Lambda_\sigma^{-1}\Lambda'_\sigma - I\right)_{\nu_1\ell_1,\nu_2\ell_2} = \delta_{\ell,\ell_1}\delta_{\ell,\ell_2}\Big\{&\delta_{\eta',\nu_1}\delta_{\eta',\nu_2}\left(\Lambda_\sigma^{-1}\Lambda'_\sigma - I\right)_{\eta'\ell,\eta'\ell}\\ &+ \delta_{\eta,\nu_1}\delta_{\eta,\nu_2}\left(\Lambda_\sigma^{-1}\Lambda'_\sigma - I\right)_{\eta\ell,\eta\ell}\\ &+ \delta_{\eta',\nu_1}\delta_{\eta,\nu_2}\left(\Lambda_\sigma^{-1}\Lambda'_\sigma - I\right)_{\eta'\ell,\eta\ell}\\ &+ \delta_{\eta,\nu_1}\delta_{\eta',\nu_2}\left(\Lambda_\sigma^{-1}\Lambda'_\sigma - I\right)_{\eta\ell,\eta'\ell}\\ &+ \delta_{\nu,\nu_1}\delta_{\nu,\nu_2}\left(\Lambda_\sigma^{-1}\Lambda'_\sigma - I\right)_{\nu\ell,\nu\ell}\Big\}\end{aligned} \tag{E.36}$$

In order to update the Green's function, we use the following expression.

$$\begin{aligned}&\left(G^\sigma_{\nu_1,\nu_2}(\ell_1,\ell_2)\right)' = G^\sigma_{\nu_1,\nu_2}(\ell_1,\ell_2)\\ &+ \sum_{\ell_3,\ell_4,\ell_5}\sum_{\nu_3,\nu_4,\nu_5}\left(G^\sigma - I\right)_{\nu_1\ell_1,\nu_3\ell_3}\left(\Lambda_\sigma^{-1}\Lambda'_\sigma - I\right)_{\nu_3\ell_3,\nu_4\ell_4}\left(A_\sigma^{-1}\right)_{\nu_4\ell_4,\nu_5\ell_5}G^\sigma_{\nu_5,\nu_2}(\ell_5,\ell_2)\end{aligned} \tag{E.37}$$

After equation E.36 is inserted in equation E.37, equation E.37 becomes

$$\begin{aligned}\left(G^\sigma_{\nu_1,\nu_2}(\ell_1,\ell_2)\right)' = G^\sigma_{\nu_1,\nu_2}(\ell_1,\ell_2)&\\ + \left(G^\sigma - I\right)_{\nu_1\ell_1,\eta'\ell}\left(\Lambda_\sigma^{-1}\Lambda'_\sigma - I\right)_{\eta'\ell,\eta'\ell}\sum_{\ell_5,\nu_5}\left(A_\sigma^{-1}\right)_{\eta'\ell,\nu_5\ell_5}G^\sigma_{\nu_5,\nu_2}(\ell_5,\ell_2)&\\ + \left(G^\sigma - I\right)_{\nu_1\ell_1,\eta\ell}\left(\Lambda_\sigma^{-1}\Lambda'_\sigma - I\right)_{\eta\ell,\eta\ell}\sum_{\ell_5,\nu_5}\left(A_\sigma^{-1}\right)_{\eta\ell,\nu_5\ell_5}G^\sigma_{\nu_5,\nu_2}(\ell_5,\ell_2)&\\ + \left(G^\sigma - I\right)_{\nu_1\ell_1,\eta'\ell}\left(\Lambda_\sigma^{-1}\Lambda'_\sigma - I\right)_{\eta'\ell,\eta\ell}\sum_{\ell_5,\nu_5}\left(A_\sigma^{-1}\right)_{\eta\ell,\nu_5\ell_5}G^\sigma_{\nu_5,\nu_2}(\ell_5,\ell_2)&\\ + \left(G^\sigma - I\right)_{\nu_1\ell_1,\eta\ell}\left(\Lambda_\sigma^{-1}\Lambda'_\sigma - I\right)_{\eta\ell,\eta'\ell}\sum_{\ell_5,\nu_5}\left(A_\sigma^{-1}\right)_{\eta'\ell,\nu_5\ell_5}G^\sigma_{\nu_5,\nu_2}(\ell_5,\ell_2)&\\ + \left(G^\sigma - I\right)_{\nu_1\ell_1,\nu\ell}\left(\Lambda_\sigma^{-1}\Lambda'_\sigma - I\right)_{\nu\ell,\nu\ell}\sum_{\ell_5,\nu_5}\left(A_\sigma^{-1}\right)_{\nu\ell,\nu_5\ell_5}G^\sigma_{\nu_5,\nu_2}(\ell_5,\ell_2)&\end{aligned} \tag{E.38}$$

Here it is seen that we only need 3×3 part of A_σ^{-1} which consists of η', η and ν. Now let us calculate A_σ^{-1} using equation E.36;

$$A_\sigma = I + (I - G^\sigma)\left(\Lambda_\sigma^{-1}\Lambda'_\sigma - I\right) \tag{E.39}$$

$$A_\sigma = I + \begin{bmatrix} \cdots & \cdot & \cdot & \cdots & \cdot & \cdot & \cdots \\ \cdot & \cdot & \cdot & \cdot & \cdot & \cdot & \cdot \\ \vdots & \cdot & \ddots & \cdot & \cdot & \cdot & \vdots \\ \cdot & \cdot & \cdot & \cdot & \cdot & \cdot & \cdot \\ \vdots & \cdot & \cdot & \ddots & \cdot & \cdot & \vdots \\ \cdot & \cdot & \cdot & \cdot & \cdot & \cdot & \cdot \\ \vdots & \cdot & \cdot & \cdot & \ddots & \cdot & \vdots \\ \cdot & \cdot & \cdot & \cdot & \cdot & \cdot & \cdot \\ \cdots & \cdot & \cdot & \cdots & \cdot & \cdot & \cdots \end{bmatrix} \begin{bmatrix} 0 & & & & & & 0 \\ & \ddots & & & & & \\ & & \bullet & & \bullet & & \\ & & & \ddots & & & \\ & & \bullet & & \bullet & & \\ & & & & & \ddots & \\ & & & & & & \bullet \\ & & & & & & & \ddots \\ 0 & & & & & & & & 0 \end{bmatrix} \tag{E.40}$$

$$A_\sigma = \begin{bmatrix} 1 & & & & & & 0 \\ & \ddots & & & & & \\ & & \bullet & & \bullet & & \\ & & & \ddots & & & \\ & & \bullet & & \bullet & & \\ & & & & & \ddots & \\ & & & & & & \bullet \\ & & & & & & & \ddots \\ 0 & & & & & & & & 1 \end{bmatrix} \tag{E.41}$$

Here all elements in the diagonal are 1 except the big dots, vertical lines indicates the non-zero elements, and all other elements are zero. The representation of A_σ is

$$\begin{aligned}(A_\sigma)_{\nu_1\ell_1,\nu_2\ell_2} = \delta_{\nu_1,\nu_2}\delta_{\ell_1,\ell_2} &+ \delta_{\eta',\nu_2}\delta_{\ell,\ell_2}(I-G^\sigma)_{\nu_1\ell_1,\eta'\ell}\left(\Lambda_\sigma^{-1}\Lambda'_\sigma - I\right)_{\eta'\ell,\eta'\ell} \\ &+ \delta_{\eta,\nu_2}\delta_{\ell,\ell_2}(I-G^\sigma)_{\nu_1\ell_1,\eta\ell}\left(\Lambda_\sigma^{-1}\Lambda'_\sigma - I\right)_{\eta\ell,\eta\ell} \\ &+ \delta_{\eta,\nu_2}\delta_{\ell,\ell_2}(I-G^\sigma)_{\nu_1\ell_1,\eta'\ell}\left(\Lambda_\sigma^{-1}\Lambda'_\sigma - I\right)_{\eta'\ell,\eta\ell} \\ &+ \delta_{\eta',\nu_2}\delta_{\ell,\ell_2}(I-G^\sigma)_{\nu_1\ell_1,\eta\ell}\left(\Lambda_\sigma^{-1}\Lambda'_\sigma - I\right)_{\eta\ell,\eta'\ell} \\ &+ \delta_{\nu,\nu_2}\delta_{\ell,\ell_2}(I-G^\sigma)_{\nu_1\ell_1,\nu\ell}\left(\Lambda_\sigma^{-1}\Lambda'_\sigma - I\right)_{\nu\ell,\nu\ell}\end{aligned} \tag{E.42}$$

Let us look at the form of A_σ^{-1}.

$$A_\sigma \cdot A_\sigma^{-1} = I \tag{E.43}$$

The matrix form of this is following;

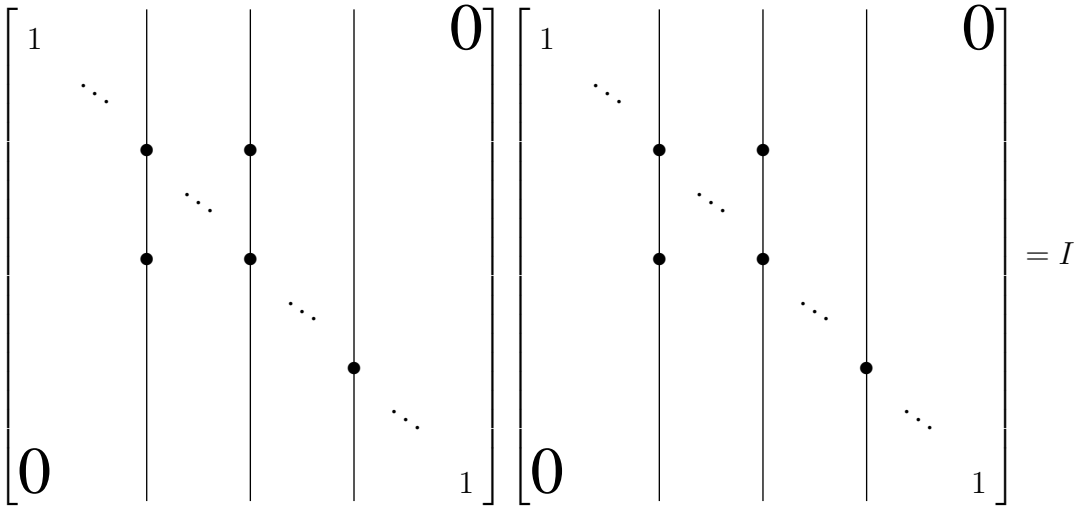

(E.44)

A_σ $\qquad\qquad$ A_σ^{-1}

It is seen from equation E.38 that we only need 9 elements of A_σ^{-1} which are indicated as big dots. Thanks to the form of A_σ^{-1}, we can work on only 3×3 part of A_σ and take the

inverse. Let us define 3×3 matrix $\widetilde{A}$ as

$$\widetilde{A} = \begin{bmatrix} (A_\sigma)_{\eta'\ell,\eta'\ell} & (A_\sigma)_{\eta'\ell,\eta\ell} & (A_\sigma)_{\eta'\ell,\nu\ell} \\ (A_\sigma)_{\eta\ell,\eta'\ell} & (A_\sigma)_{\eta\ell,\eta\ell} & (A_\sigma)_{\eta\ell,\nu\ell} \\ (A_\sigma)_{\nu\ell,\eta'\ell} & (A_\sigma)_{\nu\ell,\eta\ell} & (A_\sigma)_{\nu\ell,\nu\ell} \end{bmatrix} \tag{E.45}$$

We can find the inverse of $\widetilde{A}$ by using 2×2 determinants of $\widetilde{A}$.

$$\widetilde{A}^{-1} = \frac{1}{\det \widetilde{A}} \begin{bmatrix} \begin{vmatrix} (A_\sigma)_{\eta\ell,\eta\ell} & (A_\sigma)_{\eta\ell,\nu\ell} \\ (A_\sigma)_{\nu\ell,\eta\ell} & (A_\sigma)_{\nu\ell,\nu\ell} \end{vmatrix} & \begin{vmatrix} (A_\sigma)_{\eta'\ell,\nu\ell} & (A_\sigma)_{\eta'\ell,\eta\ell} \\ (A_\sigma)_{\nu\ell,\nu\ell} & (A_\sigma)_{\nu\ell,\eta\ell} \end{vmatrix} & \begin{vmatrix} (A_\sigma)_{\eta'\ell,\eta\ell} & (A_\sigma)_{\eta'\ell,\nu\ell} \\ (A_\sigma)_{\eta\ell,\eta\ell} & (A_\sigma)_{\eta\ell,\nu\ell} \end{vmatrix} \\ \begin{vmatrix} (A_\sigma)_{\eta\ell,\nu\ell} & (A_\sigma)_{\eta\ell,\eta'\ell} \\ (A_\sigma)_{\nu\ell,\nu\ell} & (A_\sigma)_{\nu\ell,\eta'\ell} \end{vmatrix} & \begin{vmatrix} (A_\sigma)_{\eta'\ell,\eta'\ell} & (A_\sigma)_{\eta'\ell,\nu\ell} \\ (A_\sigma)_{\nu\ell,\eta'\ell} & (A_\sigma)_{\nu\ell,\nu\ell} \end{vmatrix} & \begin{vmatrix} (A_\sigma)_{\eta'\ell,\nu\ell} & (A_\sigma)_{\eta'\ell,\eta'\ell} \\ (A_\sigma)_{\eta\ell,\nu\ell} & (A_\sigma)_{\eta\ell,\eta'\ell} \end{vmatrix} \\ \begin{vmatrix} (A_\sigma)_{\eta\ell,\eta'\ell} & (A_\sigma)_{\eta\ell,\eta\ell} \\ (A_\sigma)_{\nu\ell,\eta'\ell} & (A_\sigma)_{\nu\ell,\eta\ell} \end{vmatrix} & \begin{vmatrix} (A_\sigma)_{\eta'\ell,\eta\ell} & (A_\sigma)_{\eta'\ell,\eta'\ell} \\ (A_\sigma)_{\nu\ell,\eta\ell} & (A_\sigma)_{\nu\ell,\eta'\ell} \end{vmatrix} & \begin{vmatrix} (A_\sigma)_{\eta'\ell,\eta'\ell} & (A_\sigma)_{\eta'\ell,\eta\ell} \\ (A_\sigma)_{\eta\ell,\eta'\ell} & (A_\sigma)_{\eta\ell,\eta\ell} \end{vmatrix} \end{bmatrix} \tag{E.46}$$

As in section E.1, because of the form of A_σ, determinants of A_σ and $\widetilde{A}$ are equal.

$$\det \widetilde{A} = \det A_\sigma \tag{E.47}$$

We have all the elements that we need for updating the Green's function. From matrix E.45, we can calculate the determinant of A_σ, which is

$$\begin{aligned}\det A_\sigma = &(A_\sigma)_{\eta'\ell,\eta'\ell}\left[(A_\sigma)_{\eta\ell,\eta\ell}(A_\sigma)_{\nu\ell,\nu\ell} - (A_\sigma)_{\eta\ell,\nu\ell}(A_\sigma)_{\nu\ell,\eta\ell}\right] \\ &- (A_\sigma)_{\eta\ell,\eta'\ell}\left[(A_\sigma)_{\eta'\ell,\eta\ell}(A_\sigma)_{\nu\ell,\nu\ell} - (A_\sigma)_{\eta'\ell,\nu\ell}(A_\sigma)_{\nu\ell,\eta\ell}\right] \\ &+ (A_\sigma)_{\nu\ell,\eta'\ell}\left[(A_\sigma)_{\eta'\ell,\eta\ell}(A_\sigma)_{\eta\ell,\nu\ell} - (A_\sigma)_{\eta'\ell,\nu\ell}(A_\sigma)_{\eta\ell,\eta\ell}\right]\end{aligned} \tag{E.48}$$

From equation E.42, we know the 3×3 part of A_σ. 9 elements of A_σ are

$$\begin{aligned}(A_\sigma)_{\eta'\ell,\eta'\ell} &= 1 + \left[1 - G^\sigma_{\eta',\eta'}(\ell,\ell)\right]\left(\Lambda_\sigma^{-1}\Lambda'_\sigma - I\right)_{\eta'\ell,\eta'\ell} - G^\sigma_{\eta',\eta}(\ell,\ell)\left(\Lambda_\sigma^{-1}\Lambda'_\sigma - I\right)_{\eta\ell,\eta'\ell} \\ (A_\sigma)_{\eta'\ell,\eta\ell} &= -G^\sigma_{\eta',\eta}(\ell,\ell)\left(\Lambda_\sigma^{-1}\Lambda'_\sigma - I\right)_{\eta\ell,\eta\ell} + \left[1 - G^\sigma_{\eta',\eta'}(\ell,\ell)\right]\left(\Lambda_\sigma^{-1}\Lambda'_\sigma - I\right)_{\eta'\ell,\eta\ell} \\ (A_\sigma)_{\eta'\ell,\nu\ell} &= -G^\sigma_{\eta',\nu}(\ell,\ell)\left(\Lambda_\sigma^{-1}\Lambda'_\sigma - I\right)_{\nu\ell,\nu\ell}\end{aligned} \tag{E.49}$$

$$\begin{aligned}(A_\sigma)_{\eta\ell,\eta'\ell} &= -G^\sigma_{\eta,\eta'}(\ell,\ell)\left(\Lambda_\sigma^{-1}\Lambda'_\sigma - I\right)_{\eta'\ell,\eta'\ell} + \left[1 - G^\sigma_{\eta,\eta}(\ell,\ell)\right]\left(\Lambda_\sigma^{-1}\Lambda'_\sigma - I\right)_{\eta\ell,\eta'\ell} \\ (A_\sigma)_{\eta\ell,\eta\ell} &= 1 + \left[1 - G^\sigma_{\eta,\eta}(\ell,\ell)\right]\left(\Lambda_\sigma^{-1}\Lambda'_\sigma - I\right)_{\eta\ell,\eta\ell} - G^\sigma_{\eta,\eta'}(\ell,\ell)\left(\Lambda_\sigma^{-1}\Lambda'_\sigma - I\right)_{\eta'\ell,\eta\ell} \\ (A_\sigma)_{\eta\ell,\nu\ell} &= -G^\sigma_{\eta,\nu}(\ell,\ell)\left(\Lambda_\sigma^{-1}\Lambda'_\sigma - I\right)_{\nu\ell,\nu\ell}\end{aligned} \tag{E.50}$$

$$\begin{aligned}(A_\sigma)_{\nu\ell,\eta'\ell} &= -G^\sigma_{\nu,\eta'}(\ell,\ell)\left(\Lambda_\sigma^{-1}\Lambda'_\sigma - I\right)_{\eta'\ell,\eta'\ell} - G^\sigma_{\nu,\eta}(\ell,\ell)\left(\Lambda_\sigma^{-1}\Lambda'_\sigma - I\right)_{\eta\ell,\eta'\ell} \\ (A_\sigma)_{\nu\ell,\eta\ell} &= -G^\sigma_{\nu,\eta}(\ell,\ell)\left(\Lambda_\sigma^{-1}\Lambda'_\sigma - I\right)_{\eta\ell,\eta\ell} - G^\sigma_{\nu,\eta'}(\ell,\ell)\left(\Lambda_\sigma^{-1}\Lambda'_\sigma - I\right)_{\eta'\ell,\eta\ell} \\ (A_\sigma)_{\nu\ell,\nu\ell} &= 1 + \left[1 - G^\sigma_{\nu,\nu}(\ell,\ell)\right]\left(\Lambda_\sigma^{-1}\Lambda'_\sigma - I\right)_{\nu\ell,\nu\ell}\end{aligned} \tag{E.51}$$

From matrix E.46, we know the 9 elements of A_σ^{-1} which are

$$\begin{aligned}\left(A_\sigma^{-1}\right)_{\eta'\ell,\eta'\ell} &= (\det A_\sigma)^{-1}\left[(A_\sigma)_{\eta\ell,\eta\ell}(A_\sigma)_{\nu\ell,\nu\ell} - (A_\sigma)_{\eta\ell,\nu\ell}(A_\sigma)_{\nu\ell,\eta\ell}\right] \\ \left(A_\sigma^{-1}\right)_{\eta'\ell,\eta\ell} &= (\det A_\sigma)^{-1}\left[(A_\sigma)_{\eta'\ell,\nu\ell}(A_\sigma)_{\nu\ell,\eta\ell} - (A_\sigma)_{\eta'\ell,\eta\ell}(A_\sigma)_{\nu\ell,\nu\ell}\right] \\ \left(A_\sigma^{-1}\right)_{\eta'\ell,\nu\ell} &= (\det A_\sigma)^{-1}\left[(A_\sigma)_{\eta'\ell,\eta\ell}(A_\sigma)_{\eta\ell,\nu\ell} - (A_\sigma)_{\eta'\ell,\nu\ell}(A_\sigma)_{\eta\ell,\eta\ell}\right]\end{aligned} \tag{E.52}$$

$$
\begin{aligned}
\left(A_\sigma^{-1}\right)_{\eta\ell,\eta'\ell} &= (\det A_\sigma)^{-1}\left[(A_\sigma)_{\eta\ell,\nu\ell}(A_\sigma)_{\nu\ell,\eta'\ell} - (A_\sigma)_{\eta\ell,\eta'\ell}(A_\sigma)_{\nu\ell,\nu\ell}\right] \\
\left(A_\sigma^{-1}\right)_{\eta\ell,\eta\ell} &= (\det A_\sigma)^{-1}\left[(A_\sigma)_{\eta'\ell,\eta'\ell}(A_\sigma)_{\nu\ell,\nu\ell} - (A_\sigma)_{\eta'\ell,\nu\ell}(A_\sigma)_{\nu\ell,\eta'\ell}\right] \\
\left(A_\sigma^{-1}\right)_{\eta\ell,\nu\ell} &= (\det A_\sigma)^{-1}\left[(A_\sigma)_{\eta'\ell,\nu\ell}(A_\sigma)_{\eta\ell,\eta'\ell} - (A_\sigma)_{\eta'\ell,\eta'\ell}(A_\sigma)_{\eta\ell,\nu\ell}\right]
\end{aligned}
\tag{E.53}
$$

$$
\begin{aligned}
\left(A_\sigma^{-1}\right)_{\nu\ell,\eta'\ell} &= (\det A_\sigma)^{-1}\left[(A_\sigma)_{\eta\ell,\eta'\ell}(A_\sigma)_{\nu\ell,\eta\ell} - (A_\sigma)_{\eta\ell,\eta\ell}(A_\sigma)_{\nu\ell,\eta'\ell}\right] \\
\left(A_\sigma^{-1}\right)_{\nu\ell,\eta\ell} &= (\det A_\sigma)^{-1}\left[(A_\sigma)_{\eta'\ell,\eta\ell}(A_\sigma)_{\nu\ell,\eta'\ell} - (A_\sigma)_{\eta'\ell,\eta'\ell}(A_\sigma)_{\nu\ell,\eta\ell}\right] \\
\left(A_\sigma^{-1}\right)_{\nu\ell,\nu\ell} &= (\det A_\sigma)^{-1}\left[(A_\sigma)_{\eta'\ell,\eta'\ell}(A_\sigma)_{\eta\ell,\eta\ell} - (A_\sigma)_{\eta'\ell,\eta\ell}(A_\sigma)_{\eta\ell,\eta'\ell}\right]
\end{aligned}
\tag{E.54}
$$

Finally, after these findings equation E.38 becomes "General Expression for Updates with $(\Lambda_\sigma^{-1}\Lambda'_\sigma - I)$ Having Five Non-zero Elements";

$$
\begin{aligned}
&\left(G^\sigma_{\nu_1,\nu_2}(\ell_1,\ell_2)\right)' = G^\sigma_{\nu_1,\nu_2}(\ell_1,\ell_2) \\
&+ \left[(G^\sigma - I)_{\nu_1\ell_1,\eta'\ell}\left(\Lambda_\sigma^{-1}\Lambda'_\sigma - I\right)_{\eta'\ell,\eta'\ell} + (G^\sigma - I)_{\nu_1\ell_1,\eta\ell}\left(\Lambda_\sigma^{-1}\Lambda'_\sigma - I\right)_{\eta\ell,\eta'\ell}\right] \\
&\quad \times \left[\left(A_\sigma^{-1}\right)_{\eta'\ell,\eta'\ell} G^\sigma_{\eta',\nu_2}(\ell,\ell_2) + \left(A_\sigma^{-1}\right)_{\eta'\ell,\eta\ell} G^\sigma_{\eta,\nu_2}(\ell,\ell_2) + \left(A_\sigma^{-1}\right)_{\eta'\ell,\nu\ell} G^\sigma_{\nu,\nu_2}(\ell,\ell_2)\right] \\
&+ \left[(G^\sigma - I)_{\nu_1\ell_1,\eta\ell}\left(\Lambda_\sigma^{-1}\Lambda'_\sigma - I\right)_{\eta\ell,\eta\ell} + (G^\sigma - I)_{\nu_1\ell_1,\eta'\ell}\left(\Lambda_\sigma^{-1}\Lambda'_\sigma - I\right)_{\eta'\ell,\eta\ell}\right] \\
&\quad \times \left[\left(A_\sigma^{-1}\right)_{\eta\ell,\eta'\ell} G^\sigma_{\eta',\nu_2}(\ell,\ell_2) + \left(A_\sigma^{-1}\right)_{\eta\ell,\eta\ell} G^\sigma_{\eta,\nu_2}(\ell,\ell_2) + \left(A_\sigma^{-1}\right)_{\eta\ell,\nu\ell} G^\sigma_{\nu,\nu_2}(\ell,\ell_2)\right] \\
&+ (G^\sigma - I)_{\nu_1\ell_1,\nu\ell}\left(\Lambda_\sigma^{-1}\Lambda'_\sigma - I\right)_{\nu\ell,\nu\ell} \\
&\quad \times \left[\left(A_\sigma^{-1}\right)_{\nu\ell,\eta'\ell} G^\sigma_{\eta',\nu_2}(\ell,\ell_2) + \left(A_\sigma^{-1}\right)_{\nu\ell,\eta\ell} G^\sigma_{\eta,\nu_2}(\ell,\ell_2) + \left(A_\sigma^{-1}\right)_{\nu\ell,\nu\ell} G^\sigma_{\nu,\nu_2}(\ell,\ell_2)\right]
\end{aligned}
\tag{E.55}
$$

Equations E.48, E.49, E.50, E.51, E.52, E.53, E.54 and E.55 are the general expressions for the updates when an arbitrary spin variable changes at an orbital on which H_J is turned on and when $N_d \cdot L \times N_d \cdot L$ matrix $(\Lambda_\sigma^{-1}\Lambda'_\sigma - I)$ has 5 non-zero elements.

E.4. Single Spin-flip for "r_ℓ"

Spin-flip for r_ℓ occurs in two ways. First one is turning on the effect of H_J for imaginary-time slice ℓ, and the second one is turning it off for imaginary-time slice ℓ.

E.4.1. Turning on the effect of H_J

Let us look at the turning on case which is following;

$$r_\ell = 0 \quad \longrightarrow \quad r'_\ell = 1$$

This move turns on three auxiliary field variables at time slice ℓ, and impurity sites η, η'. These variables are q_ℓ, $t_{\uparrow\ell}$ and $t_{\downarrow\ell}$.

$$\begin{aligned} q_\ell = 0 \quad &\longrightarrow \quad q'_\ell = \pm 1 \\ t_{\uparrow\ell} = 0 \quad &\longrightarrow \quad t'_{\uparrow\ell} = \pm 1 \\ t_{\downarrow\ell} = 0 \quad &\longrightarrow \quad t'_{\downarrow\ell} = \pm 1 \end{aligned}$$

Green's function for new spin configuration is calculated with the relation

$$(G^\sigma)' = G^\sigma + (G^\sigma - I)\left(\Lambda_\sigma^{-1}\Lambda'_\sigma - I\right) A_\sigma^{-1} G^\sigma \tag{E.56}$$

Let us look at the form of $(\Lambda_\sigma^{-1}\Lambda'_\sigma - I)$. We know the forms of the matrices $[\Lambda_\sigma(\ell)]^{-1}$ and $\Lambda'_\sigma(\ell)$ from section 4.3.

$$\Lambda'_\sigma(\ell) = \begin{bmatrix} \ddots & & & 0 \\ & e^{\lambda_4 t_{\sigma\ell}} \cosh(\lambda_4 \sigma q_\ell) e^{W_{\eta',\sigma}(\ell)} & e^{\lambda_4 t_{\sigma\ell}} \sinh(\lambda_4 \sigma q_\ell) e^{W_{\eta',\sigma}(\ell)} & \\ & & \ddots & \\ & e^{\lambda_4 t_{\sigma\ell}} \sinh(\lambda_4 \sigma q_\ell) e^{W_{\eta,\sigma}(\ell)} & e^{\lambda_4 t_{\sigma\ell}} \cosh(\lambda_4 \sigma q_\ell) e^{W_{\eta,\sigma}(\ell)} & \\ 0 & & & \ddots \end{bmatrix} \tag{E.57}$$

and

$$[\Lambda_\sigma(\ell)]^{-1} = \begin{bmatrix} \ddots & & & 0 \\ & e^{-W_{\eta',\sigma}(\ell)} & & \\ & & \ddots & \\ & & e^{-W_{\eta,\sigma}(\ell)} & \\ 0 & & & \ddots \end{bmatrix} \tag{E.58}$$

After we multiply them, we get the form of $\left\{\left[\Lambda_\sigma(\ell)\right]^{-1}\Lambda'_\sigma(\ell)-I\right\}_{N_d\times N_d}$;

$$
\left[\Lambda_\sigma(\ell)\right]^{-1}\Lambda'_\sigma(\ell)-I=
\begin{bmatrix}
0 & & & & & & 0\\
& \ddots & \overset{\boldsymbol{\eta',\eta'}}{\downarrow} & & \overset{\boldsymbol{\eta',\eta}}{\downarrow} & & \\
& & e^{\lambda_4 t_{\sigma\ell}}\cosh(\lambda_4\sigma q_\ell)-1 & & e^{\lambda_4 t_{\sigma\ell}}\sinh(\lambda_4\sigma q_\ell) & & \\
& & & 0 & & & \\
& & e^{\lambda_4 t_{\sigma\ell}}\sinh(\lambda_4\sigma q_\ell) & & e^{\lambda_4 t_{\sigma\ell}}\cosh(\lambda_4\sigma q_\ell)-1 & & \\
& & \underset{\boldsymbol{\eta,\eta'}}{\uparrow} & & \underset{\boldsymbol{\eta,\eta}}{\uparrow} & \ddots & \\
0 & & & & & & 0
\end{bmatrix}
\tag{E.59}
$$

Since the change occurs only at imaginary-time slice ℓ, the form of $(\Lambda_\sigma^{-1}\Lambda'_\sigma-I)$ is the same.

$$
\Lambda_\sigma^{-1}\Lambda'_\sigma-I=
\begin{bmatrix}
0 & & & & & & 0\\
& \ddots & & & & & \\
& & e^{\lambda_4 t_{\sigma\ell}}\cosh(\lambda_4\sigma q_\ell)-1 & & e^{\lambda_4 t_{\sigma\ell}}\sinh(\lambda_4\sigma q_\ell) & & \\
& & & 0 & & & \\
& & e^{\lambda_4 t_{\sigma\ell}}\sinh(\lambda_4\sigma q_\ell) & & e^{\lambda_4 t_{\sigma\ell}}\cosh(\lambda_4\sigma q_\ell)-1 & & \\
& & & & & \ddots & \\
0 & & & & & & 0
\end{bmatrix}
\tag{E.60}
$$

All elements are zero except the four elements which are located at $(\eta'\ell,\eta'\ell)$, $(\eta'\ell,\eta\ell)$, $(\eta\ell,\eta'\ell)$ and $(\eta\ell,\eta\ell)$. For this new spin configuration, the update expression of Green's function is equation E.28, because the matrix, $(\Lambda_\sigma^{-1}\Lambda'_\sigma-I)$, has only 4 non-zero ele-

ments. The elements which are used for the Green's function update caused by

$$r_\ell = 0 \quad \longrightarrow \quad r'_\ell = 1$$

change are

$$\boxed{\begin{aligned}
\left(\Lambda_\sigma^{-1}\Lambda'_\sigma - I\right)_{\eta'\ell,\eta'\ell} &= e^{\lambda_4 t_{\sigma\ell}}\cosh(\lambda_4\sigma q_\ell) - 1 \\
\left(\Lambda_\sigma^{-1}\Lambda'_\sigma - I\right)_{\eta'\ell,\eta\ell} &= e^{\lambda_4 t_{\sigma\ell}}\sinh(\lambda_4\sigma q_\ell) \\
\left(\Lambda_\sigma^{-1}\Lambda'_\sigma - I\right)_{\eta\ell,\eta'\ell} &= e^{\lambda_4 t_{\sigma\ell}}\sinh(\lambda_4\sigma q_\ell) \\
\left(\Lambda_\sigma^{-1}\Lambda'_\sigma - I\right)_{\eta\ell,\eta\ell} &= e^{\lambda_4 t_{\sigma\ell}}\cosh(\lambda_4\sigma q_\ell) - 1
\end{aligned}} \tag{E.61}$$

E.4.2. Turning off the effect of H_J

Let us look at the turning on case which is following;

$$r_\ell = 1 \quad \longrightarrow \quad r'_\ell = 0$$

This move turns off three auxiliary field variables at time slice ℓ, and impurity sites η, η'. These variables are q_ℓ, $t_{\uparrow\ell}$ and $t_{\downarrow\ell}$.

$$\begin{aligned}
q_\ell = \pm 1 \quad &\longrightarrow \quad q'_\ell = 0 \\
t_{\uparrow\ell} = \pm 1 \quad &\longrightarrow \quad t'_{\uparrow\ell} = 0 \\
t_{\downarrow\ell} = \pm 1 \quad &\longrightarrow \quad t'_{\downarrow\ell} = 0
\end{aligned}$$

Green's function for new spin configuration is calculated with the relation

$$(G^\sigma)' = G^\sigma + (G^\sigma - I)\left(\Lambda_\sigma^{-1}\Lambda'_\sigma - I\right)A_\sigma^{-1}G^\sigma \tag{E.62}$$

Let us look at the form of $(\Lambda_\sigma^{-1}\Lambda'_\sigma - I)$. We know the forms of the matrices $[\Lambda_\sigma(\ell)]^{-1}$ and $\Lambda'_\sigma(\ell)$ from section 4.3.

$$\Lambda'_\sigma(\ell) = \begin{bmatrix} \ddots & & & 0 \\ & e^{W_{\eta',\sigma}(\ell)} & & \\ & & \ddots & \\ & & & e^{W_{\eta,\sigma}(\ell)} \\ 0 & & & \ddots \end{bmatrix} \tag{E.63}$$

and

$$[\Lambda_\sigma(\ell)]^{-1} = \begin{bmatrix} \ddots & & & 0 \\ & e^{-\lambda_4 t_{\sigma\ell}}\cosh(\lambda_4\sigma q_\ell)e^{-W_{\eta',\sigma}(\ell)} & -e^{-\lambda_4 t_{\sigma\ell}}\sinh(\lambda_4\sigma q_\ell)e^{-W_{\eta,\sigma}(\ell)} & \\ & & \ddots & \\ & -e^{-\lambda_4 t_{\sigma\ell}}\sinh(\lambda_4\sigma q_\ell)e^{-W_{\eta',\sigma}(\ell)} & e^{-\lambda_4 t_{\sigma\ell}}\cosh(\lambda_4\sigma q_\ell)e^{-W_{\eta,\sigma}(\ell)} & \\ 0 & & & \ddots \end{bmatrix} \tag{E.64}$$

After we multiply them, we get the form of $\left\{\left[\Lambda_\sigma(\ell)\right]^{-1}\Lambda'_\sigma(\ell) - I\right\}_{N_d \times N_d}$;

$$
\left[\Lambda_\sigma(\ell)\right]^{-1}\Lambda'_\sigma(\ell) - I =
$$

$$
\begin{bmatrix}
0 & & & & & & 0 \\
& \ddots & \overset{\boldsymbol{\eta',\eta'}}{\downarrow} & & \overset{\boldsymbol{\eta',\eta}}{\downarrow} & & \\
& & e^{-\lambda_4 t_{\sigma\ell}}\cosh(\lambda_4\sigma q_\ell) - 1 & & -e^{-\lambda_4 t_{\sigma\ell}}\sinh(\lambda_4\sigma q_\ell) & & \\
& & & 0 & & & \\
& & -e^{-\lambda_4 t_{\sigma\ell}}\sinh(\lambda_4\sigma q_\ell) & & e^{-\lambda_4 t_{\sigma\ell}}\cosh(\lambda_4\sigma q_\ell) - 1 & & \\
& & \underset{\boldsymbol{\eta,\eta'}}{\uparrow} & & \underset{\boldsymbol{\eta,\eta}}{\uparrow} & \ddots & \\
0 & & & & & & 0
\end{bmatrix}
\tag{E.65}
$$

Since the change occurs only at imaginary-time slice ℓ, the form of $(\Lambda_\sigma^{-1}\Lambda'_\sigma - I)$ is the same.

$$
\Lambda_\sigma^{-1}\Lambda'_\sigma - I =
$$

$$
\begin{bmatrix}
0 & & & & & & 0 \\
& \ddots & & & & & \\
& & e^{-\lambda_4 t_{\sigma\ell}}\cosh(\lambda_4\sigma q_\ell) - 1 & & -e^{-\lambda_4 t_{\sigma\ell}}\sinh(\lambda_4\sigma q_\ell) & & \\
& & & 0 & & & \\
& & -e^{-\lambda_4 t_{\sigma\ell}}\sinh(\lambda_4\sigma q_\ell) & & e^{-\lambda_4 t_{\sigma\ell}}\cosh(\lambda_4\sigma q_\ell) - 1 & & \\
& & & & & \ddots & \\
0 & & & & & & 0
\end{bmatrix}
\tag{E.66}
$$

All elements are zero except the four elements which are located at $(\eta'\ell, \eta'\ell)$, $(\eta'\ell, \eta\ell)$, $(\eta\ell, \eta'\ell)$ and $(\eta\ell, \eta\ell)$. For this new spin configuration, the update expression of Green's function is equation E.28, because the matrix, $(\Lambda_\sigma^{-1}\Lambda'_\sigma - I)$, has only 4 non-zero ele-

ments. The elements which are used for the Green's function update caused by

$$r_\ell = 1 \quad \longrightarrow \quad r'_\ell = 0$$

change are

$$\boxed{\begin{aligned}
\left(\Lambda_\sigma^{-1}\Lambda'_\sigma - I\right)_{\eta'\ell,\eta'\ell} &= e^{-\lambda_4 t_{\sigma\ell}} \cosh(\lambda_4 \sigma q_\ell) - 1 \\
\left(\Lambda_\sigma^{-1}\Lambda'_\sigma - I\right)_{\eta'\ell,\eta\ell} &= -e^{-\lambda_4 t_{\sigma\ell}} \sinh(\lambda_4 \sigma q_\ell) \\
\left(\Lambda_\sigma^{-1}\Lambda'_\sigma - I\right)_{\eta\ell,\eta'\ell} &= -e^{-\lambda_4 t_{\sigma\ell}} \sinh(\lambda_4 \sigma q_\ell) \\
\left(\Lambda_\sigma^{-1}\Lambda'_\sigma - I\right)_{\eta\ell,\eta\ell} &= e^{-\lambda_4 t_{\sigma\ell}} \cosh(\lambda_4 \sigma q_\ell) - 1
\end{aligned}} \tag{E.67}$$

E.5. Single Spin-flip for "q_ℓ"

The spin-flip for q_ℓ occurs in the following way.

$$q_\ell \quad \longrightarrow \quad q'_\ell = -q_\ell$$

Green's function for new spin configuration is calculated with the relation

$$(G^\sigma)' = G^\sigma + (G^\sigma - I)\left(\Lambda_\sigma^{-1}\Lambda'_\sigma - I\right) A_\sigma^{-1} G^\sigma \tag{E.68}$$

Let us look at the form of $(\Lambda_\sigma^{-1}\Lambda'_\sigma - I)$. We know the forms of the matrices $[\Lambda_\sigma(\ell)]^{-1}$ and $\Lambda'_\sigma(\ell)$ from section 4.3.

$$\Lambda'_\sigma(\ell) = \begin{bmatrix} \ddots & & & 0 \\ & e^{\lambda_4 t_{\sigma\ell}} \cosh(\lambda_4 \sigma q_\ell) e^{W_{\eta',\sigma}(\ell)} & -e^{\lambda_4 t_{\sigma\ell}} \sinh(\lambda_4 \sigma q_\ell) e^{W_{\eta',\sigma}(\ell)} & \\ & & \ddots & \\ & -e^{\lambda_4 t_{\sigma\ell}} \sinh(\lambda_4 \sigma q_\ell) e^{W_{\eta,\sigma}(\ell)} & e^{\lambda_4 t_{\sigma\ell}} \cosh(\lambda_4 \sigma q_\ell) e^{W_{\eta,\sigma}(\ell)} & \\ 0 & & & \ddots \end{bmatrix} \tag{E.69}$$

and

$$[\Lambda_\sigma(\ell)]^{-1} = \begin{bmatrix} \ddots & & & 0 \\ & e^{-\lambda_4 t_{\sigma\ell}} \cosh(\lambda_4 \sigma q_\ell) e^{-W_{\eta',\sigma}(\ell)} & -e^{-\lambda_4 t_{\sigma\ell}} \sinh(\lambda_4 \sigma q_\ell) e^{-W_{\eta,\sigma}(\ell)} & \\ & & \ddots & \\ & -e^{-\lambda_4 t_{\sigma\ell}} \sinh(\lambda_4 \sigma q_\ell) e^{-W_{\eta',\sigma}(\ell)} & e^{-\lambda_4 t_{\sigma\ell}} \cosh(\lambda_4 \sigma q_\ell) e^{-W_{\eta,\sigma}(\ell)} & \\ 0 & & & \ddots \end{bmatrix} \tag{E.70}$$

After we multiply them, we get the form of $\left\{[\Lambda_\sigma(\ell)]^{-1}\,\Lambda'_\sigma(\ell) - I\right\}_{N_d \times N_d}$, and the result can be reduced more by using hyperbolic identities. Since the change occurs only at imaginary-time slice ℓ, the form of $(\Lambda_\sigma^{-1}\Lambda'_\sigma - I)$ is the same. The reduced form of the

matrix is

$$\Lambda_\sigma^{-1}\Lambda'_\sigma - I = \begin{bmatrix} 0 & & & & & & 0 \\ & \ddots & & & & & \\ & & \cosh(2\lambda_4\sigma q_\ell) - 1 & & -\sinh(2\lambda_4\sigma q_\ell) & & \\ & & & 0 & & & \\ & & -\sinh(2\lambda_4\sigma q_\ell) & & \cosh(2\lambda_4\sigma q_\ell) - 1 & & \\ & & & & & \ddots & \\ 0 & & & & & & 0 \end{bmatrix} \tag{E.71}$$

All elements are zero except the four elements which are located at $(\eta'\ell, \eta'\ell)$, $(\eta'\ell, \eta\ell)$, $(\eta\ell, \eta'\ell)$ and $(\eta\ell, \eta\ell)$. For this new spin configuration, the update expression of Green's function is equation E.28, because the matrix, $(\Lambda_\sigma^{-1}\Lambda'_\sigma - I)$, has only 4 non-zero elements. The elements which are used for the Green's function update caused by

$$q_\ell \quad \longrightarrow \quad q'_\ell = -q_\ell$$

change are

$$\boxed{\begin{aligned} \left(\Lambda_\sigma^{-1}\Lambda'_\sigma - I\right)_{\eta'\ell,\eta'\ell} &= \cosh(2\lambda_4\sigma q_\ell) - 1 \\ \left(\Lambda_\sigma^{-1}\Lambda'_\sigma - I\right)_{\eta'\ell,\eta\ell} &= -\sinh(2\lambda_4\sigma q_\ell) \\ \left(\Lambda_\sigma^{-1}\Lambda'_\sigma - I\right)_{\eta\ell,\eta'\ell} &= -\sinh(2\lambda_4\sigma q_\ell) \\ \left(\Lambda_\sigma^{-1}\Lambda'_\sigma - I\right)_{\eta\ell,\eta\ell} &= \cosh(2\lambda_4\sigma q_\ell) - 1 \end{aligned}} \tag{E.72}$$

E.6. Single Spin-flip for "$t_{\sigma\ell}$"

The spin-flip for $t_{\sigma\ell}$ occurs in the following way.

$$t_{\sigma\ell} \quad \longrightarrow \quad t'_{\sigma\ell} = -t_{\sigma\ell}$$

Green's function for new spin configuration is calculated with the relation

$$(G^\sigma)' = G^\sigma + (G^\sigma - I)\left(\Lambda_\sigma^{-1}\Lambda'_\sigma - I\right) A_\sigma^{-1} G^\sigma \tag{E.73}$$

Let us look at the form of $(\Lambda_\sigma^{-1}\Lambda'_\sigma - I)$. We know the forms of the matrices $[\Lambda_\sigma(\ell)]^{-1}$ and $\Lambda'_\sigma(\ell)$ from section 4.3.

$$\Lambda'_\sigma(\ell) = \begin{bmatrix} \ddots & & & 0 \\ & e^{-\lambda_4 t_{\sigma\ell}} \cosh(\lambda_4 \sigma q_\ell) e^{W_{\eta',\sigma}(\ell)} & e^{-\lambda_4 t_{\sigma\ell}} \sinh(\lambda_4 \sigma q_\ell) e^{W_{\eta',\sigma}(\ell)} & \\ & & \ddots & \\ & e^{-\lambda_4 t_{\sigma\ell}} \sinh(\lambda_4 \sigma q_\ell) e^{W_{\eta,\sigma}(\ell)} & e^{-\lambda_4 t_{\sigma\ell}} \cosh(\lambda_4 \sigma q_\ell) e^{W_{\eta,\sigma}(\ell)} & \\ 0 & & & \ddots \end{bmatrix} \tag{E.74}$$

and

$$[\Lambda_\sigma(\ell)]^{-1} = \begin{bmatrix} \ddots & & & & 0 \\ & e^{-\lambda_4 t_{\sigma\ell}} \cosh(\lambda_4 \sigma q_\ell) e^{-W_{\eta',\sigma}(\ell)} & & -e^{-\lambda_4 t_{\sigma\ell}} \sinh(\lambda_4 \sigma q_\ell) e^{-W_{\eta,\sigma}(\ell)} & \\ & & \ddots & & \\ & -e^{-\lambda_4 t_{\sigma\ell}} \sinh(\lambda_4 \sigma q_\ell) e^{-W_{\eta',\sigma}(\ell)} & & e^{-\lambda_4 t_{\sigma\ell}} \cosh(\lambda_4 \sigma q_\ell) e^{-W_{\eta,\sigma}(\ell)} & \\ 0 & & & & \ddots \end{bmatrix} \tag{E.75}$$

After we multiply them, we get the form of $\left\{[\Lambda_\sigma(\ell)]^{-1} \Lambda'_\sigma(\ell) - I\right\}_{N_d \times N_d}$.

$$[\Lambda_\sigma(\ell)]^{-1} \Lambda'_\sigma(\ell) - I = \begin{bmatrix} 0 & & & & & & 0 \\ & \ddots & \boldsymbol{\eta',\eta'} & & & & \\ & & \downarrow & & & & \\ & & e^{-2\lambda_4 t_{\sigma\ell}} - 1 & & & & \\ & & & 0 & & & \\ & & & & e^{-2\lambda_4 t_{\sigma\ell}} - 1 & & \\ & & & & \boldsymbol{\eta},\boldsymbol{\eta} \uparrow & \ddots & \\ 0 & & & & & & 0 \end{bmatrix} \tag{E.76}$$

This can be reduced more by using hyperbolic identities. Since the change occurs only at imaginary-time slice ℓ, the form of $(\Lambda_\sigma^{-1}\Lambda'_\sigma - I)$ is the same.

$$\Lambda_\sigma^{-1}\Lambda'_\sigma - I = \begin{bmatrix} 0 & & & & & & 0 \\ & \ddots & & & & & \\ & & e^{-2\lambda_4 t_{\sigma\ell}} - 1 & & & & \\ & & & 0 & & & \\ & & & & e^{-2\lambda_4 t_{\sigma\ell}} - 1 & & \\ & & & & & \ddots & \\ 0 & & & & & & 0 \end{bmatrix} \tag{E.77}$$

All elements are zero except two elements which are located at $(\eta'\ell, \eta'\ell)$ and $(\eta\ell, \eta\ell)$. For this new spin configuration, the update expression of Green's function is equation E.31, because the matrix, $(\Lambda_\sigma^{-1}\Lambda'_\sigma - I)$, has only 2 non-zero elements. The elements which are used for the Green's function update caused by

$$t_{\sigma\ell} \quad \longrightarrow \quad t'_{\sigma\ell} = -t_{\sigma\ell}$$

change are

$$\boxed{\begin{aligned} \left(\Lambda_\sigma^{-1}\Lambda'_\sigma - I\right)_{\eta'\ell,\eta'\ell} &= e^{-2\lambda_4 t_{\sigma\ell}} - 1 \\ \left(\Lambda_\sigma^{-1}\Lambda'_\sigma - I\right)_{\eta\ell,\eta\ell} &= e^{-2\lambda_4 t_{\sigma\ell}} - 1 \end{aligned}} \tag{E.78}$$

E.7. Single Spin-flip for "$S^U_{\nu\ell}$"

The update algorithms of arbitrary field variables $S^U_{\nu'\ell}$,$S^{U'}_{\nu\nu',\ell}$ and $S^{U'-J}_{\nu\nu',\ell,\sigma}$ are modified when the changes are at the impurity orbitals on which the effects of H_J are turned on. The update algorithm of these variables do not change if the effects of H_J is turned off on that orbitals. Here, for the update algorithms of these variables, we assume that the

effects of H_J is turned on for η and η' impurity orbitals. There are two cases which $S^U_{\nu\ell}$ can be changed; for $\nu = \eta$ or $\nu = \eta'$ impurity orbitals. If $\nu \neq \eta$ or $\nu \neq \eta'$, there is no change in the algorithms.

E.7.1. Spin-flip for $S^U_{\eta'\ell}$

In this section, we will look at spin-flip for $S^U_{\eta'\ell}$ which is

$$S^U_{\eta'\ell} \quad \longrightarrow \quad \left(S^U_{\eta'\ell}\right)' = -S^U_{\eta'\ell}$$

In order to track the effect of this change let us look at $(W_{\eta'\sigma}(\ell))' - W_{\eta'\sigma}(\ell)$ which will be calculated when we multiply Λ^{-1}_σ and Λ'_σ matrices.

$$(W_{\eta'\sigma}(\ell))' - W_{\eta'\sigma}(\ell) = -2\lambda_1\sigma S^U_{\eta'\ell} \tag{E.79}$$

Green's function for new spin configuration is calculated with the relation

$$(G^\sigma)' = G^\sigma + (G^\sigma - I)\left(\Lambda^{-1}_\sigma\Lambda'_\sigma - I\right)A^{-1}_\sigma G^\sigma \tag{E.80}$$

Let us look at the form of $(\Lambda_\sigma^{-1}\Lambda'_\sigma - I)$. We know the forms of the matrices $[\Lambda_\sigma(\ell)]^{-1}$ and $\Lambda'_\sigma(\ell)$ from section 4.3.

$$\Lambda'_\sigma(\ell) = \begin{bmatrix} \ddots & & & 0 \\ & e^{\lambda_4 t_{\sigma\ell}} \cosh(\lambda_4 \sigma q_\ell) e^{\left(W_{\eta',\sigma}(\ell)\right)'} & e^{\lambda_4 t_{\sigma\ell}} \sinh(\lambda_4 \sigma q_\ell) e^{\left(W_{\eta',\sigma}(\ell)\right)'} & \\ & & \ddots & \\ & e^{\lambda_4 t_{\sigma\ell}} \sinh(\lambda_4 \sigma q_\ell) e^{W_{\eta,\sigma}(\ell)} & e^{\lambda_4 t_{\sigma\ell}} \cosh(\lambda_4 \sigma q_\ell) e^{W_{\eta,\sigma}(\ell)} & \\ 0 & & & \ddots \end{bmatrix} \tag{E.81}$$

and

$$[\Lambda_\sigma(\ell)]^{-1} = \begin{bmatrix} \ddots & & & 0 \\ & e^{-\lambda_4 t_{\sigma\ell}} \cosh(\lambda_4 \sigma q_\ell) e^{-W_{\eta',\sigma}(\ell)} & -e^{-\lambda_4 t_{\sigma\ell}} \sinh(\lambda_4 \sigma q_\ell) e^{-W_{\eta,\sigma}(\ell)} & \\ & & \ddots & \\ & -e^{-\lambda_4 t_{\sigma\ell}} \sinh(\lambda_4 \sigma q_\ell) e^{-W_{\eta',\sigma}(\ell)} & e^{-\lambda_4 t_{\sigma\ell}} \cosh(\lambda_4 \sigma q_\ell) e^{-W_{\eta,\sigma}(\ell)} & \\ 0 & & & \ddots \end{bmatrix} \tag{E.82}$$

Since the change occurs only at imaginary-time slice ℓ, the form of $(\Lambda_\sigma^{-1}\Lambda'_\sigma - I)$ is the same. All elements are zero except the four elements which are located at $(\eta'\ell, \eta'\ell)$, $(\eta'\ell, \eta\ell)$, $(\eta\ell, \eta'\ell)$ and $(\eta\ell, \eta\ell)$. For this new spin configuration, the update expression of Green's function is equation E.28, because the matrix, $(\Lambda_\sigma^{-1}\Lambda'_\sigma - I)$, has only 4 non-zero

elements. The elements which are used for the Green's function update caused by

$$S^U_{\eta'\ell} \quad \longrightarrow \quad \left(S^U_{\eta'\ell}\right)' = -S^U_{\eta'\ell}$$

change are

$$\boxed{\begin{aligned}
\left(\Lambda_\sigma^{-1}\Lambda'_\sigma - I\right)_{\eta'\ell,\eta'\ell} &= \cosh^2(\lambda_4\sigma q_\ell)\left(e^{-2\lambda_1\sigma S^U_{\eta'\ell}} - 1\right) \\
\left(\Lambda_\sigma^{-1}\Lambda'_\sigma - I\right)_{\eta'\ell,\eta\ell} &= \frac{1}{2}\sinh(2\lambda_4\sigma q_\ell)\left(e^{-2\lambda_1\sigma S^U_{\eta'\ell}} - 1\right) \\
\left(\Lambda_\sigma^{-1}\Lambda'_\sigma - I\right)_{\eta\ell,\eta'\ell} &= \frac{1}{2}\sinh(2\lambda_4\sigma q_\ell)\left(1 - e^{-2\lambda_1\sigma S^U_{\eta'\ell}}\right) \\
\left(\Lambda_\sigma^{-1}\Lambda'_\sigma - I\right)_{\eta\ell,\eta\ell} &= \sinh^2(\lambda_4\sigma q_\ell)\left(1 - e^{-2\lambda_1\sigma S^U_{\eta'\ell}}\right)
\end{aligned}} \tag{E.83}$$

E.7.2. Spin-flip for $S^U_{\eta\ell}$

In this section, we will look at spin-flip for $S^U_{\eta\ell}$ which is

$$S^U_{\eta\ell} \quad \longrightarrow \quad \left(S^U_{\eta\ell}\right)' = -S^U_{\eta\ell}$$

In order to track the effect of this change let us look at $(W_{\eta'\sigma}(\ell))' - W_{\eta'\sigma}(\ell)$ which will be calculated when we multiply Λ_σ^{-1} and Λ'_σ matrices.

$$(W_{\eta\sigma}(\ell))' - W_{\eta\sigma}(\ell) = -2\lambda_1\sigma S^U_{\eta\ell} \tag{E.84}$$

This update is the same as in the case for $S^U_{\eta'\ell}$, however the only change is the orbital indices. All elements are zero except the four elements which are located at $(\eta'\ell, \eta'\ell)$, $(\eta'\ell, \eta\ell)$, $(\eta\ell, \eta'\ell)$ and $(\eta\ell, \eta\ell)$. For this new spin configuration, the update expression of Green's function is equation E.28, because the matrix, $(\Lambda_\sigma^{-1}\Lambda'_\sigma - I)$, has only 4 non-zero

elements. The elements which are used for the Green's function update caused by

$$S^U_{\eta\ell} \quad \longrightarrow \quad \left(S^U_{\eta\ell}\right)' = -S^U_{\eta\ell}$$

change are

$$\boxed{\begin{aligned}
\left(\Lambda_\sigma^{-1}\Lambda'_\sigma - I\right)_{\eta'\ell,\eta'\ell} &= \sinh^2(\lambda_4\sigma q_\ell)\left(1 - e^{-2\lambda_1\sigma S^U_{\eta'\ell}}\right) \\
\left(\Lambda_\sigma^{-1}\Lambda'_\sigma - I\right)_{\eta'\ell,\eta\ell} &= \frac{1}{2}\sinh(2\lambda_4\sigma q_\ell)\left(1 - e^{-2\lambda_1\sigma S^U_{\eta'\ell}}\right) \\
\left(\Lambda_\sigma^{-1}\Lambda'_\sigma - I\right)_{\eta\ell,\eta'\ell} &= \frac{1}{2}\sinh(2\lambda_4\sigma q_\ell)\left(e^{-2\lambda_1\sigma S^U_{\eta'\ell}} - 1\right) \\
\left(\Lambda_\sigma^{-1}\Lambda'_\sigma - I\right)_{\eta\ell,\eta\ell} &= \cosh^2(\lambda_4\sigma q_\ell)\left(e^{-2\lambda_1\sigma S^U_{\eta'\ell}} - 1\right)
\end{aligned}} \tag{E.85}$$

E.8. Single Spin-flip for "$S^{U'}_{\nu\nu',\ell}$"

$$S^{U'}_{\nu\nu',\ell} \quad \longrightarrow \quad \left(S^{U'}_{\nu\nu',\ell}\right)' = -S^{U'}_{\nu\nu',\ell}$$

The spin-flip for $S^{U'}_{\nu\nu'\ell}$ affects just the orbital in the first index which is ν in this example. However, the effect of this change is different for up and down spin in the following way;

$$\begin{aligned}
(W_{\nu\uparrow}(\ell))' - W_{\nu\uparrow}(\ell) &= -2\lambda_2\sigma S^{U'}_{\nu\nu',\ell} \\
(W_{\nu\downarrow}(\ell))' - W_{\nu\downarrow}(\ell) &= +2\lambda_2\sigma S^{U'}_{\nu\nu',\ell}
\end{aligned} \tag{E.86}$$

Since it affects just one orbital, the update algorithm is the same as in the case of $S^{U'}_{\nu\ell}$'. One needs to check whether ν is equal to η,η' or not. If ν is equal to η or η', the update algorithm is equation E.28 and the elements of $(\Lambda_\sigma^{-1}\Lambda'_\sigma - I)$ matrix depends on the

orbital.

$$\begin{aligned} \text{If} \quad \nu = \eta' \quad &\longrightarrow \quad \text{use equations} \quad E.83 \\ \text{If} \quad \nu = \eta \quad &\longrightarrow \quad \text{use equations} \quad E.85 \\ \text{If} \quad \nu \neq \eta' \quad \text{or} \quad \nu \neq \eta \quad &\longrightarrow \quad \text{no change in the equations} \end{aligned} \tag{E.87}$$

Addition to this, exponents of the factors in the equations E.83 and E.85 should be changed depending on up and down spin using equations E.86

E.9. Single Spin-flip for "$S^{U'-J}_{\nu\nu',\ell,\sigma}$"

There are three cases in which the spin-flip for $S^{U'-J}_{\nu\nu',\ell,\sigma}$ occurs. These cases include H_J being turned on at both ν and ν' orbitals, H_J being turned on at just ν or ν' orbital. These three cases includes 5 situations. Let us assume that the effects of H_J is turned on at η and η' orbitals.

$$\begin{aligned} \text{if} \quad \nu = \eta \quad \text{and} \quad \nu' = \eta' \quad &\longrightarrow \quad S^{U'-J}_{\eta\eta',\ell,\sigma} \\ \text{if} \quad \nu \neq \eta, \eta' \quad \text{and} \quad \nu' = \eta' \quad &\longrightarrow \quad S^{U'-J}_{\nu\eta',\ell,\sigma} \\ \text{if} \quad \nu \neq \eta, \eta' \quad \text{and} \quad \nu' = \eta \quad &\longrightarrow \quad S^{U'-J}_{\nu\eta,\ell,\sigma} \\ \text{if} \quad \nu = \eta' \quad \text{and} \quad \nu' \neq \eta, \eta' \quad &\longrightarrow \quad S^{U'-J}_{\eta'\nu',\ell,\sigma} \\ \text{if} \quad \nu = \eta \quad \text{and} \quad \nu' \neq \eta, \eta' \quad &\longrightarrow \quad S^{U'-J}_{\eta\nu',\ell,\sigma} \end{aligned}$$

E.9.1. Spin-flip for $S^{U'-J}_{\eta\eta',\ell,\sigma}$

$$S^{U'-J}_{\eta\eta',\ell,\sigma} \quad \longrightarrow \quad \left(S^{U'-J}_{\eta\eta',\ell,\sigma}\right)' = -S^{U'-J}_{\eta\eta',\ell,\sigma}$$

In order to track the effect of this change let us look at $(W_{\eta'\sigma}(\ell))'-W_{\eta'\sigma}(\ell)$ and $(W_{\eta\sigma}(\ell))'-W_{\eta\sigma}(\ell)$ which will be calculated when we multiply Λ_σ^{-1} and Λ'_σ matrices.

$$\begin{aligned}(W_{\eta'\sigma}(\ell))' - W_{\eta'\sigma}(\ell) &= +2\lambda_3 S^{U'-J}_{\eta\eta',\ell,\sigma} \\ (W_{\eta\sigma}(\ell))' - W_{\eta\sigma}(\ell) &= -2\lambda_3 S^{U'-J}_{\eta\eta',\ell,\sigma}\end{aligned} \tag{E.88}$$

Green's function for new spin configuration is calculated with the relation

$$(G^\sigma)' = G^\sigma + (G^\sigma - I)\left(\Lambda_\sigma^{-1}\Lambda'_\sigma - I\right) A_\sigma^{-1} G^\sigma \tag{E.89}$$

Let us look at the form of $(\Lambda_\sigma^{-1}\Lambda'_\sigma - I)$. We know the forms of the matrices $[\Lambda_\sigma(\ell)]^{-1}$ and $\Lambda'_\sigma(\ell)$ from section 4.3.

$$\Lambda'_\sigma(\ell) = \begin{bmatrix} \ddots & & & 0 \\ & e^{\lambda_4 t_{\sigma\ell}}\cosh(\lambda_4\sigma q_\ell)e^{\left(W_{\eta',\sigma}(\ell)\right)'} & e^{\lambda_4 t_{\sigma\ell}}\sinh(\lambda_4\sigma q_\ell)e^{\left(W_{\eta',\sigma}(\ell)\right)'} & \\ & & \ddots & \\ & e^{\lambda_4 t_{\sigma\ell}}\sinh(\lambda_4\sigma q_\ell)e^{(W_{\eta,\sigma}(\ell))'} & e^{\lambda_4 t_{\sigma\ell}}\cosh(\lambda_4\sigma q_\ell)e^{(W_{\eta,\sigma}(\ell))'} & \\ 0 & & & \ddots \end{bmatrix} \tag{E.90}$$

and

$$[\Lambda_\sigma(\ell)]^{-1} = \begin{bmatrix} \ddots & & & 0 \\ & e^{-\lambda_4 t_{\sigma\ell}} \cosh(\lambda_4 \sigma q_\ell) e^{-W_{\eta',\sigma}(\ell)} & -e^{-\lambda_4 t_{\sigma\ell}} \sinh(\lambda_4 \sigma q_\ell) e^{-W_{\eta,\sigma}(\ell)} & \\ & & \ddots & \\ & -e^{-\lambda_4 t_{\sigma\ell}} \sinh(\lambda_4 \sigma q_\ell) e^{-W_{\eta',\sigma}(\ell)} & e^{-\lambda_4 t_{\sigma\ell}} \cosh(\lambda_4 \sigma q_\ell) e^{-W_{\eta,\sigma}(\ell)} & \\ 0 & & & \ddots \end{bmatrix} \tag{E.91}$$

After we multiply them, we get the form of $\left\{[\Lambda_\sigma(\ell)]^{-1} \Lambda'_\sigma(\ell) - I\right\}_{N_d \times N_d}$.

$$[\Lambda_\sigma(\ell)]^{-1} \Lambda'_\sigma(\ell) - I = \begin{bmatrix} 0 & & & & 0 \\ & \ddots & \boldsymbol{\eta',\eta'} \downarrow & \boldsymbol{\eta',\eta} \downarrow & \\ & & \bullet & \bullet & \\ & & 0 & & \\ & & \bullet & \bullet & \\ & & \boldsymbol{\eta,\eta'} \uparrow & \boldsymbol{\eta,\eta} \uparrow & \ddots \\ 0 & & & & 0 \end{bmatrix} \tag{E.92}$$

Here, all elements are zero except the big dots. Since the change occurs only at imaginary-time slice ℓ, the form of $(\Lambda_\sigma^{-1}\Lambda'_\sigma - I)$ is the same.

$$\Lambda_\sigma^{-1}\Lambda'_\sigma - I = \begin{bmatrix} 0 & & & & \mathbf{0} \\ & \ddots & & & \\ & & \bullet \quad \bullet & & \\ & & \ddots & & \\ & & \bullet \quad \bullet & & \\ & & & \ddots & \\ \mathbf{0} & & & & 0 \end{bmatrix} \tag{E.93}$$

All elements are zero except the four elements which are located at $(\eta'\ell, \eta'\ell)$, $(\eta'\ell, \eta\ell)$, $(\eta\ell, \eta'\ell)$ and $(\eta\ell, \eta\ell)$. For this new spin configuration, the update expression of Green's function is equation E.28, because the matrix, $(\Lambda_\sigma^{-1}\Lambda'_\sigma - I)$, has only 4 non-zero elements. After the results is reduced more by using hyperbolic identities, we can get the final form of the non-zero elements. The elements which are used for the Green's function update caused by

$$S^{U'-J}_{\eta\eta',\ell,\sigma} \quad \longrightarrow \quad \left(S^{U'-J}_{\eta\eta',\ell,\sigma}\right)' = -S^{U'-J}_{\eta\eta',\ell,\sigma}$$

change are

$$\boxed{\begin{aligned}
\left(\Lambda_\sigma^{-1}\Lambda'_\sigma - I\right)_{\eta'\ell,\eta'\ell} &= e^{2\lambda_3 S^{U'-J}_{\eta\eta',\ell,\sigma}}\left[1 + \sinh^2(\lambda_4\sigma q_\ell)\left(1 - e^{-4\lambda_3 S^{U'-J}_{\eta\eta',\ell,\sigma}}\right)\right] - 1 \\
\left(\Lambda_\sigma^{-1}\Lambda'_\sigma - I\right)_{\eta'\ell,\eta\ell} &= \frac{1}{2}\sinh(2\lambda_4\sigma q_\ell)\left(e^{2\lambda_3 S^{U'-J}_{\eta\eta',\ell,\sigma}} - e^{-2\lambda_3 S^{U'-J}_{\eta\eta',\ell,\sigma}}\right) \\
\left(\Lambda_\sigma^{-1}\Lambda'_\sigma - I\right)_{\eta\ell,\eta'\ell} &= \frac{1}{2}\sinh(2\lambda_4\sigma q_\ell)\left(e^{-2\lambda_3 S^{U'-J}_{\eta\eta',\ell,\sigma}} - e^{2\lambda_3 S^{U'-J}_{\eta\eta',\ell,\sigma}}\right) \\
\left(\Lambda_\sigma^{-1}\Lambda'_\sigma - I\right)_{\eta\ell,\eta\ell} &= e^{2\lambda_3 S^{U'-J}_{\eta\eta',\ell,\sigma}}\left[1 + \cosh^2(\lambda_4\sigma q_\ell)\left(e^{-4\lambda_3 S^{U'-J}_{\eta\eta',\ell,\sigma}} - 1\right)\right] - 1
\end{aligned}} \tag{E.94}$$

E.9.2. Spin-flip for $S^{U'-J}_{\nu\eta',\ell,\sigma}$

$$S^{U'-J}_{\nu\eta',\ell,\sigma} \quad \longrightarrow \quad \left(S^{U'-J}_{\nu\eta',\ell,\sigma}\right)' = -S^{U'-J}_{\nu\eta',\ell,\sigma}$$

In order to track the effect of this change let us look at $(W_{\eta'\sigma}(\ell))' - W_{\eta'\sigma}(\ell)$ which will be calculated when we multiply Λ_σ^{-1} and Λ'_σ matrices.

$$\begin{aligned}(W_{\eta'\sigma}(\ell))' - W_{\eta'\sigma}(\ell) &= +2\lambda_3 S^{U'-J}_{\nu\eta',\ell,\sigma} \\ (W_{\nu\sigma}(\ell))' - W_{\nu\sigma}(\ell) &= -2\lambda_3 S^{U'-J}_{\nu\eta',\ell,\sigma}\end{aligned} \tag{E.95}$$

Here, we should be careful about the facts that

$$\nu > \eta' \tag{E.96}$$

$$\eta > \eta'. \tag{E.97}$$

Green's function for new spin configuration is calculated with the relation

$$(G^\sigma)' = G^\sigma + (G^\sigma - I)\left(\Lambda_\sigma^{-1}\Lambda'_\sigma - I\right) A_\sigma^{-1} G^\sigma \tag{E.98}$$

Let us look at the form of $(\Lambda_\sigma^{-1}\Lambda'_\sigma - I)$. We know the forms of the matrices $[\Lambda_\sigma(\ell)]^{-1}$ and $\Lambda'_\sigma(\ell)$ from section 4.3.

$$\Lambda'_\sigma(\ell) = \begin{bmatrix} \ddots & & & & 0 \\ & e^{\lambda_4 t_{\sigma\ell}}\cosh(\lambda_4\sigma q_\ell)e^{\left(W_{\eta',\sigma}(\ell)\right)'} & e^{\lambda_4 t_{\sigma\ell}}\sinh(\lambda_4\sigma q_\ell)e^{\left(W_{\eta',\sigma}(\ell)\right)'} & & \\ & e^{\lambda_4 t_{\sigma\ell}}\sinh(\lambda_4\sigma q_\ell)e^{W_{\eta,\sigma}(\ell)} & e^{\lambda_4 t_{\sigma\ell}}\cosh(\lambda_4\sigma q_\ell)e^{W_{\eta,\sigma}(\ell)} & & \\ & & & e^{(W_{\nu,\sigma}(\ell))'} & \\ 0 & & & & \ddots \end{bmatrix} \tag{E.99}$$

and

$$[\Lambda_\sigma(\ell)]^{-1} = \begin{bmatrix} \ddots & & & & 0 \\ & e^{-\lambda_4 t_{\sigma\ell}}\cosh(\lambda_4\sigma q_\ell)e^{-W_{\eta',\sigma}(\ell)} & -e^{-\lambda_4 t_{\sigma\ell}}\sinh(\lambda_4\sigma q_\ell)e^{-W_{\eta,\sigma}(\ell)} & & \\ & -e^{-\lambda_4 t_{\sigma\ell}}\sinh(\lambda_4\sigma q_\ell)e^{-W_{\eta',\sigma}(\ell)} & e^{-\lambda_4 t_{\sigma\ell}}\cosh(\lambda_4\sigma q_\ell)e^{-W_{\eta,\sigma}(\ell)} & & \\ & & & e^{-W_{\nu,\sigma}(\ell)} & \\ 0 & & & & \ddots \end{bmatrix} \tag{E.100}$$

After we multiply them, we get the form of $\left\{\left[\Lambda_\sigma(\ell)\right]^{-1}\Lambda'_\sigma(\ell) - I\right\}_{N_d \times N_d}$.

$$\left[\Lambda_\sigma(\ell)\right]^{-1}\Lambda'_\sigma(\ell) - I = \tag{E.101}$$

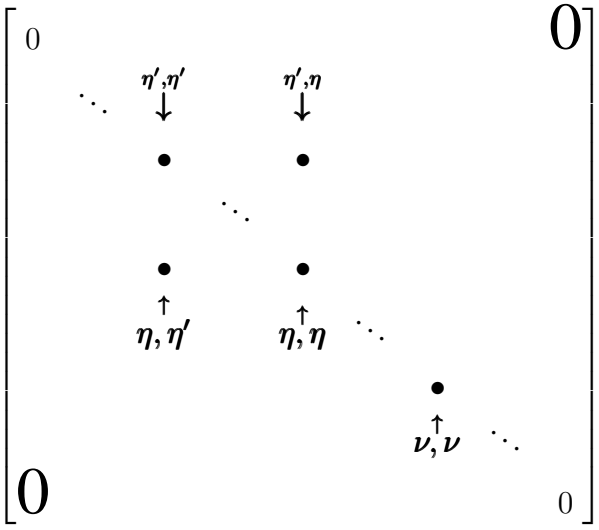

Here, all elements are zero except the big dots. Since the change occurs only at imaginary-time slice ℓ, the form of $(\Lambda_\sigma^{-1}\Lambda'_\sigma - I)$ is the same.

$$\Lambda_\sigma^{-1}\Lambda'_\sigma - I = \tag{E.102}$$

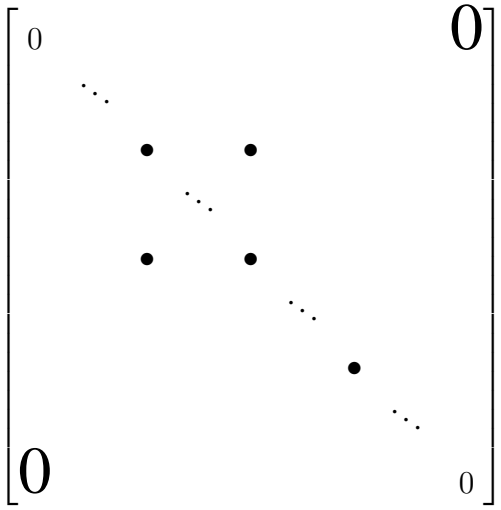

All elements are zero except five elements which are located at $(\eta'\ell, \eta'\ell)$, $(\eta'\ell, \eta\ell)$, $(\eta\ell, \eta'\ell)$, $(\eta\ell, \eta\ell)$ and $(\nu\ell, \nu\ell)$. For this new spin configuration, the update expression of Green's function is equation E.55, because the matrix, $(\Lambda_\sigma^{-1}\Lambda'_\sigma - I)$, has only 5 non-zero elements. After the results is reduced more by using hyperbolic identities, we can get the final form of the non-zero elements. The elements which are used for the Green's function

update caused by

$$S^{U'-J}_{\nu\eta',\ell,\sigma} \quad \longrightarrow \quad \left(S^{U'-J}_{\nu\eta',\ell,\sigma}\right)' = -S^{U'-J}_{\nu\eta',\ell,\sigma}$$

change are

$$\boxed{\begin{aligned}
\left(\Lambda_\sigma^{-1}\Lambda'_\sigma - I\right)_{\eta'\ell,\eta'\ell} &= \cosh^2(\lambda_4\sigma q_\ell)\left(e^{+2\lambda_3 S^{U'-J}_{\nu\eta',\ell,\sigma}} - 1\right) \\
\left(\Lambda_\sigma^{-1}\Lambda'_\sigma - I\right)_{\eta'\ell,\eta\ell} &= \frac{1}{2}\sinh(2\lambda_4\sigma q_\ell)\left(e^{+2\lambda_3 S^{U'-J}_{\nu\eta',\ell,\sigma}} - 1\right) \\
\left(\Lambda_\sigma^{-1}\Lambda'_\sigma - I\right)_{\eta\ell,\eta'\ell} &= \frac{1}{2}\sinh(2\lambda_4\sigma q_\ell)\left(1 - e^{+2\lambda_3 S^{U'-J}_{\nu\eta',\ell,\sigma}}\right) \\
\left(\Lambda_\sigma^{-1}\Lambda'_\sigma - I\right)_{\eta\ell,\eta\ell} &= \sinh^2(\lambda_4\sigma q_\ell)\left(1 - e^{+2\lambda_3 S^{U'-J}_{\nu\eta',\ell,\sigma}}\right) \\
\left(\Lambda_\sigma^{-1}\Lambda'_\sigma - I\right)_{\nu\ell,\nu\ell} &= e^{-2\lambda_3 S^{U'-J}_{\nu\eta',\ell,\sigma}} - 1
\end{aligned}} \tag{E.103}$$

E.9.3. Spin-flip for $S^{U'-J}_{\nu\eta,\ell,\sigma}$

$$S^{U'-J}_{\nu\eta,\ell,\sigma} \quad \longrightarrow \quad \left(S^{U'-J}_{\nu\eta,\ell,\sigma}\right)' = -S^{U'-J}_{\nu\eta,\ell,\sigma}$$

In order to track the effect of this change let us look at $(W_{\nu\sigma}(\ell))' - W_{\nu\sigma}(\ell)$ which will be calculated when we multiply Λ_σ^{-1} and Λ'_σ matrices.

$$\begin{aligned}
(W_{\eta\sigma}(\ell))' - W_{\eta\sigma}(\ell) &= +2\lambda_3 S^{U'-J}_{\nu\eta,\ell,\sigma} \\
(W_{\nu\sigma}(\ell))' - W_{\nu\sigma}(\ell) &= -2\lambda_3 S^{U'-J}_{\nu\eta,\ell,\sigma}
\end{aligned} \tag{E.104}$$

Here, we should be careful about the facts that

$$\nu > \eta \tag{E.105}$$

$$\eta > \eta'. \tag{E.106}$$

Green's function for new spin configuration is calculated with the relation

$$(G^\sigma)' = G^\sigma + (G^\sigma - I)\left(\Lambda_\sigma^{-1}\Lambda'_\sigma - I\right) A_\sigma^{-1} G^\sigma \tag{E.107}$$

The form of the matrix $(\Lambda_\sigma^{-1}\Lambda'_\sigma - I)$ is the same as in the case of $S^{U'-J}_{\nu\eta',\ell,\sigma}$.

$$\Lambda_\sigma^{-1}\Lambda'_\sigma - I = \begin{bmatrix} 0 & & & & & & 0 \\ & \ddots & & & & & \\ & & \bullet & & \bullet & & \\ & & & \ddots & & & \\ & & \bullet & & \bullet & & \\ & & & & & \ddots & \\ & & & & & & \ddots \\ 0 & & & & & & 0 \end{bmatrix} \tag{E.108}$$

All elements are zero except five elements which are located at $(\eta'\ell, \eta'\ell)$, $(\eta'\ell, \eta\ell)$, $(\eta\ell, \eta'\ell)$, $(\eta\ell, \eta\ell)$ and $(\nu\ell, \nu\ell)$. For this new spin configuration, the update expression of Green's function is equation E.55, because the matrix, $(\Lambda_\sigma^{-1}\Lambda'_\sigma - I)$, has only 5 non-zero elements. After the results is reduced more by using hyperbolic identities, we can get the final form of the non-zero elements. The elements which are used for the Green's function update caused by

$$S^{U'-J}_{\nu\eta,\ell,\sigma} \quad \longrightarrow \quad \left(S^{U'-J}_{\nu\eta,\ell,\sigma}\right)' = -S^{U'-J}_{\nu\eta,\ell,\sigma}$$

change are

$$\boxed{\begin{aligned}
\left(\Lambda_\sigma^{-1}\Lambda'_\sigma - I\right)_{\eta'\ell,\eta'\ell} &= \sinh^2(\lambda_4\sigma q_\ell)\left(1 - e^{+2\lambda_3 S^{U'-J}_{\nu\eta,\ell,\sigma}}\right) \\
\left(\Lambda_\sigma^{-1}\Lambda'_\sigma - I\right)_{\eta'\ell,\eta\ell} &= \frac{1}{2}\sinh(2\lambda_4\sigma q_\ell)\left(1 - e^{+2\lambda_3 S^{U'-J}_{\nu\eta,\ell,\sigma}}\right) \\
\left(\Lambda_\sigma^{-1}\Lambda'_\sigma - I\right)_{\eta\ell,\eta'\ell} &= \frac{1}{2}\sinh(2\lambda_4\sigma q_\ell)\left(e^{+2\lambda_3 S^{U'-J}_{\nu\eta,\ell,\sigma}} - 1\right) \\
\left(\Lambda_\sigma^{-1}\Lambda'_\sigma - I\right)_{\eta\ell,\eta\ell} &= \cosh^2(\lambda_4\sigma q_\ell)\left(e^{+2\lambda_3 S^{U'-J}_{\nu\eta,\ell,\sigma}} - 1\right) \\
\left(\Lambda_\sigma^{-1}\Lambda'_\sigma - I\right)_{\nu\ell,\nu\ell} &= e^{-2\lambda_3 S^{U'-J}_{\nu\eta,\ell,\sigma}} - 1
\end{aligned}} \tag{E.109}$$

E.9.4. Spin-flip for $S^{U'-J}_{\eta'\nu,\ell,\sigma}$

$$S^{U'-J}_{\eta'\nu,\ell,\sigma} \quad \longrightarrow \quad \left(S^{U'-J}_{\eta'\nu,\ell,\sigma}\right)' = -S^{U'-J}_{\eta'\nu,\ell,\sigma}$$

In order to track the effect of this change let us look at $(W_{\nu\sigma}(\ell))' - W_{\nu\sigma}(\ell)$ which will be calculated when we multiply Λ_σ^{-1} and Λ'_σ matrices.

$$\begin{aligned}
(W_{\nu\sigma}(\ell))' - W_{\nu\sigma}(\ell) &= +2\lambda_3 S^{U'-J}_{\eta'\nu,\ell,\sigma} \\
(W_{\eta'\sigma}(\ell))' - W_{\eta'\sigma}(\ell) &= -2\lambda_3 S^{U'-J}_{\eta'\nu,\ell,\sigma}
\end{aligned} \tag{E.110}$$

Here, we should be careful about the facts that

$$\eta' > \nu \tag{E.111}$$

$$\eta > \eta'. \tag{E.112}$$

Green's function for new spin configuration is calculated with the relation

$$(G^\sigma)' = G^\sigma + (G^\sigma - I)\left(\Lambda_\sigma^{-1}\Lambda'_\sigma - I\right)A_\sigma^{-1}G^\sigma \tag{E.113}$$

The form of the matrix $(\Lambda_\sigma^{-1}\Lambda'_\sigma - I)$ is the same as in the case of $S^{U'-J}_{\nu\eta',\ell,\sigma}$ with a minor difference.

$$\Lambda_\sigma^{-1}\Lambda'_\sigma - I = \begin{bmatrix} 0 & & & & & & 0 \\ & \ddots & & & & & \\ & & \bullet & & & & \\ & & & \ddots & & & \\ & & & & \bullet & \bullet & \\ & & & & & \ddots & \\ & & & & \bullet & \bullet & \\ & & & & & & \ddots \\ 0 & & & & & & 0 \end{bmatrix} \tag{E.114}$$

All elements are zero except five elements which are located at $(\eta'\ell, \eta'\ell)$, $(\eta'\ell, \eta\ell)$, $(\eta\ell, \eta'\ell)$, $(\eta\ell, \eta\ell)$ and $(\nu\ell, \nu\ell)$. For this new spin configuration, the update expression of Green's function is equation E.55, because the matrix, $(\Lambda_\sigma^{-1}\Lambda'_\sigma - I)$, has only 5 non-zero elements. After the results is reduced more by using hyperbolic identities, we can get the final form of the non-zero elements. The elements which are used for the Green's function update caused by

$$S^{U'-J}_{\eta'\nu,\ell,\sigma} \quad \longrightarrow \quad \left(S^{U'-J}_{\eta'\nu,\ell,\sigma}\right)' = -S^{U'-J}_{\eta'\nu,\ell,\sigma}$$

change are

$$\boxed{\begin{aligned}
\left(\Lambda_\sigma^{-1}\Lambda'_\sigma - I\right)_{\eta'\ell,\eta'\ell} &= \cosh^2(\lambda_4\sigma q_\ell)\left(e^{-2\lambda_3 S^{U'-J}_{\eta'\nu,\ell,\sigma}} - 1\right) \\
\left(\Lambda_\sigma^{-1}\Lambda'_\sigma - I\right)_{\eta'\ell,\eta\ell} &= \frac{1}{2}\sinh(2\lambda_4\sigma q_\ell)\left(e^{-2\lambda_3 S^{U'-J}_{\eta'\nu,\ell,\sigma}} - 1\right) \\
\left(\Lambda_\sigma^{-1}\Lambda'_\sigma - I\right)_{\eta\ell,\eta'\ell} &= \frac{1}{2}\sinh(2\lambda_4\sigma q_\ell)\left(1 - e^{-2\lambda_3 S^{U'-J}_{\eta'\nu,\ell,\sigma}}\right) \\
\left(\Lambda_\sigma^{-1}\Lambda'_\sigma - I\right)_{\eta\ell,\eta\ell} &= \sinh^2(\lambda_4\sigma q_\ell)\left(1 - e^{-2\lambda_3 S^{U'-J}_{\eta'\nu,\ell,\sigma}}\right) \\
\left(\Lambda_\sigma^{-1}\Lambda'_\sigma - I\right)_{\nu\ell,\nu\ell} &= e^{+2\lambda_3 S^{U'-J}_{\eta'\nu,\ell,\sigma}} - 1
\end{aligned}} \tag{E.115}$$

E.9.5. Spin-flip for $S^{U'-J}_{\eta\nu,\ell,\sigma}$

$$S^{U'-J}_{\eta\nu,\ell,\sigma} \quad \longrightarrow \quad \left(S^{U'-J}_{\eta\nu,\ell,\sigma}\right)' = -S^{U'-J}_{\eta\nu,\ell,\sigma}$$

In order to track the effect of this change let us look at $(W_{\nu\sigma}(\ell))' - W_{\nu\sigma}(\ell)$ which will be calculated when we multiply Λ_σ^{-1} and Λ'_σ matrices.

$$\begin{aligned}(W_{\nu\sigma}(\ell))' - W_{\nu\sigma}(\ell) &= +2\lambda_3 S^{U'-J}_{\eta\nu,\ell,\sigma} \\ (W_{\eta\sigma}(\ell))' - W_{\eta\sigma}(\ell) &= -2\lambda_3 S^{U'-J}_{\eta\nu,\ell,\sigma}\end{aligned} \tag{E.116}$$

Here, we should be careful about the facts that

$$\eta > \nu \tag{E.117}$$

$$\eta > \eta'. \tag{E.118}$$

Green's function for new spin configuration is calculated with the relation

$$(G^\sigma)' = G^\sigma + (G^\sigma - I)\left(\Lambda_\sigma^{-1}\Lambda'_\sigma - I\right) A_\sigma^{-1} G^\sigma \tag{E.119}$$

The form of the matrix $(\Lambda_\sigma^{-1}\Lambda'_\sigma - I)$ is the same as in the case of $S^{U'-J}_{\nu\eta',\ell,\sigma}$ with a minor

difference.

$$\Lambda_\sigma^{-1}\Lambda'_\sigma - I = \begin{bmatrix} 0 & & & & & & 0 \\ & \ddots & & & & & \\ & & \bullet & & & & \\ & & & \ddots & & & \\ & & & & \bullet & \bullet & \\ & & & & & \ddots & \\ & & & & \bullet & \bullet & \\ & & & & & & \ddots \\ 0 & & & & & & 0 \end{bmatrix} \tag{E.120}$$

All elements are zero except five elements which are located at $(\eta'\ell, \eta'\ell)$, $(\eta'\ell, \eta\ell)$, $(\eta\ell, \eta'\ell)$, $(\eta\ell, \eta\ell)$ and $(\nu\ell, \nu\ell)$. For this new spin configuration, the update expression of Green's function is equation E.55, because the matrix, $(\Lambda_\sigma^{-1}\Lambda'_\sigma - I)$, has only 5 non-zero elements. After the results is reduced more by using hyperbolic identities, we can get the final form of the non-zero elements. The elements which are used for the Green's function update caused by

$$S^{U'-J}_{\eta\nu,\ell,\sigma} \quad \longrightarrow \quad \left(S^{U'-J}_{\eta\nu,\ell,\sigma}\right)' = -S^{U'-J}_{\eta\nu,\ell,\sigma}$$

change are

$$\boxed{\begin{aligned}
\left(\Lambda_\sigma^{-1}\Lambda'_\sigma - I\right)_{\eta'\ell,\eta'\ell} &= \sinh^2(\lambda_4\sigma q_\ell)\left(1 - e^{-2\lambda_3 S^{U'-J}_{\eta\nu,\ell,\sigma}}\right) \\
\left(\Lambda_\sigma^{-1}\Lambda'_\sigma - I\right)_{\eta'\ell,\eta\ell} &= \frac{1}{2}\sinh(2\lambda_4\sigma q_\ell)\left(1 - e^{-2\lambda_3 S^{U'-J}_{\eta\nu,\ell,\sigma}}\right) \\
\left(\Lambda_\sigma^{-1}\Lambda'_\sigma - I\right)_{\eta\ell,\eta'\ell} &= \frac{1}{2}\sinh(2\lambda_4\sigma q_\ell)\left(e^{-2\lambda_3 S^{U'-J}_{\eta\nu,\ell,\sigma}} - 1\right) \\
\left(\Lambda_\sigma^{-1}\Lambda'_\sigma - I\right)_{\eta\ell,\eta\ell} &= \cosh^2(\lambda_4\sigma q_\ell)\left(e^{-2\lambda_3 S^{U'-J}_{\eta\nu,\ell,\sigma}} - 1\right) \\
\left(\Lambda_\sigma^{-1}\Lambda'_\sigma - I\right)_{\nu\ell,\nu\ell} &= e^{+2\lambda_3 S^{U'-J}_{\eta\nu,\ell,\sigma}} - 1
\end{aligned}} \tag{E.121}$$